Understanding the role of the TOPBP1 and BLM interaction in promoting genome stability



Elizabeth Grong Smethurst

St Catherine's College

University of Oxford

A thesis submitted for the degree of Doctor of Philosophy

Trinity term 2017

Abstract

Understanding the role of the TOPBP1 and BLM interaction in promoting genome stability

Elizabeth Smethurst
St Catherine's College
Submitted for the degree of DPhil, TT 2017

The ability to sense, respond to and repair DNA damage is essential in normal development and survival of an organism. A number of human congenital syndromes are associated with mutations in pathways involved in the DNA damage response, including Seckel and Bloom syndromes. Such diseases are often characterised by developmental abnormalities and cancer, emphasising the importance of gaining a deeper understanding of the mechanisms underlying these pathways. The protein kinase ATR, mutated in Seckel syndrome, is a critical mediator of the intra S-phase checkpoint in response to replicative stress. ATR activation is a multistep process that requires its interaction with TOPBP1. Recently published data identified an interaction between TOPBP1 and the BLM helicase. This interaction is dependent on the phosphorylation of the conserved serine 304 of BLM and mutation of this residue results in genome instability. However, exactly how TOPBP1-BLM interaction protects the genome remains unclear.

The findings presented in this thesis demonstrate that DT40 cells expressing the BLM S251A mutant are defective in activation of the ATR kinase upon DNA damage. In line with this, these cells display reduced CHK1 phosphorylation, increased origin firing and unreliable replication fork restart. Importantly, these phenotypes could be rescued by fusing the ATR activating domain of TOPBP1 to the mutated BLM. Furthermore, results from BLM-deficient human cell lines demonstrate similar phenotypes. Thus, this data establishes a non-enzymatic role for the BLM helicase in promoting genome stability via activation of the ATR kinase. This may help in explaining why many Bloom syndrome patients display many of the same symptoms as ATR-Seckel patients, including short stature and microcephaly.

Acknowledgements

I would like to thank my supervisor Wojciech Niedzwiedz for his expert advice and support throughout my DPhil project. In addition, I would like to thank my second supervisor Peter McHugh for comments along the way, and Andrew Blackford for help during my final year of research and feedback on my thesis manuscript. I am grateful to all members of the Niedzwiedz lab, past and present, for experimental advice and encouragement during my project. In particular, I would like to thank Rebekka Schwab for teaching me the DNA fibre technique which became so central to this project, and Jadwiga Nieminuszczy and Ronan Broderick for knowledgeable guidance and feedback throughout.

I would like to express my gratitude to my parents for their endless support, advice and encouragement. Without their reassuring words I would not have made it this far. Additionally, I would like to acknowledge my brother, who is an invaluable part of my life. I am grateful to my extended family, who have all taken such a keen interest in my undertakings. Finally, to everyone I have got to know during my time in Oxford, thank you for making the past 4 years here truly unique.

Abstract 2

Acknowledgements 3

Frequently used abbreviations 10

1. Introduction 12

1.1 DNA REPLICATION 12

1.1.1 Origin licensing and firing 12

1.1.2 DNA replication, progression and termination 14

1.2 DNA REPAIR MECHANISMS 15

1.2.1 DNA repair pathways 15

1.2.2 Homologous recombination 16

1.3 PIKKS, THE DNA DAMAGE RESPONSE AND ASSOCIATED DISEASES 21

1.3.1 PIKK domain structure 23

1.3.2 PIKKs and disease 26

1.4 ATR SIGNALLING PATHWAY 29

1.4.1 Sensing and signalling DNA damage 29

1.4.2 Activating ATR through TOPBP1 and ETAA1 33

1.4.3 Propagating the signal to ATR targets 37

1.4.4 ATR and CHK1 control late origin firing 39

1.5 BLM HELICASE AND ITS ROLE IN DNA REPAIR AND THE DDR 41

1.5.1 BLM protein structure and protein partners 41

1.5.2 Bloom syndrome 44

1.5.3 BLM in DNA replication and repair 44

1.5.4 The role of BLM in the S-phase checkpoint and the response to replication stress 46

1.6 HYPOTHESIS AND OBJECTIVES 47

2. Materials and methods 49

2.1 DT40 CELL CULTURE 49

2.2 HUMAN CELL CULTURE 49

2.3 SIRNA TRANSFECTION 50

2.4 COMPLEMENTATION OF HUMAN CELLS 50

2.4.1 Purification of BLM cDNA constructs 50

2.4.2 Transfection of human cells 52

2.5 CRISPR/CAS9 STRATEGY AND CELL TRANSFECTION 53

2.5.1 Verification of CRISPR/Cas9-generated cell lines 55

2.6 CHECKPOINT ANALYSIS AND WESTERN BLOTTING 56

2.6.1 Treatment of cells for the investigation of checkpoint activation 56

2.6.2 Cell harvesting and western blotting 57

2.6.3 Quantification of western blots 58

2.6.4 Buffers for western blotting 59

2.6.5 Antibodies for western blotting 60

2.7 DNA FIBRE TECHNIQUE IN DT40 CELLS 61

2.7.1 Labelling cells for DNA fibre 61

2.7.2 Staining of DNA fibres 62

2.7.3 Visualisation and quantification of fibres *62*

2.7.4 Replication fork speed by DNA fibre *64*

2.7.5 DNA fibre with drug treatments *65*

2.8 DNA FIBRE IN HUMAN CELLS 65

2.8.1 Labelling human cells under normal growth conditions *65*

2.8.2 Treatment of human cell lines for DNA fibre *66*

2.9 SISTER CHROMATID EXCHANGE ASSAY 66

3. Investigating the role of BLM in the checkpoint response in DT40 cells 68

3.1 ANALYSIS OF UNCHALLENGED DNA REPLICATION IN BLM-S251A CELLS 70

3.1.1 Replication structures in unchallenged cells *72*

3.1.2 Analysis of replication fork speed *75*

3.1.3 Analysis of replication symmetry *78*

3.2 EVALUATING CHANGES IN CHECKPOINT ACTIVATION AND DNA REPLICATION IN RESPONSE TO DSBS 81

3.2.1 Investigating the S-phase checkpoint response to DSBs *81*

3.2.2 Recovery of DNA replication in BLM-S251A cells following CPT challenge ... *85*

3.3 INVESTIGATING THE CHECKPOINT RESPONSE FOLLOWING NUCLEOTIDE DEPLETION . 91

3.3.1 Investigating the checkpoint response following replication inhibition *91*

3.3.2 Assessing DNA replication in response to HU *94*

3.4 BLM-S251A CELLS COMPLETE REPLICATION THROUGH DORMANT ORIGIN FIRING 100

3.5 RESCUING CHECKPOINT AND REPLICATION PHENOTYPES BY THE FUSION OF TOPBP1 ATR ACTIVATING DOMAIN TO BLM-S251A.....106

3.5.1 Restoring replication phenotypes with the addition of TOPBP1-AAD to BLM-S251A..... 106

4. Introducing the BLM-S304A mutation into human cell lines 111

4.1 GENERATING A BLM-S304A HUMAN CELL LINE BY CRISPR/CAS9.....111

4.2 IDENTIFYING A BLM DEFICIENT HUMAN CELL LINE.....114

4.3 COMPLEMENTING HUMAN CELL LINES WITH BLM-WT OR BLM-S304A CDNA120

5. Investigating the checkpoint response in BLM-deficient human cells 126

5.1 THE CHECKPOINT RESPONSE IN BLM-DEFICIENT RPE1 CELLS 126

5.2 ASSESSING THE CHECKPOINT RESPONSE IN HUMAN CELL LINES USING SIRNA AGAINST BLM.....131

6. Establishing novel DNA fibre technique variants in human cells.....136

6.1 INTRODUCTION 136

6.1.1 EXD2 in homologous recombination..... 136

6.2 DNA FIBRE ANALYSIS OF UNTREATED HELA AND EXD2 DEFICIENT CELLS.....138

6.3 INVESTIGATING THE DNA REPLICATION PHENOTYPES OF EXD2-DEFICIENT CELLS FOLLOWING REPLICATION FORK COLLAPSE 142

6.4 EVALUATING DNA RESECTION OF STRESSED REPLICATION FORKS IN HELA AND EXD2 DEFICIENT CELLS 146

6.5 INVESTIGATING DNA RESECTION IN EXD2$^{-/-}$ CELLS CO-DEPLETED WITH BRCA2 OR MRE11 150

6.6 CONCLUDING REMARKS 157

6.6.1 Use in the further investigations of the TOPBP1-BLM interaction 158

7. Discussion and concluding remarks 159

7.1 BLM IS REQUIRED FOR FULL CHECKPOINT ACTIVATION AND FAITHFUL DNA REPLICATION IN DT40 CELLS 160

7.1.1 TOPBP1-BLM interaction is required for efficient ATR signalling in DT40 cells 160

7.1.2 Faithful DNA replication requires BLM interaction with TOPBP1 161

7.2 BLM DEFICIENCY IN HUMAN CELLS RESULTS IN AN S-PHASE CHECKPOINT DEFECT 165

7.2.1 Identification of a BLM-deficient RPE1 cell line 166

7.2.2 BLM-deficient RPE1 cells exhibit an ATR signalling defect 166

7.2.3 BLM function in ATR signalling is conserved in other human systems 167

7.3 DEVELOPING TOOLS TO FURTHER STUDY THE INVOLVEMENT OF BLM IN CHECKPOINT SIGNALLING AND DNA REPLICATION IN HUMAN CELLS 169

7.4 QUESTIONS ARISING FROM THIS WORK 169

7.4.1 The contribution of TOPBP1-BLM interaction in Bloom syndrome phenotypes 170

7.4.2 BLM may interact with ETAA1 to activate ATR 173

7.4.2 The phosphorylation BLM and its recruitment to chromatin..... 174

CONCLUDING REMARKS 175

References.....177

Frequently used abbreviations

Abbreviation	
911	Rad9-Rad1-Hus1 complex
AAD	ATR activation domain
ATM	Ataxia telangiectasia mutated
ATR	Ataxia telangiectasia and Rad3-related
ATRIP	ATR interacting protein
BLM	Bloom syndrome RecQ like helicase
BRCT	BRCA1 C-terminus domain
bp	Base pair
CDC25	Cell division cycle 25
CDC45	Cell division cycle 45
CDK	Cyclin dependent kinase
CHK1	Checkpoint kinase 1
Cl	Clone
CldU	5-Chloro-2’-deoxyuridine
CPT	Camptothecin
DDR	DNA damage response
dHJ	Double Holliday junction
DNA	Deoxyribonucleic acid
DNA-PKcs	DNA-dependent protein kinase catalytic subunit
DSB	Double strand break
dsDNA	Double-stranded DNA
ETAA1	Ewing’s tumour-associated antigen 1
EXD2	Exonuclease 3'-5' Domain Containing 2

Abbreviation	
EXO1	Exonuclease 1
GFP	Green fluorescent protein
HR	Homologous recombination
HU	Hydroxyurea
IdU	5-Iodo-2'-deoxyuridine
MCM2-7	Minichromosome maintenance proteins 2-7
MDC1	Mediator of DNA damage checkpoint protein 1
MRN	MRE11-RAD50-NBS1 complex
NHEJ	Non-homologous end-joining
PCNA	Proliferating cell nuclear antigen
PIKK	Phosphoinositide 3-kinase-related kinase
Polα	DNA polymerase α
Polδ	DNA polymerase δ
Polε	DNA polymerase ε
RFC	Replication factor C
RMI1/2	RecQ mediated genome instability 1 and 2
RNA	Ribonucleic acid
RPA	Replication protein A
S-phase	Synthesis phase
s.e.m.	Standard error mean
SCE	Sister chromatid exchange
ssDNA	Single-stranded DNA
TOP3A	Topoisomerase IIIα
TOPBP1	DNA topoisomerase II binding protein 1
WRN	Werner syndrome RecQ like helicase

1. Introduction

Cells must faithfully duplicate their genome with every cell cycle. This in itself is an enormous task, further complicated by obstructions and DNA lesions encountered by the replication fork. Cells circumvent the challenge of such replication stress by drawing upon robust DNA repair mechanisms, known collectively as the DNA damage response (DDR). The DDR consists of a complex network of signalling pathways, each responding to different lesions. This ensures the accurate replication of the genome with every cell cycle (Zhou & Elledge 2000; Ciccia & Elledge 2010). The work presented here will further probe into one of the mechanisms fundamental to the DDR, investigating the activation and signalling of the S-phase checkpoint.

1.1 DNA replication

DNA replication in eukaryotes takes place during the synthesis (S) phase of the cell cycle. The replication programme is initiated from numerous origins of replication, spaced throughout the genome. Initiating replication from a number of locations is advantageous as it dramatically reduces the time required to complete replication of the large genomes of eukaryotic cells (Remus & Diffley 2009; Sacco et al. 2012).

1.1.1 Origin licensing and firing

In yeast, a DNA replication origin is a defined sequence of DNA from which initiation of DNA replication occurs (Stinchcomb et al. 1979; Nieduszynski et al. 2006). Although the

identification of such sequences in mammalian cells has proved a challenge, it is clear that mammalian genomes encode information specific to replication initiation (Heinzel et al. 1991; Calos et al. 1993; Prioleau & MacAlpine 2016). In eukaryotes, replication is initiated in two steps: origin licensing and firing. First, the origin is recognised by the origin recognition complex (ORC) (Bell & Stillman 1992). Then follows the recruitment of cell division cycle 6 (CDC6) and cell division cycle 10-dependent transcript 1 (CDT1), that in turn loads two copies of the replicative helicase complex which consists of minichromosome maintenance proteins 2-7 (MCM2-7). Together these proteins make up the pre-replicative complex (pre-RC) (Gambus et al. 2011; Yamazaki et al. 2013). The number of origins licensed by the loading of MCM2-7 greatly surpasses the number of origins that fire during S-phase. Evidence suggests that these dormant origins can be drawn upon in the event of replication stress, providing a mechanism to salvage DNA replication when the original replication forks become compromised (Woodward et al. 2006; Ge et al. 2007).

The second step of replication initiation, origin firing, is triggered by the activation of the two MCM2-7 hexamers, culminating in the formation of two replication forks orientated in opposite directions on DNA, each with a single MCM2-7 helicase (Mazouzi et al. 2014). Crucial to origin firing is the recruitment of cell division cycle 45 (CDC45) and GINS to the MCM2-7 helicase, together forming the CMG complex (Moyer et al. 2006). The CMG complex allows for the initial unwinding of the DNA sequence within the origin and thus replisome assembly (Ilves et al. 2010). This then allows for replication to proceed from two bi-directional forks emanating from a single origin of replication.

Interestingly, not all origins utilised for replication fire simultaneously. An early study in human cells demonstrated that origins fire at different stages of the cell cycle. A subset of origins remain licensed but dormant during the early stages of replication, only to fire later in S-phase (Jackson & Pombo 1998). More recently, research has suggested that origin firing in early S-phase occurs randomly and sparsely throughout the genome. As S-phase progresses, additional origins fire in unreplicated regions of the genome to ensure complete replication (Kaykov & Nurse 2015).

1.1.2 DNA replication, progression and termination

Prior to replication, unwinding of the origin must take place to allow for the generation of the single stranded DNA (ssDNA) required for synthesis of an RNA primer. This primer is needed for the initiation of DNA replication. In eukaryotes replication priming is carried out by a DNA-dependent RNA primase alongside DNA polymerase α (Polα), known as the pol α - DNA primase complex (Frick & Richardson 2001; Kilkenny et al. 2013; Muzi-Falconi et al. 2003). As DNA replication on the lagging strand is discontinuous, the pol α - DNA primase complex is also required throughout the elongation stage of replication. The elongation of DNA replication on the lagging strands requires DNA polymerase δ (Polδ), whereas the leading strand is replicated in a continuous fashion by DNA polymerase ε (Polε) (Pursell et al. 2007; Nick McElhinny et al. 2008; Larrea & Lujan 2010). To increase processivity, both Polδ and Polε require the proliferating cell nuclear antigen (PCNA) which is loaded to DNA by the replication factor C (RFC) clamp loader (Fukuda et al. 1995; Kelman 1997; Bloom 2009; Chen et al. 2009). As replication nears completion, DNA replication forks converge. The termination of DNA replication is completed when the replisome is removed from chromatin by the

ubiquitin-dependent segregase p97 following the ubiquitination of MCM7 (Priego Moreno et al. 2014; Maric et al. 2014). p97 binds the ubiquitinated MCM7, and proceeds to remove the CMG complex from chromatin using its ATPase activity (Maric et al. 2014). In addition, DNA crossovers, known as catenanes, arising from topological stress caused by the converging forks must be resolved (Dewar & Walter 2017).

1.2 DNA repair mechanisms

The genome of cells is constantly subjected to stress factors, causing damage to the DNA sequence and obstructing DNA replication. Lesion-inducing stress factors can be both endogenous and exogenous to the cell. Errors made during DNA replication are an example of an endogenous stress factor, whereas UV-light and ionising radiation are examples of exogenous DNA damaging agents (Yazinski & Zou 2016).

1.2.1 DNA repair pathways

DNA lesions can be varied in nature and therefore require repair by different mechanisms. Mismatched bases in DNA are replaced by mismatch repair (MMR), whereas small chemical changes to bases require the base to be replaced by the base excision repair (BER) pathway (Robertson et al. 2009). Lesions such as pyrimidine dimers are repaired by nucleotide excision repair (NER), resulting in the removal of damaged bases as well as surrounding bases (Marteijn et al. 2014). Historically, Interstrand crosslinks (ICLs) were thought to be repaired through the Fanconi anaemia pathway which organises secondary processes, including translesion synthesis, NER and homologous recombination (HR), to fully repair the lesion (Lopez-Martinez et al. 2016;

Moldovan & D'Andrea 2009). However, recent work has identified an alternative repair mechanism relying upon the cleavage of an N-glycosyl bond by the NEIL3 DNA glycosylase (Semlow et al. 2016). Single stranded DNA breaks (SSB) are repaired through single stranded break repair (SSBR) (Caldecott 2008).

DNA double strand breaks (DSB) are extremely toxic lesions which are repaired by one of two pathways. These are HR, discussed in the following section, and non-homologous end-joining (NHEJ). NHEJ provides a rapid repair mechanism by ligating the two DNA ends of a DSB together. Central to the NHEJ pathway is DNA-dependent protein kinase catalytic subunit (DNA-PKcs) which is recruited to the DSB and activated by DNA-bound Ku70/80 (Gottlieb & Jackson 1993). DNA-PKcs tethers the two DNA ends together, before the ends are aligned and ligated (Graham et al. 2016). Alignment and ligation requires DNA ligase IV (Lig4), X-ray cross complementation group 4 (XRCC4) and XRCC4-like factor (XLF) (Cottarel et al. 2013; Wu et al. 2009; Graham et al. 2016). In addition, paralogue of XRCC4 and XLF (PAXX) has been shown to be involved in promoting Ku-dependent ligation (Ochi et al. 2015). In some cases, when the DSB requires some level of resection, the structure-specific nuclease Artemis is required for re-joining of DNA (Riballo et al. 2004).

1.2.2 Homologous recombination

When a DSB occurs during S-phase the lesion is preferentially repaired through HR (**Figure 1**) (Wyman & Kanaar 2006). When a DSB is detected, the 5' end of the break is subjected to nucleolytic digestion, a process known as resection (Cejka 2015). Initially the break is processed by the MRE11-RAD50-NBS1 (MRN) complex. In yeast the initial

endonuclease activity of MRE11 is dependent on its interaction with Sae2, creating the initial entry site for resection to take place (Cannavo & Cejka 2014). In human cells CTIP is responsible for stimulating the nuclease activity of MRE11 in this way (Sartori et al. 2007). Resection from the nick is carried out by MRE11 exonuclease activity and is accelerated through its interaction with exonuclease 3'-5' Domain Containing 2 (EXD2), which is then followed by more extensive resection carried out by exonuclease 1 (EXO1) and DNA2 to generate ssDNA tails proximal to the break site (Zhu et al. 2008; Mimitou & Symington 2008; Nicolette et al. 2010; Broderick et al. 2016). For resection of DNA to be efficient, the nucleases require the helicase function of BLM and WRN to unwind DNA (Zhu et al. 2008; Nimonkar et al. 2011; Mimitou & Symington 2008; Sturzenegger et al. 2014). The ssDNA generated is then coated by replication protein A (RPA). The recombination mediator breast and ovarian cancer susceptibility protein 2 (BRCA2) proceeds to replace the RPA coating with the recombinase Rad51, creating the active Rad51-coated nucleoprotein filament known as the presynaptic filament (San Filippo et al. 2008). This filament then captures double stranded DNA and identifies a region of homology, resulting in the formation of a D-loop structure (Sung 1994). The strand invasion and subsequent DNA replication result in the formation of a DNA crossover intermediate, known as a double Holliday junction (dHJ), between the two chromatids. dHJs can be resolved by two separate mechanisms, either through dissolution or resolution (**Figure 2**) (Bizard & Hickson 2014; Wyatt & West 2014). The resolution of dHJs results from the nicking of the junction by nucleases, followed by the religation of the duplexes. This can lead to both crossover and non-crossover products depending on how cleavage takes place (Matos & West 2014). On the other hand, dHJ dissolution results exclusively in non-crossover events (Karow et al. 2000; Bizard & Hickson 2014).

The dissolution of a dHJ requires branch migration of the junctions, carried out by Sgs1 (human BLM) with the topoisomerase Top3 (human TOP3A) and additional stimulation from Rmi1 (human RMI1). Branch migration results in a hemicatanane, which can be removed by Top3 decatenation, stimulated by Rmi1, thus producing non-crossover recombination products (Cejka, Plank, et al. 2010; Cejka et al. 2012)

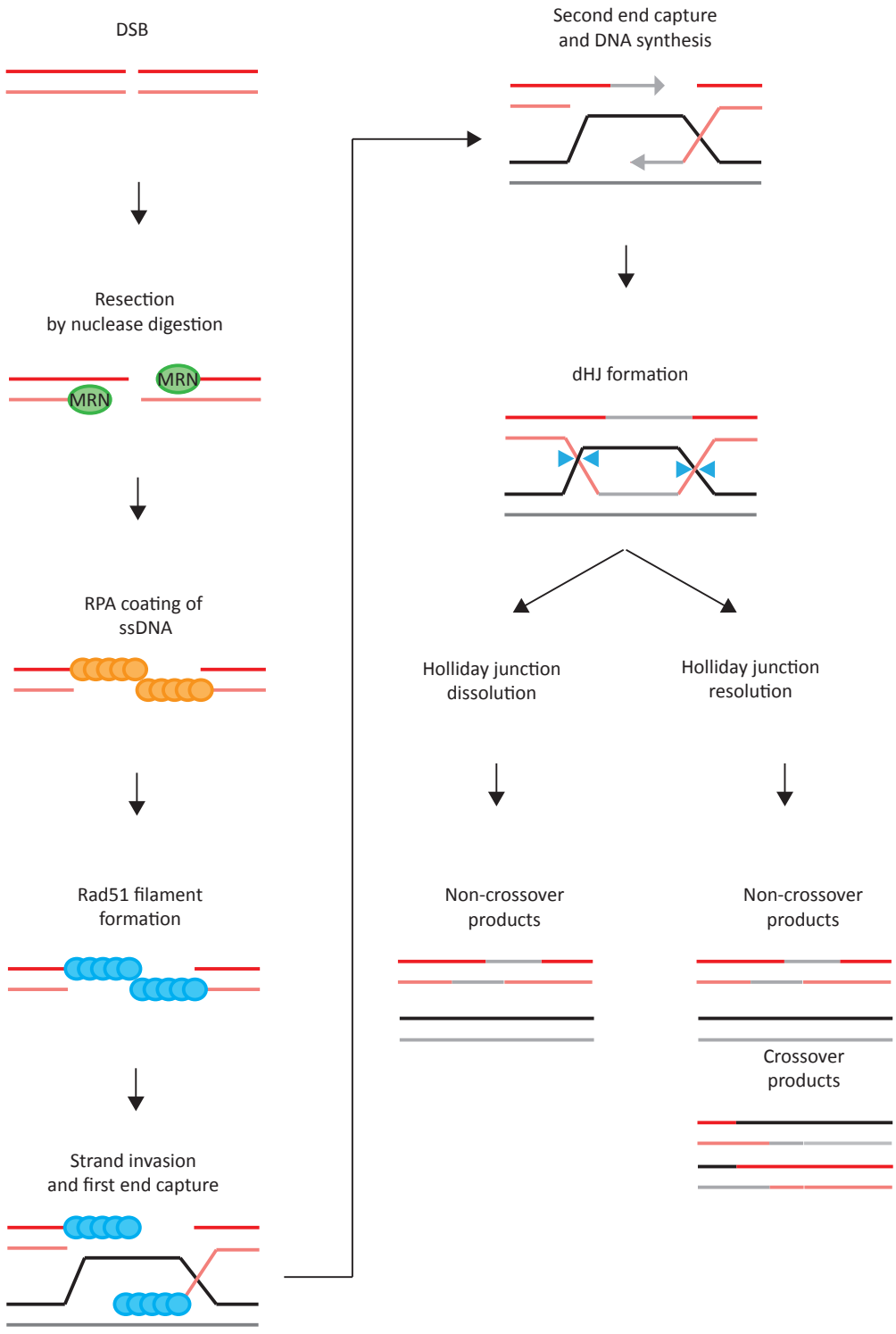


Figure 1. Schematic illustrating DSB repair through homologous recombination.

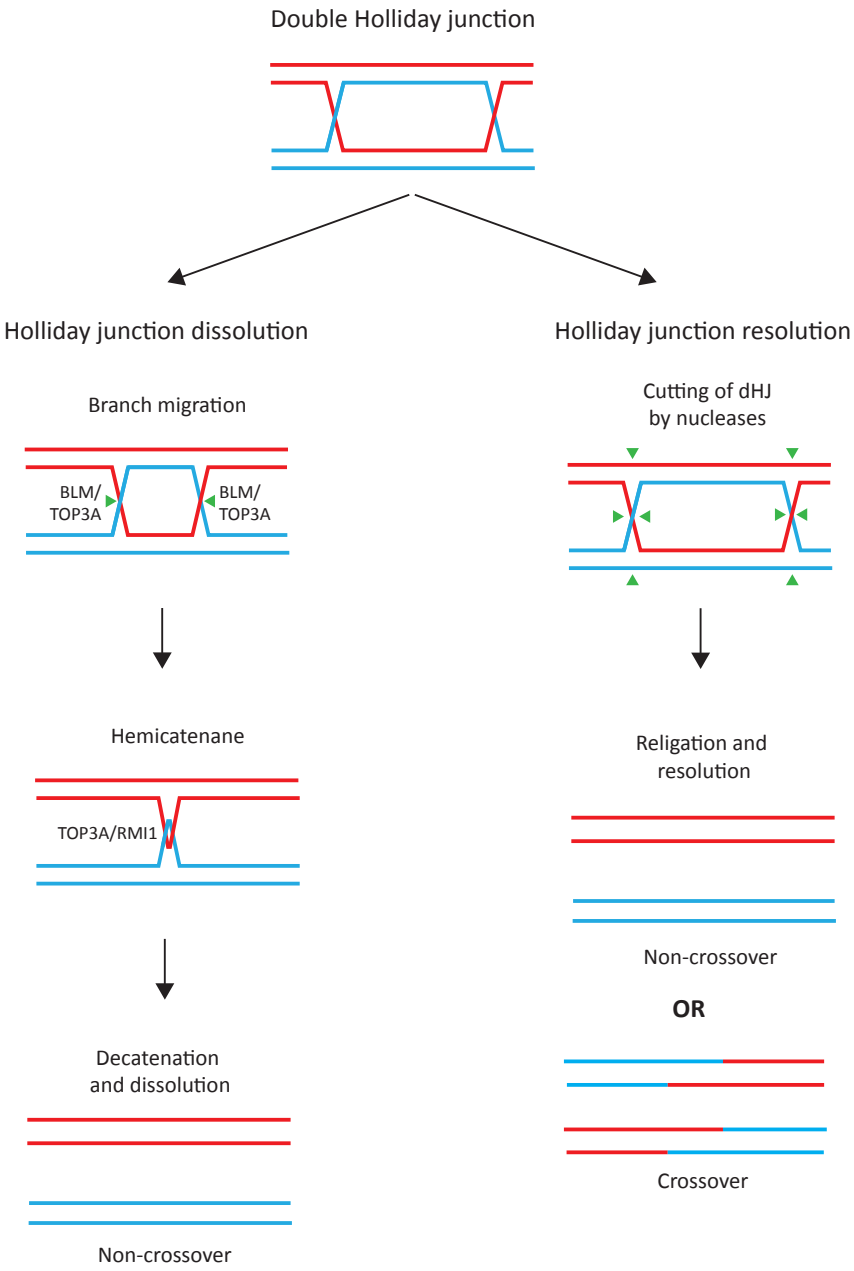


Figure 2. Schematic illustrating the dissolution and resolution of double Holliday junctions

1.3 PIKKs, the DNA damage response and associated diseases

Central to signalling DNA damage and facilitating repair are the protein kinases ataxia telangiectasia mutated (ATM), ataxia telangiectasia and Rad3 related (ATR) and DNA-PKcs. These three kinases all belong to the phosphoinositide 3-kinase-related (PIKK) family of kinases, and are all highly conserved (Blackford & Jackson 2017). As pivotal components of the DDR, these kinases all work within signalling cascades often considered to consist of sensors, transducers and effectors (**Figure 3**) (Maréchal & Zou 2013). In this simplified model, DNA damage is detected by sensor proteins. The signal is then transmitted to transducers, which propagate the signal further to effector proteins, leading to the activation of the checkpoint. Mediators are responsible for supporting the propagation of the signal. In some cases the interaction with the mediator is required for full activation of the signalling cascade (Niida & Nakanishi 2006; Houtgraaf et al. 2006).

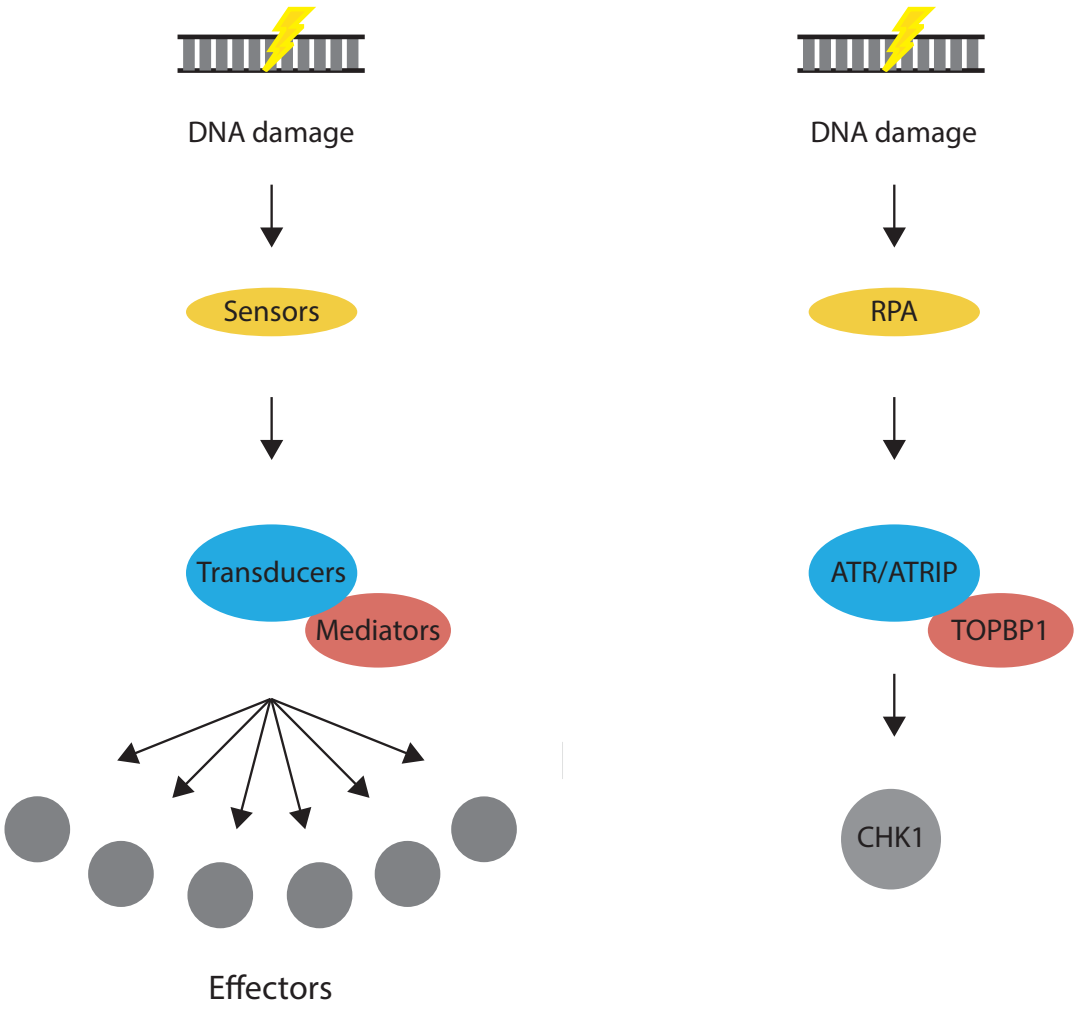


Figure 3. Left - schematic of a simplified representation of the DDR signalling cascade, right – schematic of the backbone of the ATR signalling cascade as an example of DDR signalling.

The efficient recruitment of ATM, ATR and DNA-PKcs to damaged DNA is dependent upon binding to a stable binding partner; these are the MRE11-RAD50-NBS1 (MRN) complex, ATR interacting protein (ATRIP) and Ku70/80 heterodimer for ATM, ATR and DNA-PKcs respectively (Cortez et al. 2001; Ciccia & Elledge 2010; Gottlieb & Jackson 1993). There is evidence from work with DNA-PKcs and Ku70/80 that the binding partners may change the confirmation of the kinase, making the kinase domain accessible to substrates (Spagnolo et al. 2006). Post-translational modifications may also impact upon the activity of PIKKs. Loss of acetylation of the ATM-FACT domain renders the kinase unable to become fully activated in the presence of DNA damage, despite not affecting its basal activity (Jiang et al. 2006; Sun et al. 2007).

While ATM and DNA-PKcs primarily respond to DSBs, ATR is activated by the presence of ssDNA. As ssDNA is a by-product of DNA replication and is present primarily during S-phase, ATR activity predominantly occurs during this cell cycle phase (Saldivar et al. 2017). Interestingly, in *Xenopus laevis* egg extracts the level of ssDNA generated dictates the level of ATR activation, suggesting there may be a threshold for ATR activation (Byun et al. 2005).

1.3.1 PIKK domain structure

When the PIKKs become active through the detection of DNA damage, the kinases preferentially target and phosphorylate serine or threonine residues that are followed by a glutamine (SQ/TQ sites) (Kim et al. 1999; O'Neill et al. 2000). Although ATR, ATM and DNA-PKcs are generally thought to phosphorylate different downstream targets

there is evidence suggesting some overlap between targets can occur in certain situations (Jazayeri et al. 2006; Gatei et al. 2003).

ATR, ATM and DNA-PKcs all contain a conserved C-terminal domain structure, critical to maintain kinase function (**Figure 4**). This domain structure is made up of a FRAP-ATM-TRRAP (FAT) domain, a PIKK regulatory domain (PRD) and a FAT-C-terminal (FACT) domain flanking the kinase domain (Bosotti et al. 2000; Jiang et al. 2006; Mordes et al. 2008). Although all three kinases contain a PRD, the sequence of this domain is not conserved. This results in the kinases having specificity for binding of their unique mediator protein, directing the kinase towards specific substrates (Mordes et al. 2008). Downstream of the FACT domain follow a varying number of Huntingtin, Elongation factor 3, A subunit of protein phosphatase 2A and TOR1 (HEAT) repeats, thought to facilitate protein-protein interactions between the kinase and its substrates (Perry & Kleckner 2003).

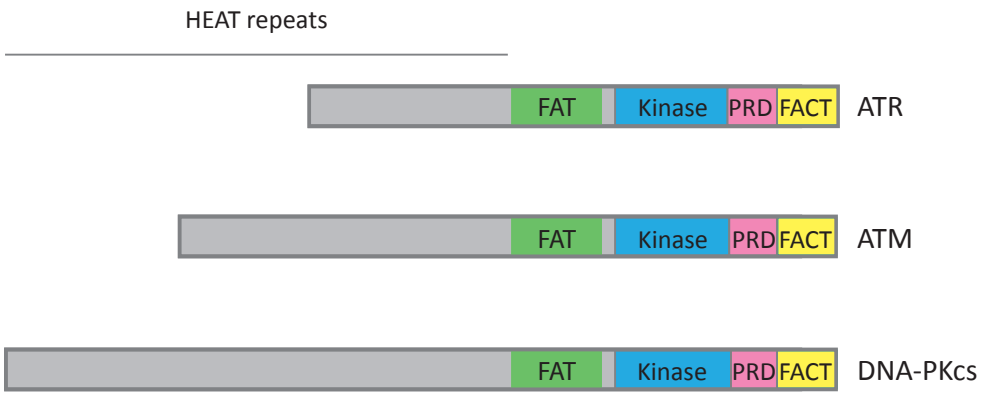


Figure 4. Schematic showing ATR, ATM and DNA-PKcs with their shared protein domains.

1.3.2 PIKKs and disease

As a properly functioning DDR is essential for maintaining genome integrity, it comes as no surprise that disruption of the DDR is closely linked to disease (Jackson & Bartek 2009). A number of congenital diseases are associated with the mutation of proteins acting within the DDR. Examples include Seckel syndrome, Bloom syndrome, Werner syndrome and Ataxia telangiectasia (**Table 1**) (Kerzendorfer & O'Driscoll 2009; Bachrati & Hickson 2008). These syndromes share many clinical and cellular phenotypes, indicative of roles in related cellular pathways. Characteristic of several of these diseases is growth defects, observed in ataxia telangiectasia, Bloom syndrome, Fanconi anaemia and Seckel syndrome. In addition, sufferers often display immunological defects and an increased susceptibility to cancer (Ciccia & Elledge 2010).

Syndrome	Causative gene	Repair pathway affected	Phenotypes			
			Cancer	Microcephaly	Growth defects	Other
Bloom syndrome	*BLM*	HR,	++	+	+	Hypersensitivity to sunlight
Werner syndrome	*WRN*	HR, BER	+	-	+	Premature aging
Rothmund-Thomson	*RecQ4*	BER	+	-	+	Skin and skeletal defects
Seckel syndrome	*ATR*	DSB repair, DNA damage signalling	-	+	+	Facial dysmorphisms
Ataxia telangiectasia	*ATM*	DSB repair, DNA damage signalling	+	-	-	Cerebral ataxia Mental retardation
Nijmegen breakage syndrome	*NBS1*	DSB repair, DNA damage signalling	+	+	+	Immunodeficiency
Cockayne syndrome	*CSA, CSB*	TC-NER	-	+	+	Neurodegeneration
Fanconi anaemia	FA complementation group	ICL repair, HR	+	-	+	Bone marrow failure

Table 1. Examples of diseases caused by defective DNA damage responses, highlighting similarities in clinical phenotypes. Adapted from Ciccia & Elledge 2010.

Interestingly, of all the PIKKs involved in the DDR, ATR is the only one essential for life. In fact, depletion results in early embryonic lethality in animals and apoptosis in cultured cells (Brown & Baltimore 2000; De Klein et al. 2000; Cortez et al. 2001). The shattered chromosomes observed in ATR-deficient mouse embryos emphasises the importance of ATR in maintaining genome stability (Brown & Baltimore 2000). Hypomorphic mutation of ATR gives rise to Seckel syndrome in humans, characterised by intrauterine growth retardation, severe proportional short stature and microcephaly (De Klein et al. 2000; O'Driscoll et al. 2003). Evidence suggests that the marked microcephaly and dwarfism associated with the syndrome is consistent with substantial cell death during embryonic proliferation and indeed somatic cell propagation (O'Driscoll et al. 2004)

Genomic instability is also hallmark of cancer cells, and DDR proteins are frequently found to be mutated in cancers (Jeggo et al. 2016). In fact, the most frequently inactivated gene in human cancer is *TP53,* the product of which is known to function in the checkpoint response to DSBs (Hollstein et al. 1991; Halazonetis 2004). It is thought that the DDR could play a dual role in cancer development. In early pre-cancerous lesions, the DDR pathways may protect against tumour progression, becoming activated by replication stress caused by oncogenic transformation. This leads to senescence or apoptosis in affected cells, hence containing cancer development. Over time, this will result in a selective advantage for cells with mutations in the DDR, eventually leading to cancer growth (Bartkova et al. 2005; Bartek et al. 2007; Gorgoulis et al. 2005). However, this will also mean that cancer cells become overly reliant on a second repair mechanism to maintain genome stability. With increased understanding of the DDR network, the reliance of the cancer on a second pathway can be exploited to induce synthetic lethality

exclusively in the cancerous cells of a patient (O'Connor 2015). This approach is currently being used in the clinic, taking advantage of the sensitivity of BRCA1 and BRCA2 mutated cancers to the inhibition of poly(ADP-ribose) polymerase (PARP) (Lord & Ashworth 2017; Helleday 2011)

1.4 ATR signalling pathway

ATR is the major responder to DNA damage and replication stress during S-phase. It responds to DNA damage caused by a broad range of damaging agents, including UV radiation, inhibition of DNA polymerase, topoisomerase poisons, depletion of the deoxyribonucleoide pool, among others. All these genotoxic agents cause the slowing or stalling of the DNA polymerases, thereby disrupting DNA replication (Saldivar et al. 2017). The activation of ATR requires the independent assembly and recruitment of multiple protein complexes to DNA (Byun et al. 2005; Melo et al. 2001). Once initiated, the ATR signalling cascade results in the phosphorylation of numerous other proteins, and the inhibition of DNA replication and progression to mitosis (Saldivar et al. 2017). Thus, activation of ATR promotes DNA repair, but can also signal towards senescence and apoptosis (Toledo et al. 2008; Maréchal & Zou 2013).

1.4.1 Sensing and signalling DNA damage

Essential to ATR function and recruitment to chromatin is its interaction with its binding partner ATRIP, first identified by Elledge and colleagues (Cortez et al. 2001). This study determined that ATRIP is required for ATR stability, and vice versa, demonstrating that the two are mutually dependent biding partners. The C-terminal end of ATRIP was found

to facilitate the interaction with ATR (**Figure 5**), and disruption of the interaction prevents both ATR and ATRIP from localising to sites of DNA damage (Ball et al. 2005; Melo et al. 2001).

ATR activation is dependent on its recruitment to damaged DNA. Crucial in this process is the coating of ssDNA by the ssDNA-binding protein complex RPA, first purified and identified as a ssDNA binding protein in simian virus 40 (SV40) (Wold & Kelly 1988). The interaction between ssDNA and RPA facilitates the recruitment of ATRIP via its checkpoint protein recruitment domain (CRD) (Ball et al. 2007). The recruitment of ATR to chromatin by this mechanism is required for ATR activation and phosphorylation of chromatin-bound ATR substrates (Ball et al. 2005; Zou & Elledge 2003).

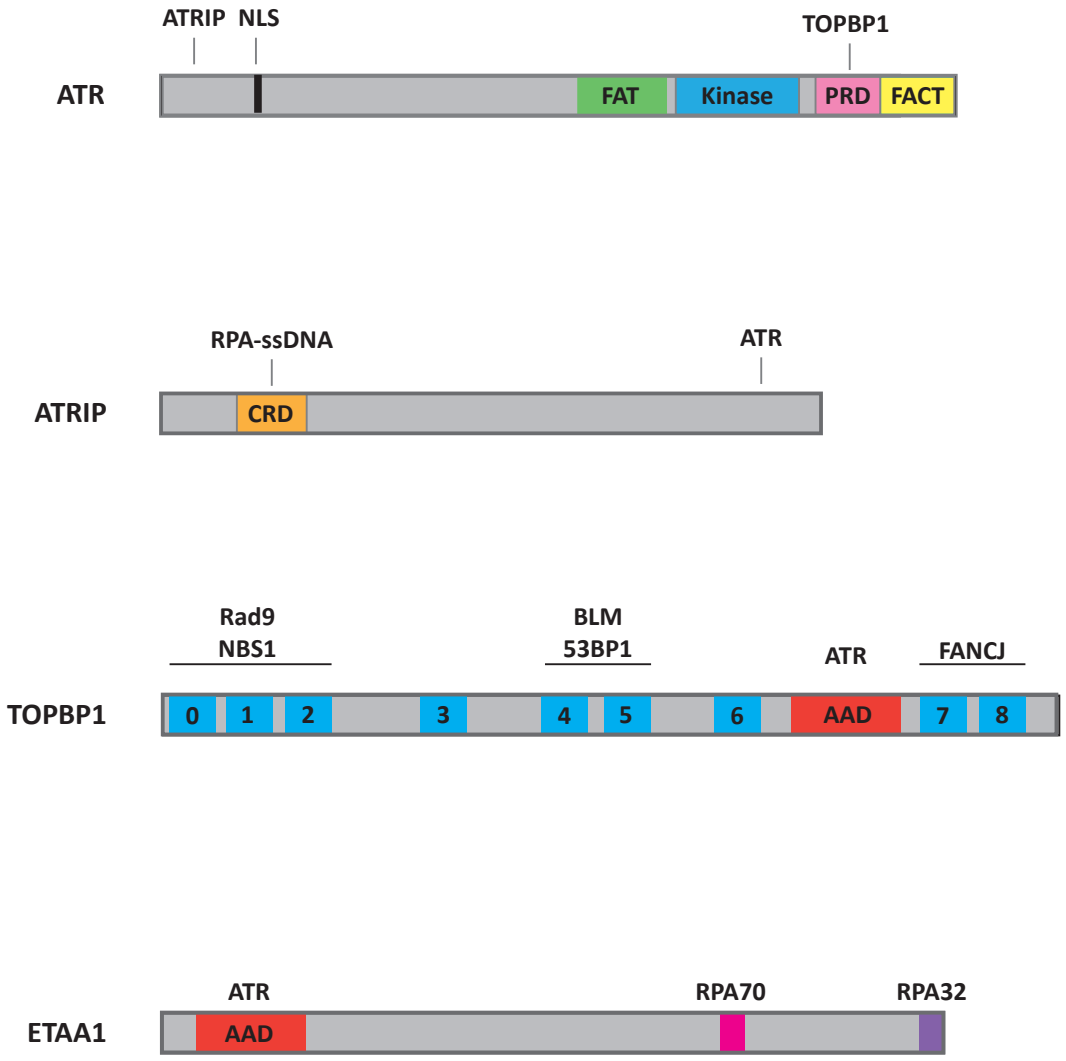


Figure 5. Schematic showing the protein domains of ATR and its binding partners. Indicated above each protein are additional interactions mediated by each protein.

ATR activity can be triggered by the ssDNA generated when the DNA replicative helicase MCM2-7 uncouples from the DNA polymerase. The uncoupling of the helicase and replicative polymerase can occur as a result of encountering lesions produced by clastogens such as UV-radiation or hydroxyurea (HU), resulting in stretches of ssDNA at the replication fork (Byun et al. 2005; Sogo et al. 2002). The ssDNA present at the replication fork functions to elevate the checkpoint response, with 800bp of ssDNA being sufficient to trigger phosphorylation of checkpoint kinase 1 (CHK1) by ATR. Additional unwinding increases the strength of the response, perhaps by facilitating the recruitment of multiple kinase complexes (Byun et al. 2005). This close link between DNA replication and ATR activation is further confirmed by the finding that depletion of MCM2-7 results a diminished S-phase checkpoint response (Cortez et al. 2004; Tsao et al. 2004).

In addition to the presence of RPA-coated ssDNA and the recruitment of ATR-ATRIP to damaged DNA, several other protein complexes are required to be present at DNA for the full activation of the S-phase checkpoint. These complexes are the Rad9-Rad1-Hus1 (911) checkpoint clamp and the Rad17-replication factor C (RFC) clamp loader (Melo et al. 2001). Following DNA damage, the 911 complex is recruited to the single strand/double strand DNA (ss/dsDNA) junction at the replication fork by the Rad17-RFC loading clamp by a mechanism similar to the loading of PCNA by the RFC clamp loader (Rauen et al. 2000; Zou et al. 2002; Bermudez et al. 2003; Majka, Binz, et al. 2006). Localisation of the 911 complex requires the interaction between Rad17 and 911, and occurs in parallel to and independently of ATR-ATRIP recruitment (Kondo et al. 2001; Melo et al. 2001; Zou et al. 2002). The presence of Rad17 is required for the

phosphorylation of ATR target CHK1, providing further evidence that both 911-Rad17-RFC and ATR-ATRIP have to be present at damaged DNA to ensure full activation of the S-phase checkpoint (Zou et al. 2002). In addition to the recruitment of the 911-complex, Rad17 has been identified as an interaction partner of MCM7. This provides a role for the replicative helicase in checkpoint activation beyond its role in generating ssDNA at the replication fork (Tsao et al. 2004; Cortez et al. 2004).

In addition to the accumulation of RPA-coated ssDNA, some DNA synthesis is also required for efficient phosphorylation of ATR downstream targets, including Rad1 and CHK1 (MacDougall et al. 2007). Full inhibition of the polymerase activity of Polα results in the presence of RPA-ssDNA but no checkpoint response as seen by phosphorylation of ATR target CHK1 (Byun et al. 2005; Michael et al. 2000). This observation could be due to the synthesis and elongation of primers on the unwound ssDNA, generating multiple ss/dsDNA junctions. The additional junctions could act as substrates for the loading of the 911-complex by Rad17. In this way, primer synthesis at stalled forks could provide a possible mechanism to amplify the checkpoint response (Majka, Niedziela-Majka, et al. 2006; Van et al. 2010; MacDougall et al. 2007; Giannattasio & Branzei 2017).

1.4.2 Activating ATR through TOPBP1 and ETAA1

In addition to its recruitment to chromatin, ATR requires the stimulation by a mediator protein for full kinase activity. So far, two ATR mediators have been identified in higher organisms; DNA topoisomerase II binding protein 1 (TOPBP1) and Ewing's tumour-associated antigen 1 (ETAA1) (**Figure 5**) (Kumagai et al. 2006; Bass et al. 2016; Haahr et

al. 2016; Lee et al. 2016). It remains unclear why the cell requires two ATR activators, however, there is evidence to suggest that ETAA1 and TOPBP1 act in distinct, parallel pathways (Bass et al. 2016; Haahr et al. 2016). It is possible that ETAA1 and TOPBP1 activate ATR in response to different stresses, direct ATR towards different targets or increase the strength of the ATR response to damage.

Both TOPBP1 and ETAA1 contain an ATR activating domain (AAD) which interacts directly with the ATR PRD. The AAD is required to stimulate ATR activity towards its downstream targets (Kumagai et al. 2006; Mordes et al. 2008). A recent structural analysis of ATR-ATRIP demonstrated that the complex forms a dimer, however, the determined structure exhibited a closed confirmation where the kinase domains remained inaccessible. It has therefore been suggested that the binding of TOPBP1 or ETAA1 is required for the ATR-ATRIP dimer to undergo a conformational change and assume its active form (Sawicka et al. 2016; Mordes et al. 2008; Saldivar et al. 2017).

The association of TOPBP1 to ATR and TOPBP1 stimulation of ATR activity requires a further interaction between TOPBP1 and ATRIP. Loss of the interaction between TOPBP1 and ATRIP results in the failure of TOPBP1 to associate either ATR or ATRIP, hence failing to activate the S-phase checkpoint (Mordes et al. 2008; Ball et al. 2005). Furthermore, recent work has established RHINO as an interaction partner of TOPBP1 (Cotta-Ramusino et al. 2011). This interaction between TOPBP1 and RHINO is also required for ATR signalling.

TOPBP1 and ETAA1 do not share sequence similarities beyond their AAD domain, suggesting that the proteins utilise different mechanisms to activate ATR signalling (Feng et al. 2016; Haahr et al. 2016; Bass et al. 2016). It has been suggested that TOPBP1 may serve as the major ATR activator, as disruption of the AAD of TOPBP1 is embryonically lethal in mice, whereas disruption of ETAA1-AAD does not significantly alter the growth of human cells (Zhou et al. 2013; Bass et al. 2016; Cescutti et al. 2010). However, it is notable that TOPBP1 plays numerous additional roles in DNA metabolism, and the role of the TOPBP1-AAD in these functions has not been thoroughly explored (Wardlaw et al. 2014).

It is thought that the ATR mediators are recruited to DNA damage separately of ATR-ATIRIP. ETAA1 contains two unique RPA binding sites, allowing for its direct recruitment to sites of DNA damage (Bass et al. 2016; Haahr et al. 2016; Lee et al. 2016). Earlier work proposed that TOPBP1 is recruited to chromatin by the 911 complex (J. Lee et al. 2007). However, this possibility is now disputed as mutation of the residue of Rad9 facilitating TOPBP1 interaction does not affect TOPBP1 localisation to chromatin or ATR activity towards targets beyond CHK1 (Lee & Dunphy 2010; MacDougall et al. 2007). Recent work has established an interaction between the MRN complex and TOPBP1 (Duursma et al. 2013). MRN has been shown to recruit TOPBP1 to ss/dsDNA junctions, providing a possible mechanism for TOPBP1 recruitment. However, this finding is also controversial as it concludes that TOPBP1 recruitment is dependent on BRCT 3-6, whereas a second study found that BRCT 1-2 of TOPBP1 is required for the formation of nuclear foci (Cescutti et al. 2010; Duursma et al. 2013). It has been proposed that mediator of DNA damage checkpoint protein 1 (MDC1) may interact with TOPBP1

BRCT1-2, thus providing another possible mechanism for TOPBP1 recruitment to chromatin (Blackford et al. 2015). However, also this has been disputed, as MDC1 has also been found to interact with TOPBP1 BRCT 4-5 (Wang et al. 2011). Therefore, the mechanism of recruitment of TOPBP1 to chromatin remains elusive.

In addition to its AAD domain TOPBP1 also contains 9 BRCA1 C-terminus (BRCT) domains. These domains specifically recognise and bind phosphorylated serine or threonine residues of other proteins (Manke et al. 2003; Yu et al. 2003). Working in tandem, the BRCT domains of TOPBP1 facilitate a large number of phospho-protein interactions, including interactions with Rad9 via BRCT1-2, 53BP1 and BLM via BRCT4-5 and FANCJ via BRCT7-8 (Delacroix et al. 2007; Cescutti et al. 2010; Gong et al. 2010; Blackford et al. 2015). Consistent with this, TOPBP1 was found to co-localise with Rad9, BRCA1, NBS1 and 53BP1 following DNA damage (Mäkiniemi et al. 2001; Yamane et al. 2002). This suggests that TOPBP1 can act as a scaffold, facilitating the checkpoint response. In support of this, disruption of the phosphorylation of Rad9 at S387 results in abrogation of TOPBP1-Rad9 interaction and an S-phase checkpoint defect (Roos-Mattjus et al. 2003; St. Onge et al. 2003; Delacroix et al. 2007; J. Lee et al. 2007). The interaction between TOPBP1 and the 911-complex is thought to be mediated by Rad17, demonstrating that multiple complexes are linked by a number of interactions to facilitate ATR activation (Lee & Dunphy 2010).

Interestingly, the TOPBP1 interaction with NBS1 may provide a second mechanism for ATR activation in the context of DNA resection. The MRN complex may recognise RPA-coated ssDNA through NBS1. In turn, NBS1 is then proposed to recruit TOPBP1, resulting

in the activation of ATR-ATRIP and the phosphorylation of RPA at S33 (Shiotani et al. 2013; Yoo et al. 2009). This activation of ATR requires the interaction of NBS1 with RPA and loss of this interaction results in failure to recover collapsed forks, implying that activation of ATR by NBS1 is central to repair of DSBs associated with replication (Shiotani et al. 2013).

1.4.3 Propagating the signal to ATR targets

Activated ATR is responsible for the targeted phosphorylation of many checkpoint proteins, hence propagating the signal of DNA damage. One ATR target, CHK1, was first identified as a checkpoint protein in fission yeast where it was found to be phosphorylated in response to a wide range of DNA damaging agents (Walworth & Bernards 1996; Q Liu et al. 2000). Loss of CHK1 is in itself embryonically lethal at the preimplantation stage in mice and causes defects in proliferation of ES cells (Q Liu et al. 2000). These findings emphasise the importance of the maintenance of the ATR signalling cascade.

CHK1 is commonly thought of as one of the main targets of ATR and the phosphorylation of CHK1 S345 is frequently used as a readout for ATR activation (Q Liu et al. 2000; Lopez-Girona et al. 2001). The phosphorylation of CHK1-S345 remains low during unperturbed replication, becoming phosphorylated in response to replication block (Feijoo et al. 2001). Mutation of CHK1-S345 to an alanine results in increased sensitivity to DNA damaging agents and loss of checkpoint related control of cell cycle progression following DNA damage in fission yeast, and is lethal in human cells (Lopez-Girona et al.

2001; Wilsker et al. 2008). This demonstrates the importance of CHK1 in checkpoint activity and maintenance of genome stability.

Once phosphorylated, the active CHK1 goes on to phosphorylate cell division cycle 25 c (CDC25C) at S216, inhibiting the phosphatase function of CDC25C (Sanchez et al. 1997; Peng et al. 1997; Furnari et al. 1997; Matsuoka et al. 1998). During unperturbed replication CDC25C dephosphorylates cyclin dependent kinase 1 (CDK1), allowing cell cycle transitioning to take place. However, when phosphorylated by CHK1, CDC25C is bound by the ubiquitously expressed 14-3-3 proteins and shuttled to the cytoplasm and degraded, resulting in a transient arrest of the cell cycle and full checkpoint activation (Sanchez et al. 1997; Peng et al. 1997; Dalal et al. 1999; Giono et al. 2017). This proposed mechanism provides a relatively simplistic view on the mechanisms involved in the arrest of the cell cycle by ATR signalling. Some controversy surrounds the involvement in CDC25C in mitotic entry, as contradictory results regarding the effect of CDC25C depletion on mitotic entry have been published (Lindqvist et al. 2005; Bulavin et al. 2003). It is likely that other members of the CDC25 family play a role in the control of mitotic entry. In fact, CHK1 has been suggested to also regulate CDC25A, thus preventing premature entry into mitosis (Chen et al. 2003). Evidence from human cell lines demonstrates that the depletion of CDC25A or CDC25B resulted in delayed entry into mitosis. Co-depletion of these two factors further prolonged this delay (Lindqvist et al. 2005). Interestingly, a study carried out in mice demonstrates that the loss of CDC25B and CDC25C does not adversely affect mitotic entry or DNA damage responses (Ferguson et al. 2005). Together these results suggest a complex mechanism for control of cell cycle transitioning following DNA damage.

In addition to interaction with ATR, activation of CHK1 requires an interaction with phosphorylated Claspin (Kumagai & Dunphy 2000; Kumagai & Dunphy 2003). Claspin has been shown to bind chromatin in an RPA-dependent manner (Lee et al. 2003). It is therefore possible that Claspin is responsible for bringing CHK1 into proximity of ATR, that is localised to chromatin by ATRIP. In support of this hypothesis, depletion of Claspin results in reduced phosphorylation of CHK1 (Kumagai et al. 2004). Once at chromatin, CHK1 is rapidly phosphorylated at S345 by ATR. The phosphorylation of CHK1 facilitates its dissociation from chromatin (Smits et al. 2006). Dissociation of CHK1 following DNA damage may allow CHK1 to interact with its downstream targets in order to propagate the DNA damage signal throughout the nucleoplasm and arrest the cell cycle.

1.4.4 ATR and CHK1 control late origin firing

It is vital that the genome is accurately replicated and replicated only once during each cell cycle. It is therefore essential that the use of origins and timing of origin firing is tightly controlled (Fragkos et al. 2015). ATR has been implicated in the control of late origin firing for a number of years. Findings in yeast demonstrated that the blocking of late origin firing was defective in cells carrying mutations of the *rad53* (CHK1/2 homologue) and *mec1* (ATR homologue) genes (Santocanale & Diffley 1998). The use of CHK1 inhibitors revealed that CHK1 depleted cells display a gradual change in the pattern of origin firing (Feijoo et al. 2001). Furthermore, inhibiting ATR and ATM in *Xenopus laevis* egg extracts resulted in excessive origin firing, particularly in early S-phase (Shechter et al. 2004; Marheineke & Hyrien 2004). The same was later

demonstrated in avian DT40 cells, where the inhibition of CHK1 or ATR/ATM resulted in the super-activation of replication factories and loss of the normal temporal replication programme (Maya-Mendoza et al. 2007). Additionally, depletion or loss of CHK1 or ATR has been demonstrated to result in reduced replication fork speed (Petermann et al. 2006; Eykelenboom et al. 2013). It was later shown that this phenotype could be reversed in CHK1 deficient cells by the simultaneous depletion of proteins promoting origin firing, suggesting that CHK1 is involved in regulating replication fork speed by controlling origin firing (Petermann, Woodcock, et al. 2010). These findings strongly support a role for the S-phase checkpoint in the control of late origin firing as well as timely replication progression.

Mechanistically, ATR and CHK1 involvement in the control of origin firing is thought to be tied to the role of the S-phase checkpoint in controlling cell cycle progression. Cell cycle progression is prevented through the inhibitory phosphorylation of CDKs by the tyrosine kinase WEE1 (Parker & Piwnica-Worms 1992; Watanabe et al. 1995). CDKs can then be activated by the phosphatase action of CDC25A. However, when the S-phase checkpoint is active the phosphorylation of CDC25A by CHK1 inhibits the phosphatase action of CDC25A, resulting in its rapid degradation and thus preventing cell cycle progression (Xiao et al. 2003; Molinari et al. 2000; Mailand et al. 2000). CDKs phosphorylate a number of substrates, including the TOPBP1 interacting protein Treslin (Sanchez-Pulido et al. 2010; Sansam et al. 2010). The phosphorylated Treslin interacts with TOPBP1 BRCT 1-2 to facilitate the loading of CDC45 to replication origins, thus regulating a pivotal step in the initiation of DNA replication (Kumagai et al. 2010; Sansam et al. 2010). Together these results demonstrate that ATR signalling through CHK1

prevents the firing of dormant origins by blocking the loading of CDC45, required for origin firing (Moyer et al. 2006).

1.5 BLM helicase and its role in DNA repair and the DDR

BLM belongs to the RecQ helicase family (Ellis et al. 1995). This is a family of helicases conserved from bacteria to humans, and members of this family play central roles in DNA metabolism. RecQ helicases are of particular interest as mutation or disruption of the helicases result in well recognised disorders such as Bloom syndrome, Werner syndrome and Rothmund-Thomson syndrome (Wu 2007; Bachrati & Hickson 2008).

1.5.1 BLM protein structure and protein partners

BLM is a 159 kDa protein, containing multiple recognisable domain structures at its C-terminal: a helicase domain, a RecQ carboxy-terminal (RQC) domain, and the helicase and RNase D C-terminal (HRDC) domain (**Figure 6**). The helicase domain facilitates unwinding of a variety of DNA structures in the 3'-5' direction. It does this with the support of the RQC domain, thought to contribute towards the binding of DNA (Croteau et al. 2014). As a helicase, BLM can efficiently unwind short DNA duplexes up to 71 bp in length. When interacting directly with RPA, this can be increased to over 200 bp (Brosh et al. 2000). WRN helicase, a second RecQ helicase, is also stimulated by RPA, suggesting this mechanism is conserved in this helicase family (Brosh et al. 1999). The HRDC of RecQ helicases direct the protein towards specific DNA structures (Wu & Hickson 2006). Differences in the HRDC sequence has been suggested to provide specificity of each helicase towards their particular roles in DNA metabolism (Bernstein

& Keck 2005). In addition to these domains, BLM contains a nuclear localisation signal at its C-terminus (Kaneko, Orii, et al. 1997). The N-terminus of BLM is required for its interaction with topoisomerase IIIα (TOP3A) and RecQ mediated genome instability (RMI)1 and 2 (Hu et al. 2001; Raynard et al. 2006; Chen & Brill 2007). The BLM-TOP3A interaction is important in regulating recombination in somatic cells (Hu et al. 2001). RMI1/2 stimulates TOP3A towards its role alongside BLM in DHJ dissolution (Raynard et al. 2008).

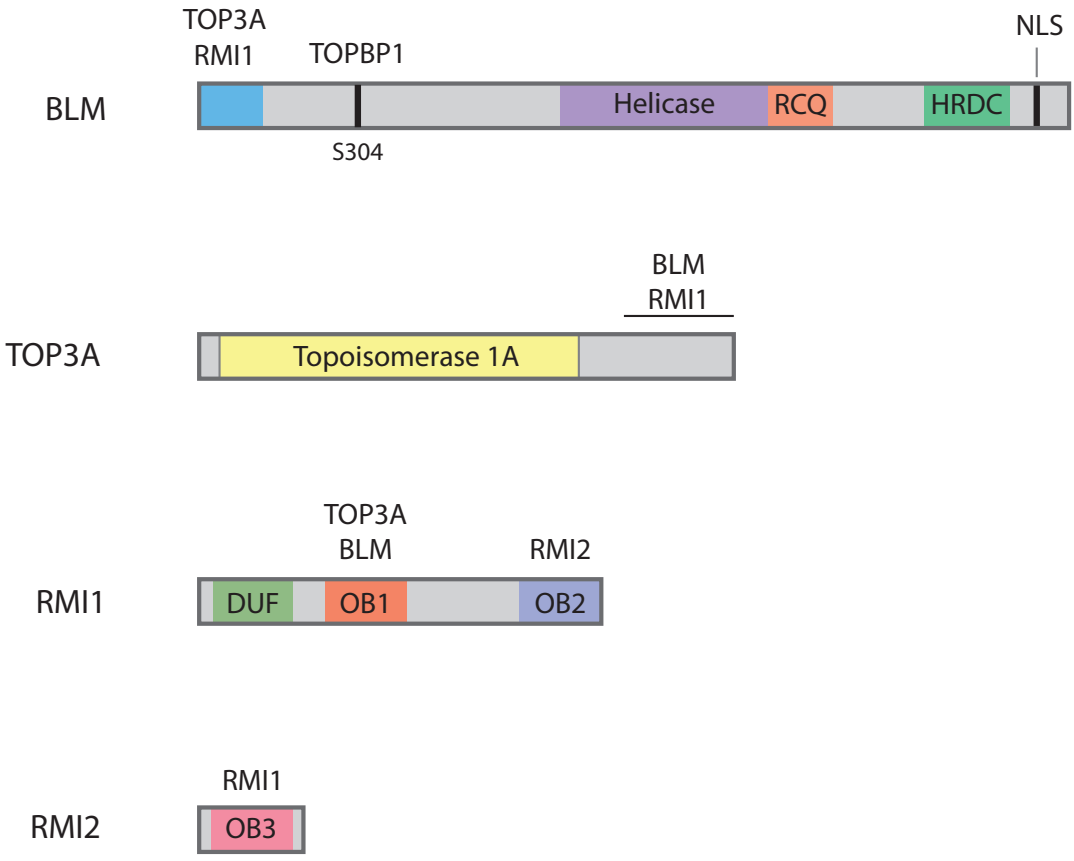


Figure 6. Schematic showing the protein domain structure of BLM and its interacting partners.

1.5.2 Bloom syndrome

Bloom syndrome is a rare autosomal recessive disorder caused by mutation in the *BLM* gene. The syndrome is characterised by facial abnormalities, microcephaly, sun sensitivity, infertility, immunodeficiency, stunted growth and predisposition to a variety of cancers (German 1993; Kaneko, Inoue, et al. 1997). A hallmark for Bloom syndrome is high levels of genomic instability, as seen by highly increased levels of sister chromatid exchanges (SCEs) in patient cells (Chaganti et al. 1974) The phenotype is unique to sufferers of Bloom syndrome, and is not seen in individuals with heterozygous mutation of the gene or in patients with other genome instability syndromes. The increase in SCEs is therefore used as a diagnostic tool to identify new Bloom syndrome patients (Kaneko, Inoue, et al. 1997; Chaganti et al. 1974).

1.5.3 BLM in DNA replication and repair

The helicase function of BLM is vital in maintaining genome stability through its involvement in HR (Ouyang et al. 2008). Evidence of this has been provided through the complementation of BLM deficient cells with wildtype BLM or helicase-dead BLM mutants (Neff et al. 1999). Only complementation with wildtype BLM could rescue the SCE phenotype of the BLM-deficient cells. Complementation with BLM can also partially rescue genome instability phenotypes in sgs1 (*S. cerevisiae* BLM homologue) mutant strains of *S. cerevisiae* (Neff et al. 1999). These findings demonstrate that the catalytic activities of BLM are evolutionary conserved and are important in maintaining genome integrity. Furthermore, the genome instability caused by defective BLM activity could underlie the broad range cancer susceptibility of Bloom syndrome patients.

The genomic instability observed in Bloom syndrome and in BLM deficient cells is telling of the multiple roles BLM plays in DNA replication, recombination and repair. BLM plays a prominent role in repair through HR, acting at multiple steps of the pathway. Consistent with this, Sgs1 levels in cells are at their highest in late S/G2-phases, when HR is taking place (Frei & Gasser 2000).

Coupled to nucleases such as DNA2, BLM facilitates the unwinding of DNA in a 3' – 5' direction, required for long-range DNA end-resection during HR (Gravel et al. 2008; Nimonkar et al. 2008; Sturzenegger et al. 2014). Furthermore, it is thought that RPA and the MRN complex stimulates this role of BLM (Nimonkar et al. 2011). In yeast it has been shown that Sgs1 binding partners Top3 and Rmi1 also contribute towards the stimulation of Sgs1 in resection (Cejka, Cannavo, et al. 2010). Additionally, BLM has been implicated in resection by EXO1, although its helicase domain is not required for this interaction (Nimonkar et al. 2008). Separate depletion of EXO1 or BLM did not result in a resection defect, suggesting that the two act in separate pathways (Gravel et al. 2008). BLM may therefore play a stimulatory but non-essential role in EXO1-mediated resection. Through its role in resection, BLM is involved in the generation of ssDNA, hence initiating repair by HR.

Secondly, BLM plays a key role in the dissolution of dHJ at the end stages of HR. Indicative of this is the elevated levels of SCEs in Bloom syndrome cells, thought to arise as a consequence of defects in tackling HR intermediates (Sonoda et al. 1999). In yeast, the depletion of either Sgs1 or Top3 results in the persistence of dHJs in yeast (Mankouri et al. 2011). In human cells, dHJs only persist when nucleases from the dHJ resolution

pathway are depleted alongside BLM, resulting in severe chromosomal abnormalities, indicating that BLM-deficient cells are dependent on the resolution pathway to remove dHJs (Wechsler et al. 2011). As dHJ resolution can result in both crossover and non-crossover events, the reliance of BLM-deficient cells on this pathway could explain the increased levels of SCEs observed.

1.5.4 The role of BLM in the S-phase checkpoint and the response to replication stress

Evidence from *S. cerevisiae* supports a role for Sgs1 in the S-phase checkpoint, as yeast strains lacking it are partially defective in the S-phase checkpoint response (Frei & Gasser 2000). Furthermore, a second study showed that depletion of Sgs1 results in hypersensitivity to DSB-inducing agents due to compromised DNA resection. The study went on to show that BLM functions in parallel to EXO1 in promoting resection and simultaneous depletion of both proteins renders U2OS cells unable to properly activate CHK1 (Gravel et al. 2008).

Some controversy is tied to the sensitivity of BLM to HU. Bloom syndrome patient cells have been shown to be hypersensitive to HU, whereas other BLM-deficient human cell lines did not display this phenotype (Davies et al. 2004; Lahkim Bennani-Belhaj et al. 2010). Findings from yeast demonstrate that RecQ helicase mutants confer sensitivity to replication inhibitors and fork stalling due to lack of nucleotide precursors (Bachrati & Hickson 2008). In addition, DNA fibre experiments in BLM deficient human cells have provided evidence for a role of BLM in replication fork restart and control of new origin firing following replication stress (Davies et al. 2007).

Although evidence from previous studies has pointed at a role for BLM in S-phase checkpoint activation, much of this has been centred around the role of BLM in HR. However, a study investigating the role of the yeast homologues of BLM, Sgs1 in checkpoint activation has revealed the helicase activity of Sgs1 is not required for stimulation of the checkpoint kinase Rad53p, suggesting that Sgs1 may play a dual role in maintaining genome stability (Bjergbaek et al. 2005). In support of this finding, more recently published work from two separate groups identified an interaction between BLM and TOPBP1, implicating BLM directly in the activation of ATR for the first time. Both groups identified BRCT4-5 of TOPBP1 as being the site of interaction with BLM, however the phosphorylated residue of BLM identified differed between the studies, one identifying S338 and the other S304 (Blackford et al. 2015; Wang et al. 2013).A recent study of the structure of the TOPBP1-BLM interaction supports a role for BLM-S304 rather than BLM-S338 in mediating the interaction (Sun et al. 2017).

1.6 Hypothesis and objectives

Because of the overlapping phenotypes between Bloom and Seckel syndromes, one can hypothesise that a putative role for BLM in ATR signalling may explain some of these similarities. Despite numerous studies reporting a link between BLM and the activation the S-phase checkpoint, little is known about the mechanism underlying the involvement of BLM in this process. Previous work has predominantly relied upon the use of cells depleted of BLM, either through mutation or gene silencing, and focussed on the role of BLM in HR, without examining the possibility of a direct role of BLM in ATR activation. Thus, the newly identified interaction between TOPBP1 and BLM could

shed new light on the mechanism underlying a role for BLM in ATR activation and control of the replication programme. The overall aim of this project is to address this hypothesis by focussing the objectives as follows:

- To determine if BLM plays a role in activating ATR signalling through its interaction with TOPBP1
- To determine whether BLM is involved in maintaining the DNA replication programme via its interaction with TOPBP1
- To generate tools to investigate the role of BLM in ATR activation in human cells
- To establish and build upon existing techniques to further investigate the role of BLM-TOPBP1 interaction in DNA end-resection and processing of collapsed replication forks

To address the final objective, EXD2 deficient cells was be used as a model to establish the techniques. The background, results and discussion of these results will be addressed separately in chapter 6.

2. Materials and methods

2.1 DT40 cell culture

The DT40 cell line is a chicken B-cell line which is derived from an avian leucosis virus-induced bursal lymphoma (Winding & Berchtold 2001). These cell lines are grown in Roswell Park Memorial Institute (RPMI) 1640 medium (Gibco, Thermo Fisher, cat no. 11875093), supplemented with 7% foetal bovine serum (Gibco, Thermo Fisher, cat no. 10270106), 3% chicken serum (Sigma, cat no. C5405) and 10μM β-mercaptoethanol (Sigma, cat no. M6250). Cell cultures were grown in a humidified incubator at 37°C with 5% CO_2. All cell lines were split daily to maintain confluency in the range of 5×10^5 and 2×10^6 cells/ml. Complemented DT40 cells lines were generated by Jadwiga Nieminuszczy (Blackford et al. 2015).

2.2 Human cell culture

HeLa, U2OS and RPE1 cell lines were grown in Dulbecco's Modified Eagle Medium (DMEM, Gibco, Thermo Fisher, cat no. 11965092) supplemented with 10% foetal bovine serum and 1% penicillin streptomycin (PenStrep, Gibco, Thermo Fisher, cat no. 15140122). Cell cultures were grown in a humidified incubator at 37°C with 5% CO_2. HeLa EXD2$^{-/-}$ cell lines were generated by Ronan Broderick and Jadwiga Nieminuszczy (Broderick et al. 2016). RPE1 BLM$^{-/-}$ were generated in collaboration with Carl Morrow and Samuel Jones from the Blackford lab, WIMM.

2.3 siRNA transfection

siRNA targeting BLM, BRCA2 or MRE11, as well as control siRNA targeting luciferase was used in this analysis. HeLa or U2OS cell lines were transfected with siRNA as follows; per transfection, 3μl 20μM siRNA stock, giving a final concentration of 25nM (siBLM Dharmacon, siLuciferase, siBRCA2 and siMRE11 LifeTechnologies) was combined with 90μl Opti-MEM (Gibco, Thermo Fisher, ca no. 31985070) and 12μl HiPrefect (Qiagen, cat no. 301705). The mixture was incubated at room temperature for 10 minutes. Cells were trypsinised and counted using a haemocytometer, and 500 000 cells were added to a single 6 cm dish per condition. The siRNA-HiPerfect mixture was added directly to the cell suspension and the final volume was topped with normal growth medium to a final volume of 2.4 ml. After 24 hours, a second pulse so siRNA was added directly to cells, using the same siRNA-HiPerfect mixture as above. After 48 hours cells were trypsinised and 300 000 cells were plated per well of a 6-well-plate. At 72 hours wells were labelled for DNA fibre or treated for checkpoint analysis as outlined below.

2.4 Complementation of human cells

2.4.1 Purification of BLM cDNA constructs

The BLM-WT and BLM-S304A constructs (in pEGFP-C3 plasmid, Clontech, **Figure 7**) were grown on from glycerol stocks of DH5α *Escherichia coli*, and expanded to a 200ml bacterial culture. The plasmids were purified by midi-prep (GenElute HP Plasmid Midiprep Kit, Sigma Aldrich, cat no. NA0200), and the final concentration determined by nano-drop.

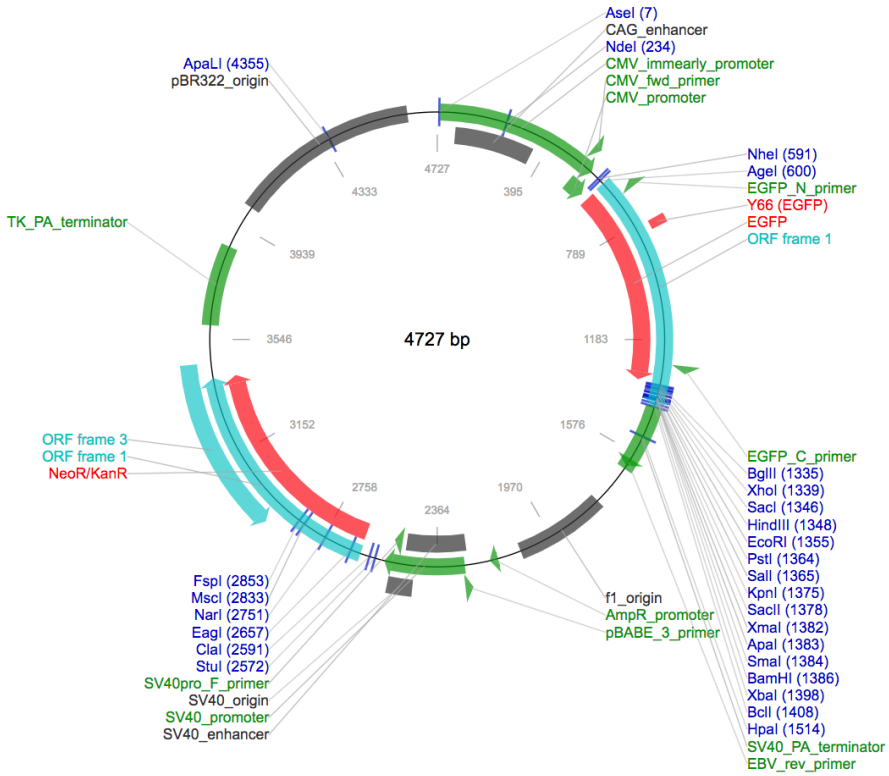


Figure 7. Vector map of plasmid used for the expression of BLM-S304A and BLM-WT in human cell lines, or BLM$^{-/-}$ -S251A, BLM$^{-/-}$ -WT, BLM$^{-/-}$ -S251A-AAD and BLM$^{-/-}$ - S251A-AAD-W1145R in DT40 cells (diagram by Addgene, https://www.addgene.org/vector-database/2489/).

2.4.2 Transfection of human cells

In order to obtain HeLa and RPE1 cell lines stably expressing either BLM-WT-GFP or BLM-S304A-GFP cDNA cells were split to be a 60% confluency at time of transfection. For a transfection in a 6-well-plate, growth medium was added to the cells to a final volume of 2ml.

Reagent	**Amount**
Opti-MEM	125μl
Lipfectamine 3000	1.5μl
P3000 reagent	3μl
DNA	1.5μg

Table 2. Reagents used for transfection of human cells with BLM-WT or BLM-S304A cDNA

Lipofectamine 3000 was diluted in Opti-MEM in an Eppendorf tube and vortexed for 3 seconds. DNA was diluted in Opti-MEM in a separate tube, before the addition of the P3000 reagent. The mixtures in the two tubes were then combined and incubated for 10 minutes at room temperature. The mixture was subsequently added to the cells. Cells were then placed back in the incubator for 24 hours. The BLM construct used in these experiments contain a geneticin resistance cassette, which is used to select transfected cells. After 24 hours, the growth medium was changed to medium containing geneticin at a final concentration of 500μg/ml (Thermo Fisher, Cat no 10131035). To ensure the selection was working, medium containing geneticin was added to a well containing untransfected cells. When there were no surviving cells in

the control well, transfected cells were trypsinised, resuspended in growth medium and sorted based on GFP positivity to 96-well-plates with the help of Kevin Clark at the WIMM FACS facility. The individual clones were then expanded. Individual clones were then harvested, washed twice in 2 ml cold PBS, resuspended in 2 ml cold PBS and screened for expression of the transgene by western blot and FACS.

2.5 CRISPR/Cas9 strategy and cell transfection

The CRISPR strategy to generate the BLM S304A point mutation in human cells was developed by Dr Andrew Blackford. The strategy to introduce the BLM S304A mutation is shown in **Figure 31**, and relies upon the cutting action of the CRISPR/Cas9 as outlined in (Ran et al. 2013). The vector pX330 (Addgene, cat no 42230) was used as the backbone for generating the CRISPR/Cas9 construct. The original Addgene vector had been modified to include a GFP tag on Cas9, allowing for rapid screening for successfully transfected clones by FACS. The guide RNAs were cloned into the pX330 vector using the protocol as described by Ran and colleagues. Briefly, the oligos encoding the two guide RNAs were phosphorylated and annealed using a thermocycler. The annealed oligos were introduced into the pX330-GFP plasmid through a digestion-ligation reaction, introducing the oligos into the vector at the *Bbs*I cut site of the vector (Fermentas, cat no ER1011). The ligation reaction was incubated at 37°C for 5 mins, then at 23 °C for another 5 minutes in a thermocycler, repeating this cycle a total of 6 cycles. The plasmid was treated with PlasmidSafe (Lucigen, cat no E3101K) exonuclease to prevent unwanted recombination products. The plasmid was transformed into competent DH5α *E. coli*, selecting colonies based on ampicillin resistance conferred by

the expression of the plasmid. Following midi-prep and purification as outlined in section 2.4.1, the plasmid was ready for transfection into cells.

To introduce the mutation at BLM S304A, a 200bp ssDNA template was introduced during the transfection of cells. This template contained the S304A mutation as well as a mutation introducing a novel restriction enzyme cut site, allowing for efficient screening. The transfection of cells was carried out using the same protocol as when complimenting human cells (**Table 2**), with the simple modification of adding 1μl of the ssDNA template at a concentration of 10μM to the DNA/Opti-MEM/P3000 mixture, giving a final concentration of the template of 5nM. 24h hours post-transfection cells were taken to FACS to sort of GFP positive cells, thus selecting only cells successfully transfected with the plasmid containing Cas9 and the guide sequences. The sorted cells were left to grow on for a week before FACS sorting again, this time for GFP negative cells. These cells will have lost the expression of Cas9, and there is no more cutting activity in these cells. GFP-negative cells were sorted to single cells in 96-well-plates. Once clones had expanded sufficiently, a portion of the cells were harvested for genomic DNA extraction. FACS sorting of cells was carried out with the help of Mr Kevin Clark from the WIMM FACS facility.

2.5.1 Verification of CRISPR/Cas9-generated cell lines

Cells were harvested from expanded clones and genomic DNA was extracted from the cells using the Qiagen DNA extraction kit (Qiagen, Cat no 158906, 158910). Following DNA extraction, DNA was rehydrated in 30ul of TE. PCR was then used to amplify the region of BLM where mutilations should be introduced, has the strategy been successful (**Table 3**, **Table 4**, **Table 5**). The polymerase used was Marathon (A&A Biotechnology SC, cat no. 1003-1000).

Primer name	**Sequence**
BLM-S304A PCR primer, forward	ACAGCAACAATTTGGGTTGTG
BLM-S304A PCR primer, reverse	GGACTTCATCTTTAGAATGCAACC
BLM-S304A sequencing primer	GGTGTGATTGTTTGTGACTTGC

Table 3. PCR and sequencing primers for the validation of in introduction of BLM-S304A mutation following CRISPR/Cas9 targeting

PCR mixture component	**Volume, μl (per reaction)**
Marathon polymerase	0.5
Marathon 2X buffer	12.5
dNTPs (10mM)	0.75
Primers (forward/reverse)	0.1
Template	0.5
Water	10.55
Total volume	25

Table 4. Reagent mixture used for PCR of CRISPR/Cas9 BLM-S304A targeted cell lines

PCR programme	Temperature (°C)/ time
Denature	98/20 sec
Denature	95/20 sec
Primer annealing	56/30 sec
Elongation	68/60 sec
Repeat steps 2-4 for an additional 34 cycles	
Final elongation	60/ 10 min
Hold at 4°C	

Table 5. PCR programme used to amplify the region surrounding BLM-S304

Following PCR, the fragment incubated with the enzyme Acu1 (NEB, Cat no R0641). 8ul of the PCR product was combined with 1µl of the enzyme, 1µl 10X CutSmart buffer, 0.5µl of S-adenosylmethionine (SAM). The mixture was incubated at 37°C for 1 hour. After digestion, 1ul of Orange DNA loading dye was added to 5ul of PCR product and run at 70V on a 1.2% agarose gel with a 1kb DNA ladder (Thermo Fisher, Cat no SM0312). The digested PCR product was visualised using a trans-illuminator.

2.6 Checkpoint analysis and western blotting

2.6.1 Treatment of cells for the investigation of checkpoint activation

Exponentially growing DT40 or human cells were treated with 100nM camptothecin (Sigma Aldrich, cat no. C9911) or 1mM HU (Sigma Aldrich, cat no. H8627) for the times

indicated prior to harvesting for western blot. In RPE1 checkpoint experiments ATR inhibitor (AZ20, Sigma Aldrich, SML1328) was added at 3μM, 30 minutes in advance of camptothecin or HU treatment.

2.6.2 Cell harvesting and western blotting

Human cells were harvested from 6-well-plates for western blotting by trypsinisation. For DT40 western blots, 1.5ml of exponentially growing cells was harvested. Cells were spun down at 4°C and 500g in a bench-top centrifuge. The resulting cell pellet was washed two times in ice cold PBS. The pellets were lysed in 1X sample loading buffer (SLB) (**Table 6**) at room temperature. The lysed pellets were vortexed to ensure complete lysis, before being heated to 100°C on a heat block for 5 minutes. The samples were vortexed and spun down at 3000g for 1 minute. The supernatant was transferred to fresh Eppendorf tubes, and the protein concentration of each sample was measured in triplicate using a nano-drop. 20μg of sample per sample was used for each blot, the samples were diluted with 1X SLB so all samples were of similar volumes. 2μl of 2X SLB with added bromophenol blue was added to each sample. Samples were vortexed, boiled for 5 minutes at 100°C and loaded to a 4-12% Bis-Tris protein gel (Invitrogen, cat no NP0321BOX, WG1402A) alongside a protein ladder (Cleaver Scientific, CSL-BBL). The gel was run in MOPS buffer (**Table 7**).

Following running, the blot was transferred to a PVDF membrane (GE Healthcare, cat no 10600023) in a chilled wet transfer tank at 90V for 90 minutes (**Table 8**). The membrane was the blocked in 5% milk in TBS-T for 1 hour. Excess milk was washed off in TBS-T before the incubation with primary antibodies overnight at 4°C (**Table 9**). The

following morning the primary antibodies were removed, and the membrane was washed three times for 10 minutes in TBS-T. The membrane was then incubated for one hour in the appropriate horseradish peroxidase-conjugated secondary antibody diluted in 5% milk in TBS-T (**Table 10**). The membrane was again washed in TBS-T three times for 10 minutes each. The membrane was then developed using a chemiluminescent HRP substrate (Millipore, cat no WBKLS0500) and X-ray films (SLS, cat no MOL7016). Following development, the membrane was thoroughly washed in TBS-T before re-probing with further primary antibodies. Each western blot was repeated in full a minimum of two times.

2.6.3 Quantification of western blots

Quantification of was performed using FIJI imaging software. For each protein analysed, measurements of the pixel density of each protein band were taken, making sure to maintain the identical measuring frame (area measured) across all bands. In addition, a background measurement for each band was taken, making sure to avoid marks on the film. The measurements were then inverted by subtracting the measured value from 255 (the value if all pixels were white). Then the background measurement was subtracted from the corresponding protein band measurement, leaving the intensity of the protein band only. The final quantification is given as a ratio of the intensity of the band of the protein of interest divided by the intensity of the loading control corresponding to that band.

2.6.4 Buffers for western blotting

Reagent	Volume for 40 ml	Final concentration
1 M Tris-HCL (pH 6.8)	2.5 ml	0.06 M
SDS, 20%	4 ml	2%
Glycerol	4 ml	2%
β-mercaptoethanol	2 ml	1%
Water	27.5 ml	-

Table 6. Recipe for sample loading buffer

Reagent	Amount	Final concentration (1X)
MOPS (3-(N-morpholino)-propane sulfonic acid)	104.6 g	50 mM
Tris base	60.6 g	50mM
SDS	10 g	3.5 mM
EDTA	3 g	1mM
Distilled water	Up to 500 ml final volume	

Table 7. Composition of 20X MOPS running buffer, diluted to 1X in distilled water

Reagent	Amount	Final concentration (1X)
Tris Base	29 g	12 mM
Glycine	144 g	96 mM
Distilled water	Up to 2 l final volume	

Table 8. Composition of 10X transfer buffer. Diluted to 1x in distilled water and 20% methanol

2.6.5 Antibodies for western blotting

Antibody	Dilution	Species	Supplier/Cat no
BLM	1:2000/5% milk in TBS-T	Rabbit	Bethyl/A300-110A
GFP	1:2000/5% milk in TBS-T	Mouse	Roche/11 814 460 001
MCM2-pS102	1:10000/5% milk in TBS-T	Rabbit	Bethyl/A300-094A
CHK1	1:1000/5% milk in TBS-T	Mouse	Santa Cruz/sc-8408
CHK1-pS345	1:1000/5% BSA in TBS-T	Rabbit	Cell signalling/133D3
RPA2	1:1000/5% milk in TBS-T	Mouse	Calbiochem/Ab-2
γH2AX	1:2000/5% milk in TBS-T	Mouse	Millipore/JBW301
p53	1:3000/5% milk in TBS-T	Mouse	Santa Cruz/ sc-126

Table 9. Primary antibodies used for western blotting

Immunoglobulins	Dilution	Species	Supplier/Cat no
HRP-conjugated Mouse	1:2000/5%milk in TBS-T	Goat	Dako/P0447
HRP-conjugated Rabbit	1:5000/5% milk in TBS-T	Goat	Dako/P0448

Table 10. Secondary antibodies used for western blotting

2.7 DNA fibre technique in DT40 cells

2.7.1 Labelling cells for DNA fibre

DT40 cells were split to 500 000 cell/ml and left to grow exponentially in normal growth conditions. Cell cultures were then pulse labelled for 20 minutes with 25μM 5-Iodo-2'-deoxyuridine (IdU, Sigma Aldrich, Cat no. I7125)) followed by labelling with 250μM 5-Chloro-2'-deoxyuridine (CldU, Sigma, C6891) for 20 minutes. Cells were harvested and spun down at 500g and 4°C, the pellet washed with cold PBS, and resuspended in PBS to a concentration of 1×10^6 cells/ml. 2μl of the cell suspension was placed onto a microscope slide (VWR), the droplet was left to evaporate slightly for 1 minute before the addition of 7μl of cell lysis solution (**Table 11**). Immediately following the addition of the lysis solution, the droplet was gently mixed and left for 2 minutes to ensure lysis and to allow for some evaporation from the droplet. The microscope slide was then left on an incline with the droplet at the top for the slide, allowing for the droplet to slowly move down the full length of the slide, leaving a trail of spread DNA fibres on the slide. Slides were left to dry at room temperature overnight.

Reagent	**Final concentration**
EDTA	50mM
SDS	0.5%
Tris-HCl (pH 7.5)	200mM

Table 11. Composition of DNA fibre lysis solution

2.7.2 Staining of DNA fibres

Slides were fixed in 3:1 methanol: acetic acid (Fisher scientific) for 10 minutes before washing 3 times in distilled water. Fibres were then denatured by submersion of slides in 2.5M HCl for 80 minutes, followed by three washes in PBS on a rocking platform for 5 minutes each. Excess PBS was removed by tapping slides on tissue paper. 50μl of blocking buffer (5% bovine serum albumin (Sigma) in PBS) was added to the slides and slides covered with a glass coverslip, ensuring the removal of any trapped air bubbles under the coverslips. Slides were incubated with the blocking agent for 20 minutes in a humidified chamber, preventing the coverslips from sticking to the slides. The primary antibodies are diluted in blocking buffer: anti-BrdU (rat- abcam) recognising CldU and anti-BrdU (mouse-BD bioscience) recognising IdU (**Table 12**). Following blocking, 50μl of the primary antibody dilution is added to each slide, covered with a glass coverslip and incubated in a humidified chamber for 2 hours. Following the incubation, the slides were washed 3 times in PBS on a rocker for 10 minutes per wash. Secondary fluorescent antibodies Alexa fluor 488 and Cy3 were diluted in blocking buffer. 50μl of the secondary antibody mixture was added to each slide, slides were covered with a coverslip and incubated in the humidified chamber for 1 hour. Slides were washed three times in PBS for 10 minutes and slides were mounted with a cover slip using Vectashield mounting medium (Vector Laboratories, H-1000).

2.7.3 Visualisation and quantification of fibres

DNA fibres were visualised using Zeiss LSM 510 Meta confocal microscope. Images were taken from randomly selected regions of untangled fibres from two slides per condition per repeat. The images were analysed using the FIJI software package. Each experiment

was repeated at least 3 times, and a minimum of 100 individual DNA fibres were scored per experiment when investigating frequency of replication structures. Track length data was measured from a minimum of 30 randomly selected DNA fibres per condition, or as many structures as possible. Results were presented as a ratio between the first and second label, or as the length of the second label only. Fork symmetry is presented as the ratio between the long and short arm resulting from a first origin firing event, as many events as possible were measured per experimental repeat. Statistics for tract length ratio and fork symmetry was calculated using the Mann-Whitney unpaired t-test. DNA fibre structures were counted and categorised as described. A minimum of 100 structures were counted per condition, per repeat. Statistics for replication structures were calculated using the Student's t-test. Statistics and graphs were generated using the GraphPad Prism 7 software package.

Primary antibody	Species	Dilution	Company/product code	Application
Anti-BrdU	Rat	1:400	Abcam/ab6326	DNA fibre
Anti-BrdU	Mouse	1:25	BD bioscience/347580	DNA fibre
Secondary antibody	**Species**	**Dilution**	**Company/product code**	**Application**
Alexa fluor 488	Anti-rat	1:400	Invitrogen/A-11006	DNA fibre
Cy3	Anti-mouse	1:500	Sigma Aldrich/C2181	DNA fibre

Table 12. Primary and secondary antibodies used for the staining of DNA fibres

2.7.4 Replication fork speed by DNA fibre

Measurement of the second (green) label of elongating forks acted as the basis for this calculation, providing the distance travelled by the replication fork over 20 minutes (the labelling time). To convert the measurement from μm to kb, the measured value was multiplied by 2.59, the estimated bases needed to make up 1μM of a DNA fibre tract (Jackson & Pombo 1998). This value was then divided by 20, to give fork speed in kb/min.

2.7.5 DNA fibre with drug treatments

When investigating replication fork restart, cells were treated with camptothecin at 2.5μM for 90 minutes alongside the first label as indicated in figure 13. Following the first label, cells were washed with growth medium containing 250μM CldU to remove the drug, before labelling with the second label for 15 minutes. Cells were then harvested and treated as above. For experiments investigating the response of ongoing replication to replication stress, HU was added to a final concentration of 200μM alongside the second label following 20 minutes labelling with the primary label. The inhibitor roscovitine (Sigma Aldrich, cat no. R7772-1MG) was added to cultures at a final concentration of 100μM for 1 hour before labelling and then maintained throughout the labelling.

2.8 DNA fibre in human cells

2.8.1 Labelling human cells under normal growth conditions

HeLa or RPE1 cells were plated to a 6-well-plate the day prior to labelling to give a confluency of 50% on the day of the experiment. Labelling was carried out as for DT40 cell cultures. Cells were then harvested by trypsinisation, and cells washed in cold PBS. Cells were then resuspended to a concentration of 6.5×10^4 cells/ml before spreading and staining as outlined for DT40 cells.

2.8.2 Treatment of human cell lines for DNA fibre

When investigating recovery from replication fork collapse HeLa cell lines were labelled with IdU as above for 20 minutes. Cells were then washed with warm growth medium, before cells were incubated with HU at the final concentration of 4mM for 4 hours. Cells were again washed with warm growth medium to remove the drug, before addition of CldU for 20 minutes as above. DNA fibres were spread, stained and visualised as before.

To investigate resection rates in HeLa cell lines, cells were labelled consecutively with IdU and CldU for 20 minutes as before. Following labelling cells were exposed to 4mM HU for 4 hours. DNA fibre spreading, staining and visualisation was carried out as before.

2.9 Sister chromatid exchange assay

BrdU was added to exponentially growing cells for 48 hrs (two cell divisions) in a 10cm tissue culture dish with 0.15μg/ml colcemid (Invitrogen, Thermo Fisher, cat no. 15212012) added for the final 4 hours before harvesting to enrich for mitotic cells. Medium and trypsinised cells were transferred to a tube and spun at 400g for 5 minutes. The pellet was resuspended in pre-warmed 75mM KCl and incubated at 37°C for 25 minutes. Cells were spun down at 400g for 10 minutes. KCl was removed, leaving 200μl in the tube to gently resuspend the pellet. 5ml of freshly prepared ice cold 3:1 methanol: acetic acid was added to the cells. The fixative is added dropwise for the first 3ml whilst gently vortexing. Cells were spun down at 400g for 10 minutes at 4°C. The fixative step was repeated an additional 2 times. The final pellet was resuspended in 300μl fixative. Cells were spread onto microscope slides by dropping a droplet of the cell suspension from a 200μl pipette onto a microscope slide held at arm's length and at a 45° angle.

Slides are left to dry on a slant overnight at room temperature. 5ml of fixative was added to the remainder of the cell suspension, and stored at 4°C.

To stain the DNA, slides were placed in a glass staining jar on a rocker and immersed in bisbenzimide (Sigma Aldrich, cat no. B1155-25MG), diluted in to a final concentration of 15μg/ml in water, for 30 minutes whilst protected from light. Slides were then washed in PBS. Slides were placed horizontally in a plastic box and immersed in PBS so the slides were just covered. The slides were then exposed to UVA light for 2 hours whilst protected from outside light sources. Following exposure to UV-light slides were washed in PBS before being incubated in pre-heated 2x SSC for one hour at 62°C. Slides were the washed four times in miliQ water. Staining was carried out using Gurr staining. 2ml Gurr staining reagent was added to 50ml Gurr staining buffer. Effort was made to remove the thin film present at the meniscus of the diluted staining reagent. Slides were kept in an upright staining jar and covered with the dye solution for 2 minutes. Excess stain was removed by overflowing the slides with miliQ water. SCEs were scored using an Axioscope microscope from two separate experiments. Results are shown as number of SCEs/metaphase with the standard error, and statistics calculated using the Mann-Whitney unpaired t-test.

3. Investigating the role of BLM in the checkpoint response in DT40 cells

Recently published work establishes BLM as a novel interactor of TOPBP1. BLM interacts with BRCT4-5 of TOPBP1 via a conserved serine residue at position S304 of the BLM N-terminus (Blackford et al. 2015; Sun et al. 2017). The interaction between TOPBP1 and BLM was demonstrated to be dependent on the phosphorylation of BLM S304, allowing for interaction with TOPBP1 (**Figure 8**). Abrogation of the interaction between TOPBP1 and BLM results in increased levels of SCEs and chromosomal aberrations in cells. In addition, origin firing was increased when the interaction was abrogated when cells were exposed to conditions of replication stress induced by 2.5μM CPT for 90 minutes. This work therefore suggests that through its interaction with TOPBP1, BLM plays a direct role in control of replication, as well as a in maintaining genome stability (Blackford et al. 2015).

To further investigate the role of BLM in ATR activation and replication the avian DT40 model system was used. In this system, the BLM S304 residue equates to the BLMS251 residue. Thus, $BLM^{-/-}$ DT40 cell lines complemented with either BLM-WT-GFP or BLM S251A-GFP were used, as previously described in Blackford et al 2015. The mutation of serine 251 of BLM to an alanine abrogates the interaction between TOPBP1 and BLM, hence allowing for the investigation of the possible direct role of BLM in checkpoint activation and DNA replication.

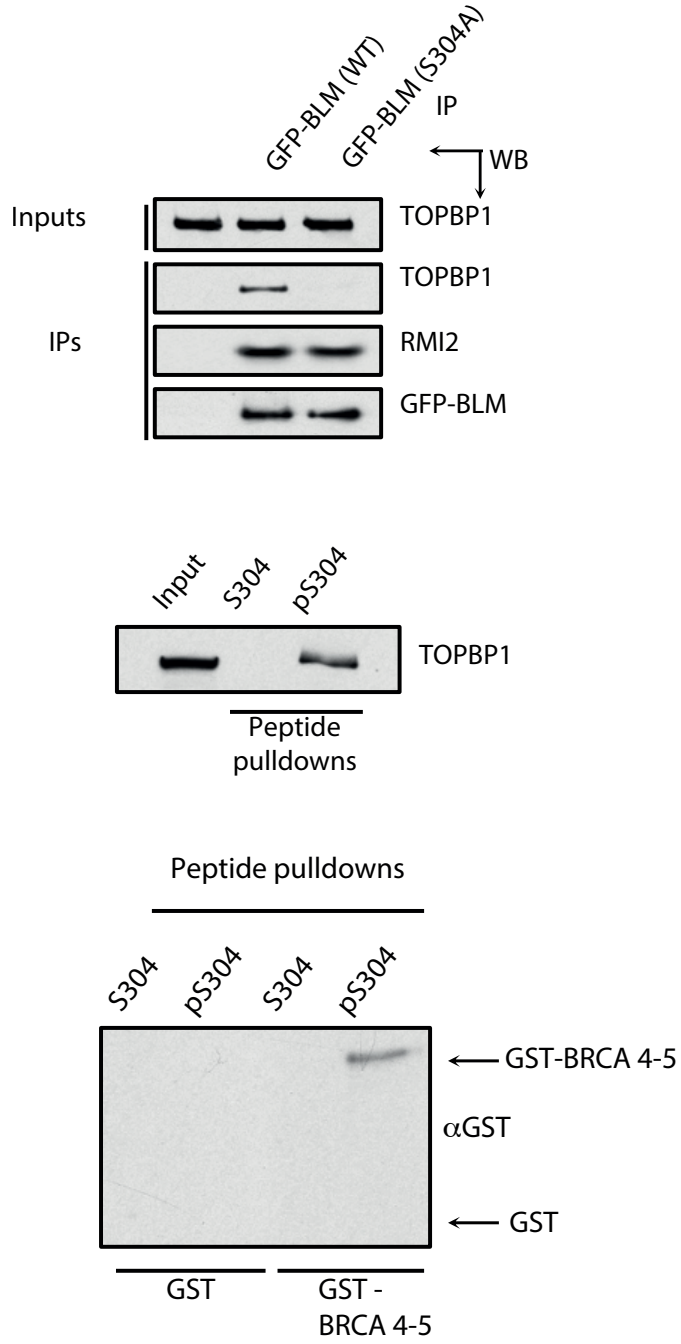


Figure 8. TOPBP1 interacts with BLM via the phosphorylated S304 residue of BLM. Top – mutation of BLM-S304 specifically prevents the interaction with TOPBP1. Middle – BLM-S304 must be phosphorylated to interact with TOPBP1. Bottom – TOPBP1 BRCT 4-5 interact directly with phosphorylated BLM-S304. Figures curtesy of Blackford et al. 2015, Mol Cell.

3.1 Analysis of unchallenged DNA replication in BLM-S251A cells

To establish if there are any underlying replication phenotypes associated with the BLM-S251A mutation in an unchallenged setting, DT40 wildtype, $BLM^{-/-}$, and $BLM^{-/-}$+ BLM WT or $BLM^{-/-}$+ BLM S251A were examined by DNA fibre analysis. This technique allows for the identification of replication patterns as seen in **Figure 9**. The relative frequency of these structures can be used to assess the spatio-temporal replication programme in cells, both in an unchallenged setting and when cells experience replication stress.

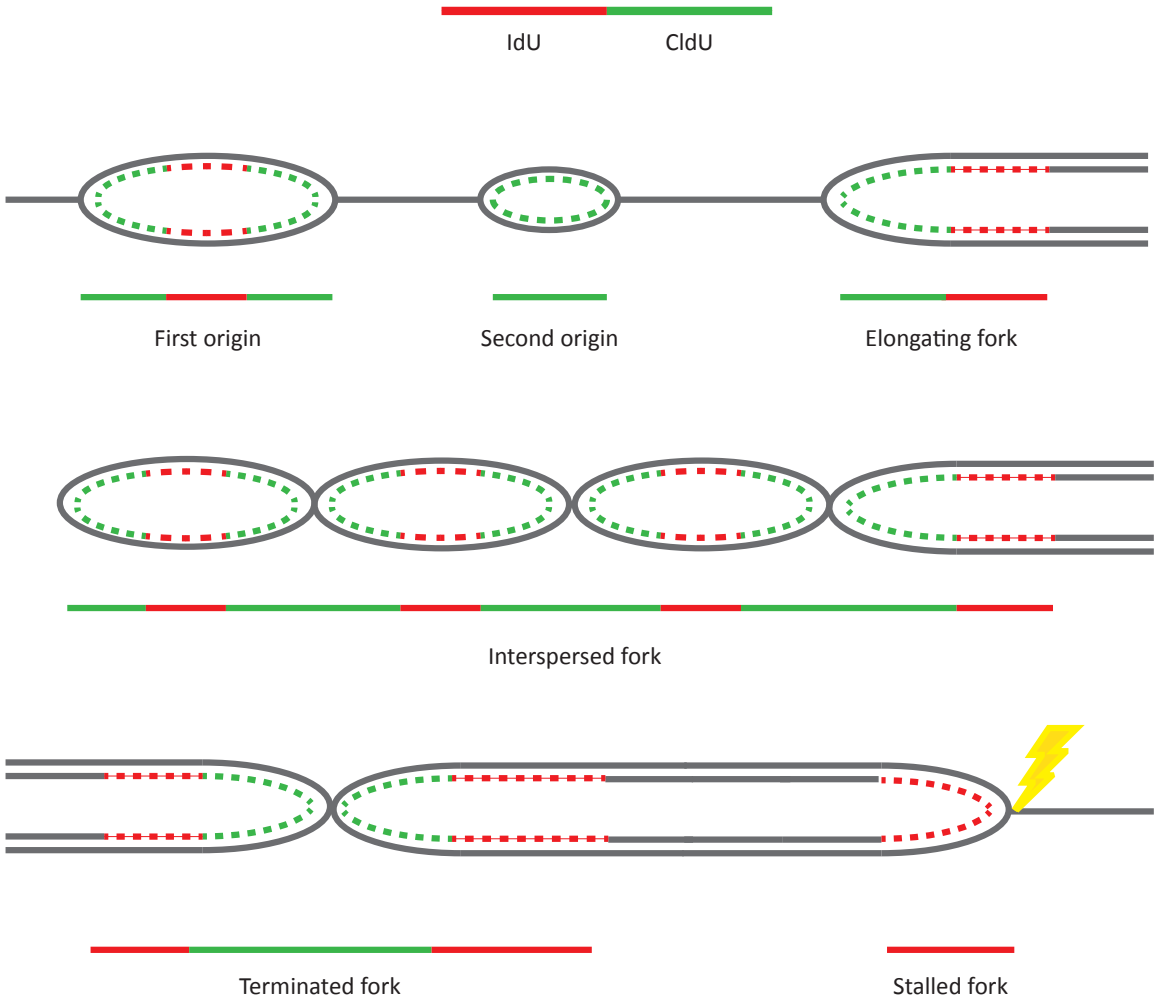


Figure 9. Schematic demonstrating DNA replication structures that can be analysed using the DNA fibre technique and how they arise.

3.1.1 Replication structures in unchallenged cells

To investigate if abrogation of the TOPBP1-BLM interaction affects DNA replication in an unchallenged situation, cells were labelled consecutively with IdU and CldU for 20 minutes each, before being harvested and analysed by microscopy (**Figure 10**). The images generated were scored for the presence of elongating forks, stalled forks, new origins and terminated replication events. Statistical analysis of these structures demonstrated that there was no significant difference between cell lines in the frequency of any of the structures examined (**Figure 11**). This result suggests that the abrogation of TOPBP1-BLM interaction does not adversely affect unchallenged replication.

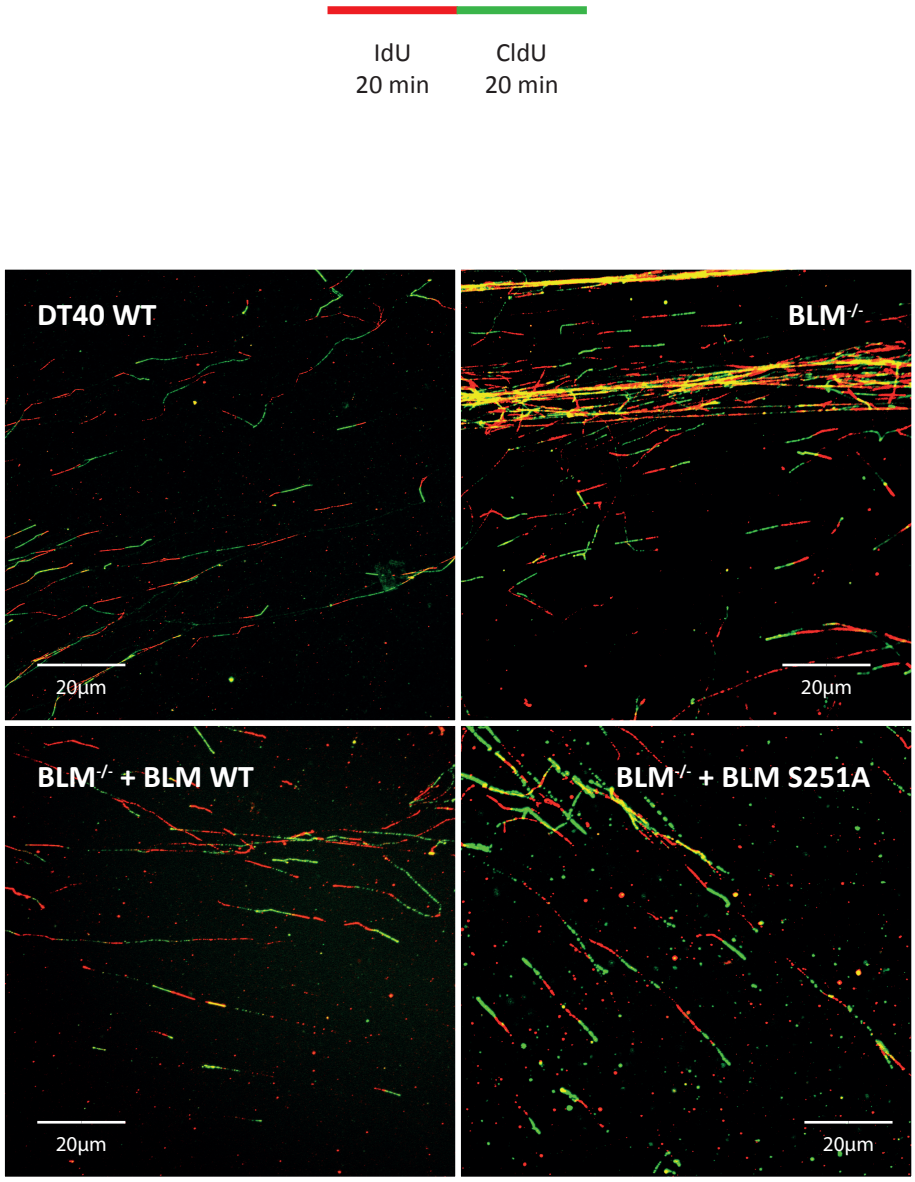


Figure 10. Top – schematic of the DNA fibre labelling experiment investigating DNA replication in unchallenged conditions. Below - representative images of actual DNA fibres from DT40 WT, $BLM^{-/-}$, $BLM^{-/-}$+BLM WT and $BLM^{-/-}$ + BLM S251A.

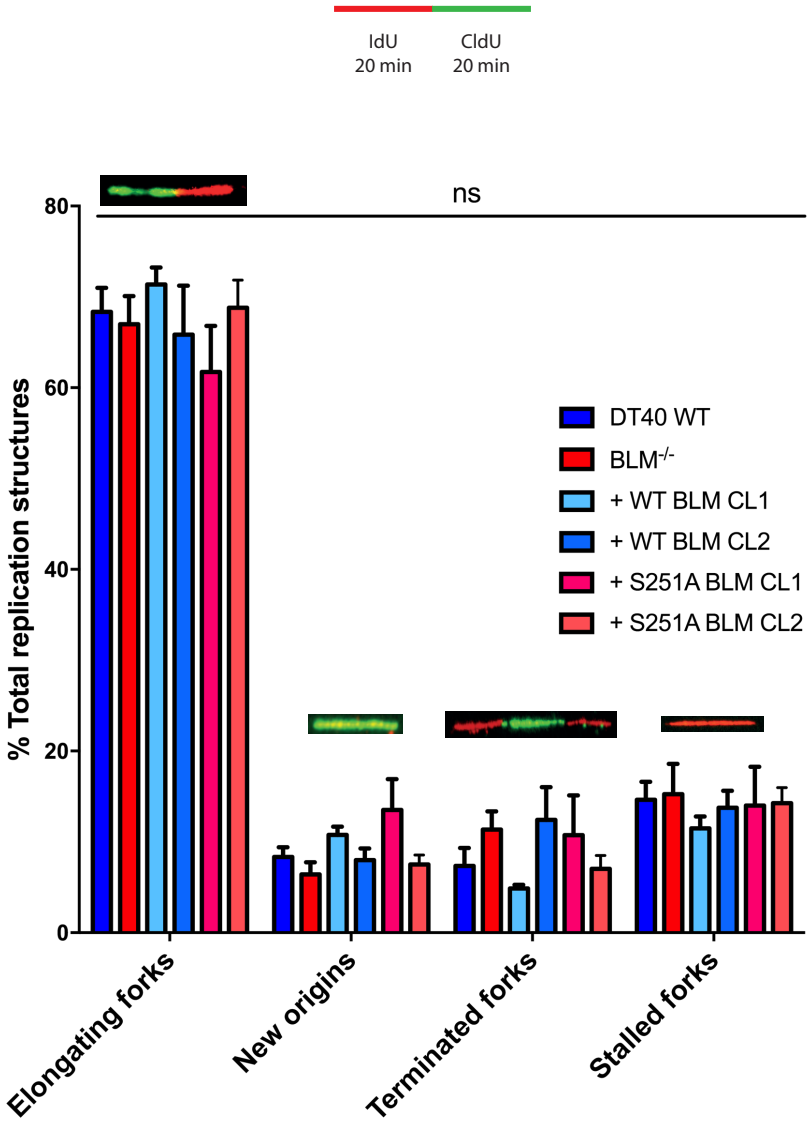


Figure 11. Top – schematic of the DNA fibre labelling experiment investigating DNA replication in unchallenged conditions. Below – quantification of the frequency of occurrence of replication structures in unchallenged DT40 WT, BLM$^{-/-}$, BLM$^{-/-}$+BLM WT and BLM$^{-/-}$ + BLM S251A cell lines (ns P> 0.05, Student's t-test, calculated from 3 independent experimental repeats with a minimum of 100 replication structures counted per cell line, per repeat). The bars represent ± s.e.m

3.1.2 Analysis of replication fork speed

To further investigate if the TOPBP1-BLM interaction plays a role in DNA replication, replication fork velocity in untreated cells was investigated.

The slowing of replication fork progression is a well-documented phenotype of cells with defective ATR signalling. Work using inhibitors of ATR have demonstrated that inhibition of ATR kinase activity slows replication speed and induces other phenotypes, including rapid cell death, disruption of replication initiation timing and increased fork collapse (Couch et al. 2013; Técher et al. 2016). Inhibition or depletion of CHK1 also results in reduced fork speed, and it has been suggested that this may be a result of starvation of DNA precursors. The cell compensates for the reduced replication fork speed phenotypes by increasing origin firing, thus completing replication (Petermann et al. 2006; Técher et al. 2016; Sanjiv et al. 2016; Técher et al. 2017).

Replication progression was monitored in BLM-WT, BLM$^{-/-}$ and BLM-S251A cells to establish if BLM plays a role in maintaining replication fork progression through its interaction with TOPBP1. This was done by measuring the green tract of elongating forks in untreated WT DT40, BLM$^{-/-}$, BLM$^{-/-}$ - WT and BLM$^{-/-}$ - S251A cell lines (**Figure 12**). Fork speed was calculated based on the finding that 1μM of a DNA fibre tract equates to approximately 2.59 kb (Jackson & Pombo 1998). The results from this analysis demonstrated that there was no significant difference in fork speed between DT40 WT and BLM$^{-/-}$ cells. There is a significant difference between BLM$^{-/-}$ - WT cl1 and BLM$^{-/-}$ - S251A cl1 and between BLM$^{-/-}$ - WT cl2 and BLM$^{-/-}$ - S251A cl2. However, a similar difference in results is seen between the two BLM$^{-/-}$ - S251A clones and BLM$^{-/-}$ - WT

clones, suggesting that the difference observed may not reflect a true causative impact of the BLM mutation on replication progression, but rather reflect a difference between individual clones. Overall, the BLM and the BLM – S251 residue are not required to maintain replication progression in unchallenged cells, unlike CHK1 and ATR. This result suggests that BLM is not required for basal ATR activity in unchallenged cells.

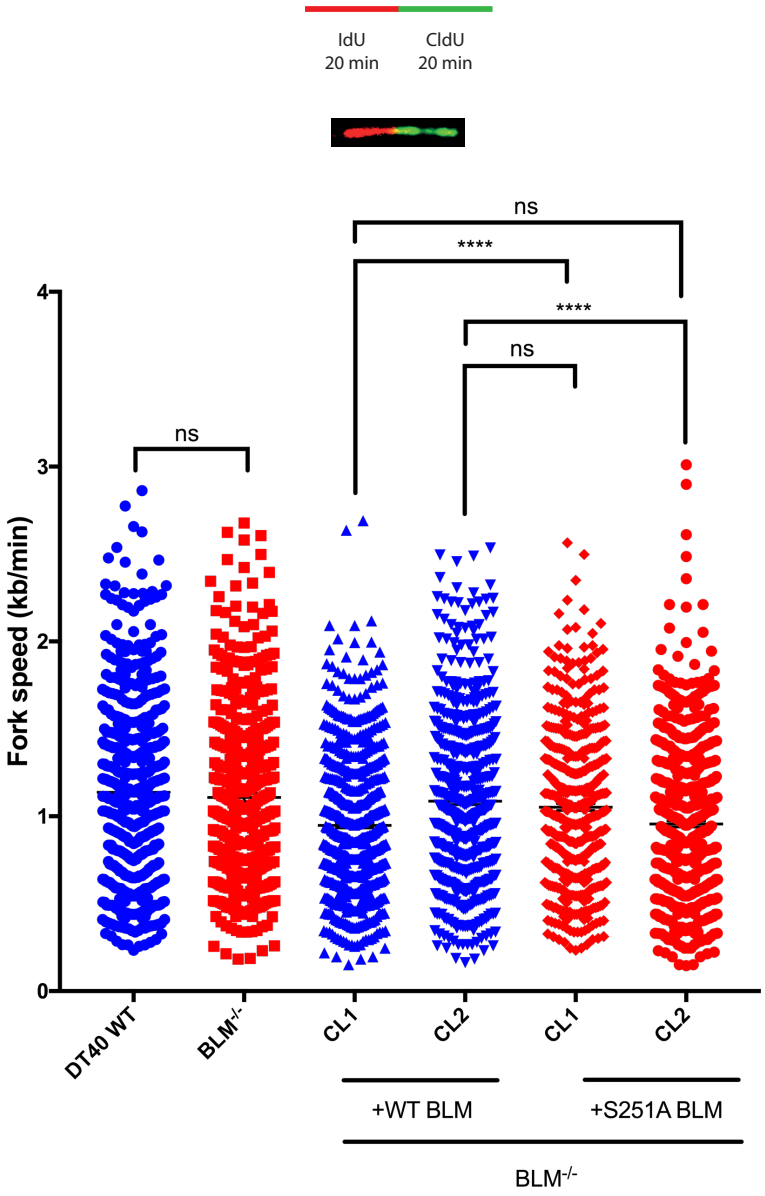


Figure 12. Top – schematic of the DNA fibre labelling experiment investigating DNA replication in unchallenged conditions. Below – dot blot showing the fork speed of elongating forks in unchallenged DT40 WT, BLM$^{-/-}$, BLM$^{-/-}$+BLM WT and BLM$^{-/-}$ + BLM S251A cell lines (ns $P > 0.05$, **** $P \leq 0.0001$ Mann-Whitney test, calculated from 3 independent experimental repeats with a minimum of 150 elongating replication forks were measured per cell line, per repeat). The bars represent ± s.e.m.

3.1.3 Analysis of replication symmetry

By using a double labelling technique, it is possible to monitor the fates of two forks emanating from a single origin. Bi-directional replication forks moving from one origin tend to exhibit the same fork velocity (Conti et al. 2007). If both forks are proceeding at the same speed, this gives rise to a symmetric fork. However, if individual forks are more prone to stalling this will give rise to asymmetric forks (**Figure 13**). This analysis provides a very sensitive and quantitative assessment of the replication programme, and a sensitive measure of the rate of fork stalling. Measuring the length of the second label of either fork allows one to calculate the ratio, reflecting the level of symmetry between the forks. If the ratio between the two arms is close to 1, the fork can be said to be symmetrical. However, if one arm is shorter than the other and the ratio is >1, the fork is asymmetrical. If there is a high prevalence of asymmetric forks this suggests that individual forks are more prone to stalling.

When the fork symmetry of untreated cells was investigated, all asymmetric forks observed in the images were quantified. However very few of these replication patterns were seen, particularly when visualising patterns in $BLM^{-/-}$ - S251A cl2 cells. Analysis of fork symmetry suggests that there is no difference in the ratio of fork progression between BLM-WT and BLM-S251A cell lines, indicating that the BLM-S251A mutation does not affect the replication of unchallenged cells (**Figure 14**). However further measurements would be required to draw a conclusion from these data.

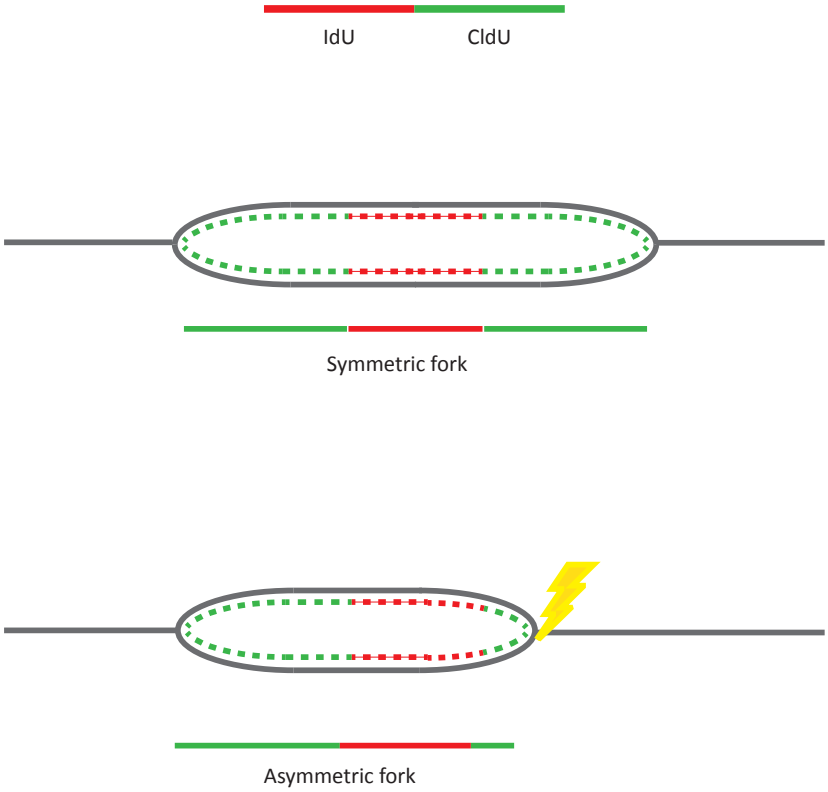


Figure 13. Schematic showing, top – an example of a DNA fibre labelling setup. Middle - a bi-directional fork emanating from a single origin to give a symmetric fork. Bottom – a bi-directional fork where a single fork has stalled, resulting in an asymmetric fork.

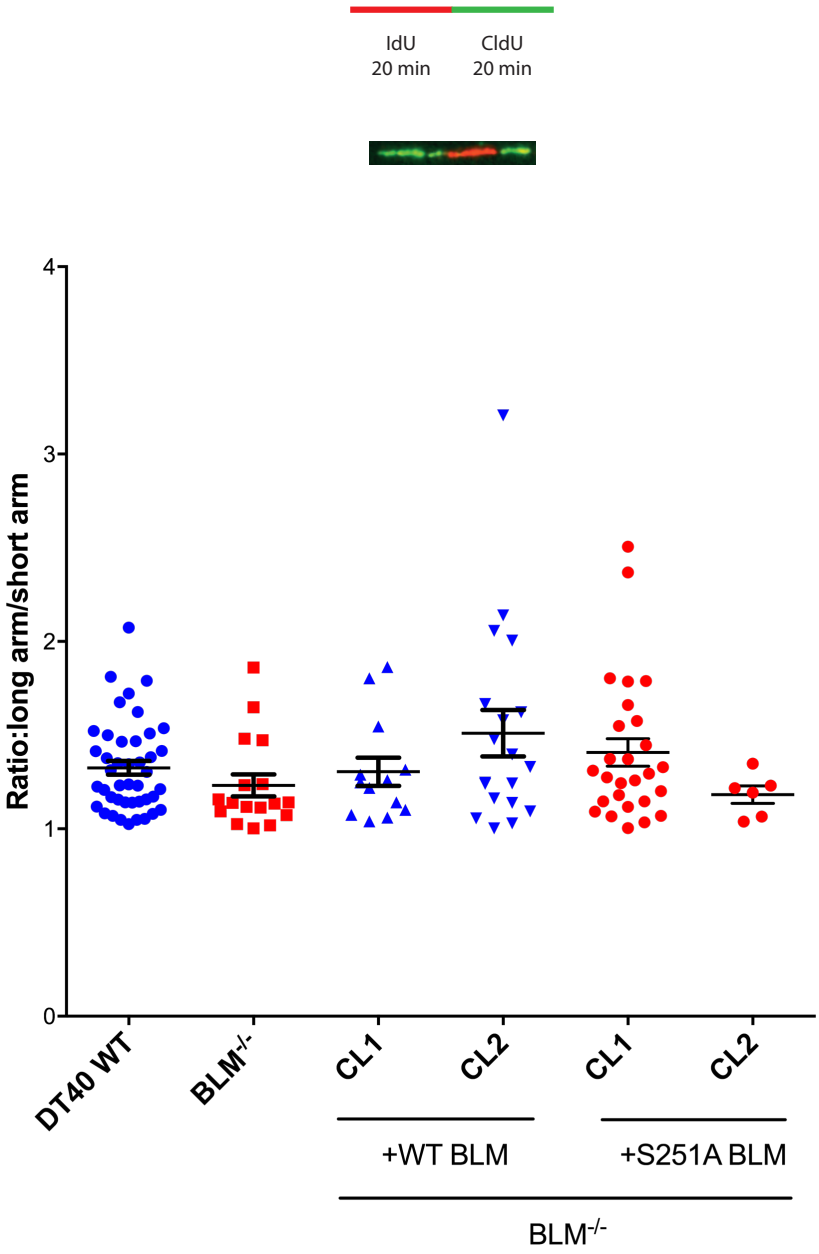


Figure 14. Top – schematic of the DNA fibre labelling experiment investigating DNA replication in unchallenged conditions. Below – dot blot showing the distribution of CldU tract length ratios of bi-directional forks in unchallenged DT40 WT, $BLM^{-/-}$, $BLM^{-/-}$+BLM WT and $BLM^{-/-}$ + BLM S251A cell lines (Quantified from 3 independent experimental repeats. All quantifiable asymmetric forks were included in the analysis, a minimum of 6 asymmetric forks were observed and measured per cell line). The bars represent ± s.e.m.

3.2 Evaluating changes in checkpoint activation and DNA replication in response to DSBs

BLM deficient cell lines have previously been shown to be sensitive to DNA damaging agents (Bachrati & Hickson 2008). Sgs1, *S. cerevisiae* homologue of BLM, has been implicated in DSB repair and resection, but it remains unclear if BLM also contributes to activation of ATR signalling in response to DSBs and genotoxic stress (Mimitou & Symington 2008; Gravel et al. 2008). Therefore, camptothecin (CPT), a topoisomerase 1 poison that causes the trapping of the Top1 cleavage complex leading to replication fork collapse , was used to induce replication stress in BLM-S251A cells (Seiler et al. 2007). Mild treatment with 25nM CPT has been shown to induce fork stalling and reversal in cells possibly limiting DSB formation, whereas treatment with 1μM CPT results in rapid formation of DSBs as well as fork stalling and reversal (Zellweger et al. 2015; Ray Chaudhuri et al. 2012). Here, a dose of 100nM CPT was used, likely resulting in fork stalling and slowing of replication fork progression (Mijic et al. 2017; Zellweger et al. 2015). This treatment allows for the investigation of the ability of mutant cells to establish a checkpoint response following such replicative stresses. In addition, the ability of cells to recover replication forks following fork stalling and DSBs induced by challenge with 2.5μM CPT was evaluated using the DNA fibre technique.

3.2.1 Investigating the S-phase checkpoint response to DSBs

Exponentially growing cells were treated with 100 nM CPT for 20 or 60 minutes to evaluate the ability of cells to activate ATR signalling. The phosphorylation of CHK1-S345 has been shown to be dependent on ATR kinase activity and is required for checkpoint-

mediated arrest of the cell cycle (Qinghua Liu et al. 2000; Capasso et al. 2002; Piwnica-Worms 2001; Guo et al. 2000). The phosphorylation of this residue was therefore utilised as a readout for activation of ATR (**Figure 15**). Following induction of replication stress by CPT, phosphorylation of CHK1-S345 was reduced in both BLM-deficient and BLM-S251A cells when compared to WT cells. However, some residual phosphorylation of CHK1 was detected in $BLM^{-/-}$ and BLM-S251A cells. The result of this analysis therefore suggests that BLM-S251A cells were unable to fully activate the S-phase checkpoint following CPT challenge, however, some low-level ATR activity is still present. Notably, CHK1 is used as a loading control for these experiments. Interestingly, a report has found that CHK1 is targeted for degradation following phosphorylation as S345. However, this degradation was only detectable 4 hours after the onset of phosphorylation, and is therefore unlikely to impact upon the results of these experiments (Zhang et al. 2005).

Although this result suggests that the TOPBP1-BLM is important in activation of ATR signalling, it does not provide conclusive results of this. The addition of cell cycle analysis of $BLM^{-/-}$ and BLM-S251A cells lines compared to wild type cells would provide evidence that these observations were due to a true defect in ATR signalling and not a problem in cell cycle progression, resulting in fewer mutant cells entering into S-phase, thus skewing the result to suggest a checkpoint defect.

The phosphorylation of histone H2AX, known as γH2AX, has been included in this analysis as an indicator of DNA damage (Kuo & Yang 2008). H2AX has been found to be a target for ATM, ATR and DNA-PKcs, with ATM being considered the major mediator of

this phosphorylation (Podhorecka et al. 2010; Ward & Chen 2001; Kuo & Yang 2008). The result of this analysis does suggest reduced phosphorylation of H2AX in the $BLM^{-/-}$ cell line in particular. This provides some support for the involvement of BLM in ATR signalling, and is in line is with a previous observations demonstrating delayed phosphorylation of H2AX in Bloom syndrome patient cell lines following CPT challenge (Shastri & Schmidt 2016). However, this phenotype is not as evident in BLM-S251A mutant cells. It is possible that BLM deficiency may also impact the activity of other PIKKs towards the phosphorylation of H2AX and not only ATR, therefore a stronger phenotype is seen in the $BLM^{-/-}$ cells. Another explanation could be that the TOPBP1-BLM interaction does not impact upon the ability of ATR to phosphorylate H2AX. Notably, the phosphorylation of H2AX was found to be high in control cells, also before CPT treatment. This could be a result of the nature of DT40 cells. This cell type has a short doubling time and exhibits a hyper-recombinogenic phenotype, which could result in high levels of phosphorylation of H2AX (Winding & Berchtold 2001; Buerstedde & Takeda 1991).

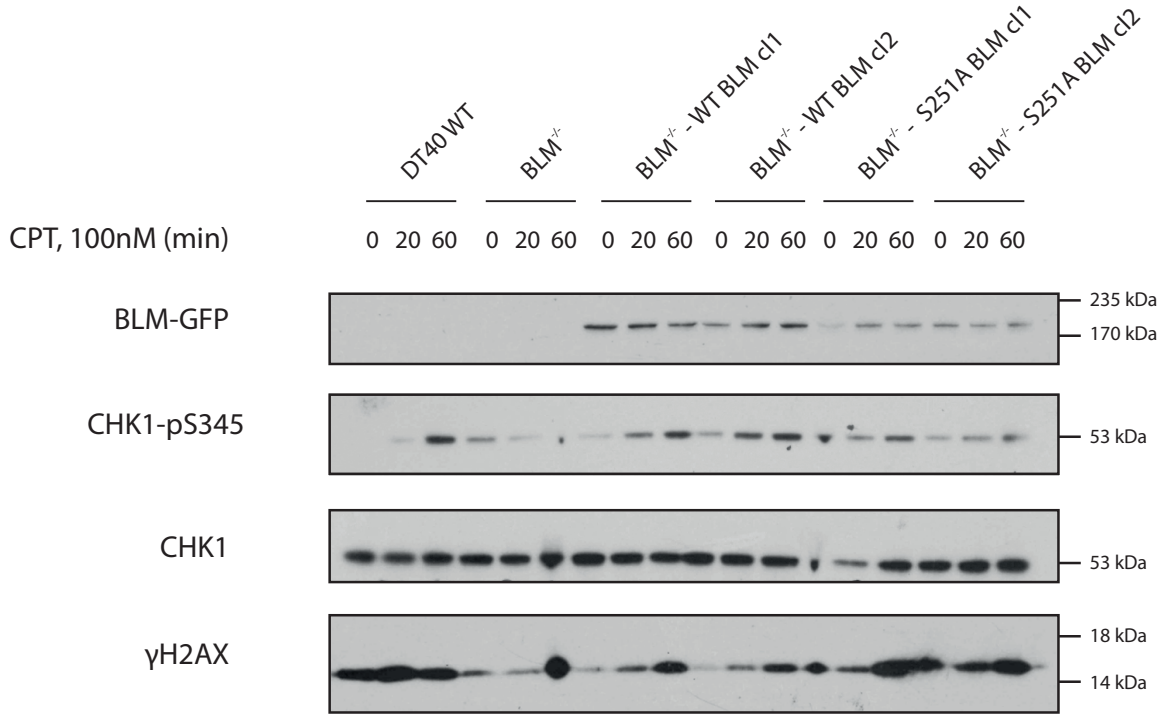


Figure 15. DT40 WT, $BLM^{-/-}$, $BLM^{-/-}$+BLM WT and $BLM^{-/-}$ + BLM S251A cell lines were treated with 100 nM CPT for the indicated times before harvesting for SDS-PGE and western blotting with the antibodies as indicated.

3.2.2 Recovery of DNA replication in BLM-S251A cells following CPT challenge

DNA fibre was used to evaluate if the checkpoint defect observed following CPT challenge also affects the DNA replication programme in $BLM^{-/-}$ and BLM-S251A cells. Cells were treated with 2.5 μM CPT alongside the first label for 90 minutes before washing away the drug and labelling the cells with CldU for 15 minutes. This setup introduces replication stress with the first label, and thus allows for the evaluation of the ability of cells to recover replication by comparing the lengths of the second (green) tract between cell lines (**Figure 16**). During the first label cells are encountering DSBs caused by CPT, and forks may stall or collapse as lesions are repaired. Once the drug is removed and the second label added, cells are no longer challenged, and repair of remaining lesions can take place. If cells are unable to carry out repair and restart replication forks, forks will remain stalled and only red tracts would be observed. However, if cells are able to repair and restart replication forks, the second label would be incorporated resulting in a red and green tract. The length of the green tract provides information on how efficiently restart is taking place; longer tracts signify faster restart whereas shorter tracts suggest slower restart.

Analysis of replication recovery shows that the green track is longer in mutant cell lines than in DT40 WT cells (**Figure 17**). This suggests that replication is restarting more efficiently in BLM mutant cell lines when compared to WT cells.

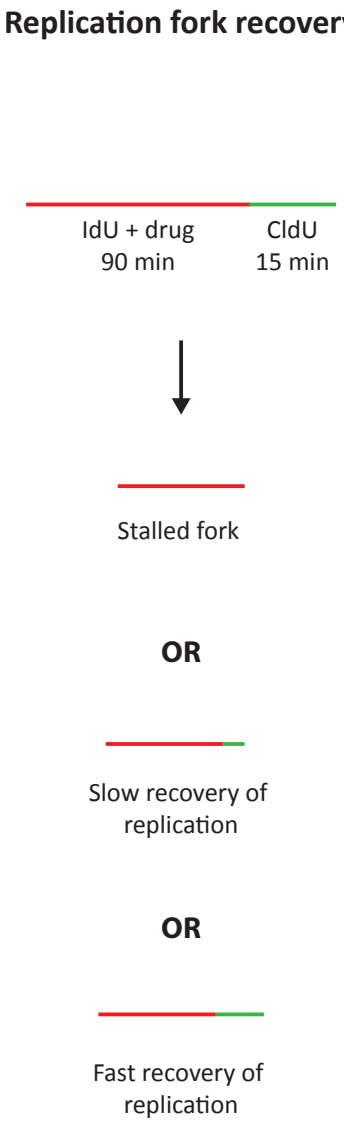


Figure 16. Schematic illustrating the possible outcomes of replication fork recovery following CPT challenge.

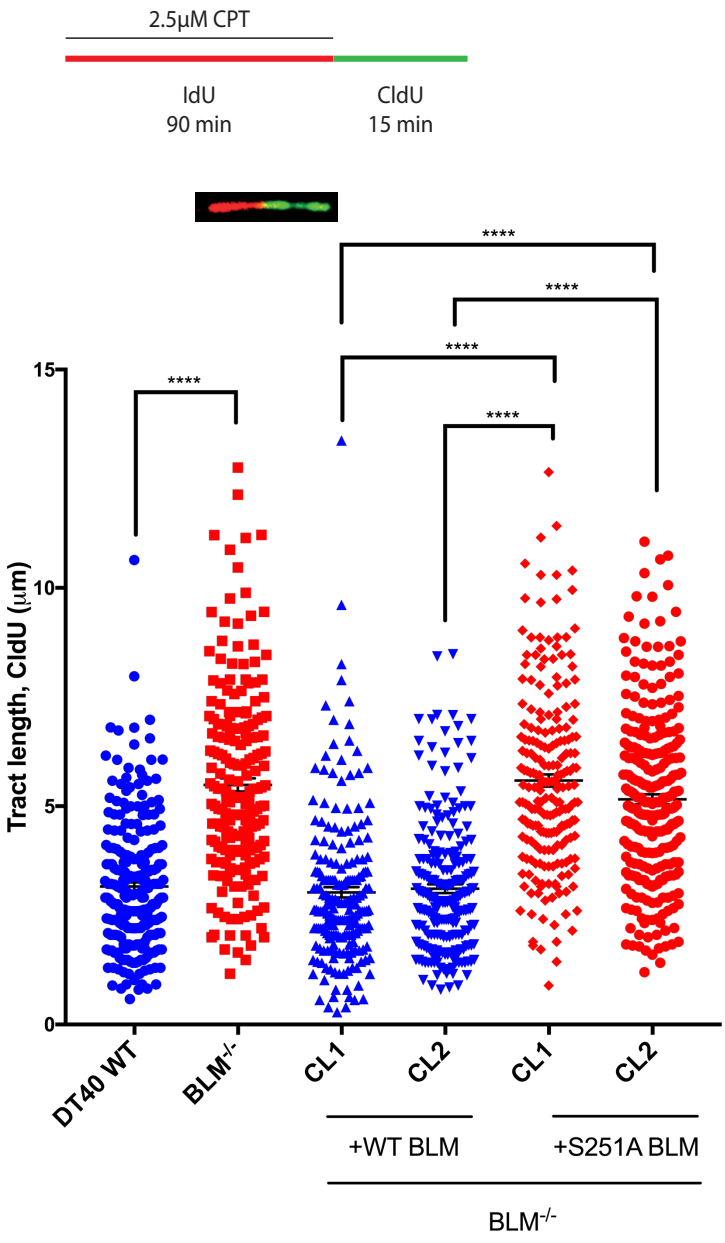


Figure 17. Top – schematic of the DNA fibre labelling experiment investigating DNA replication restart in response to challenge. Below – quantification of the length of the second label to investigate the efficiency of replication restart following CPT challenge (**** $P \leq 0.0001$ Mann-Whitney test, calculated from 3 independent experimental repeats with a minimum of 70 elongating forks measured per cell line). The bars represent ± s.e.m.

Next, analysis of the frequency of replication structures revealed that there was an increased level of origin firing in BLM-S251A cells compared to WT cells, consistent with previously published data (**Figure 18**) (Blackford et al. 2015). Furthermore, analysis of fork symmetry revealed that both $BLM^{-/-}$ and BLM-S251A cells display a higher level of fork asymmetry than WT cells, indicating that replication restart is less efficient in mutant cells as compared to WT cells (**Figure 19**). Overall, these results suggest that through its interaction with TOPBP1, BLM is involved in control of origin firing and replication fork recovery in response to DSBs.

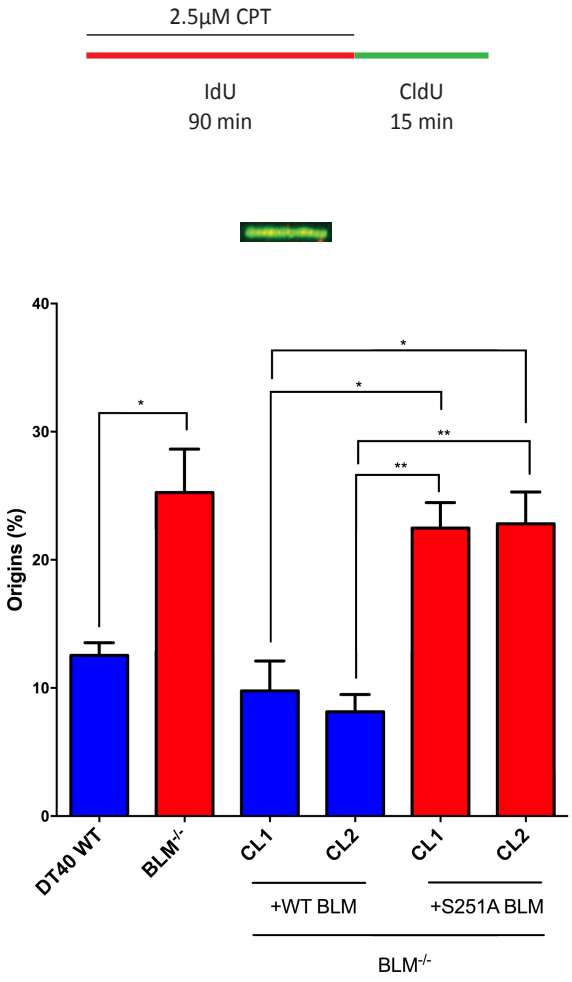


Figure 18. Top – schematic of the DNA fibre labelling experiment investigating DNA replication restart in response to challenge. Below – quantification of the frequency of new origin firing in DT40 WT, BLM$^{-/-}$, BLM$^{-/-}$+BLM WT and BLM$^{-/-}$ + BLM S251A cell lines following treatment with 2.5 µM CPT (* $P \leq 0.05$, ** $P \leq 0.01$, Student's t-test, calculated from 3 independent experimental repeats with a minimum of 100 replication structures per cell line, per repeat). The bars represent ± s.e.m.

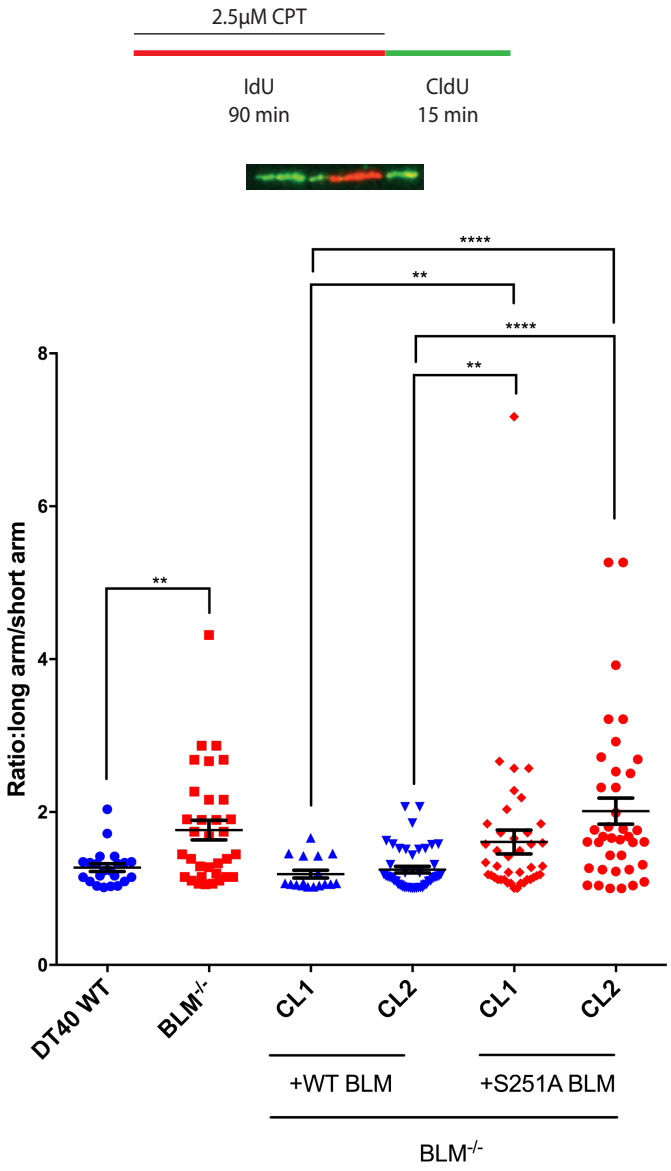


Figure 19. Top – schematic of the DNA fibre labelling experiment investigating DNA replication restart in response to challenge. Below – dot blot showing the distribution of CldU tract length ratios of bi-directional forks in DT40 WT, $BLM^{-/-}$, $BLM^{-/-}$+BLM WT and $BLM^{-/-}$ + BLM S251A cell lines following challenge with 2.5 μM CPT (** $P \leq 0.01$, **** $P \leq 0.0001$, Mann-Whitney test, calculated from 3 independent experimental repeats with a minimum of 30 bi-directional forks per cell line). The bars represent ± s.e.m.

3.3 Investigating the checkpoint response following nucleotide depletion

Bloom syndrome patient cells lines have previously been shown to be sensitive to inhibition of DNA replication (Davies et al. 2004). HU inhibits replication by blocking the active site of ribonucleotide reductase , thus the nucleotide pool becomes depleted and replication progression is prevented (Slater 1973; Yarbro 1992). Initial treatment with HU leads to fork stalling, unlike treatment with CPT which can lead to immediate fork collapse, although prolonged exposure to HU does eventually lead to collapse into a DSB (Petermann, Orta, et al. 2010; Zellweger et al. 2015). Therefore, HU was used to investigate if checkpoint activation in response to fork stalling, as opposed to fork collapse, requires the TOPBP1-BLM interaction.

3.3.1 Investigating the checkpoint response following replication inhibition

To induce replication stress, cells were treated with 1 mM HU for 1 or 2 hours and harvested for western blot (**Figure 20**). Both WT and BLM-S251A cells show robust induction of ATR activity following 1 hour of HU treatment. However, after two hours of treatment, phosphorylation of CHK1 is no longer detectable in BLM-S251A cells but is still present in WT cells. Notably, $BLM^{-/-}$ cells are unable to phosphorylate CHK1 at any of the time points investigated, suggesting that full-length BLM is required for the initial phosphorylation of CHK1, as well as the maintenance of the signal. BLM-S251A cells are able to induce a checkpoint response but are unable maintain ATR signalling and the checkpoint during prolonged challenge. It may be that the BLM-S251A mutation can facilitate the stimulation of ATR through a TOPBP1-independet mechanism, e.g. through an interaction with ETAA1, and that activation through this alternative mechanism is impossible when the full-length BLM is lost (Bass et al. 2016). Such alternative

stimulation of ATR could be enough to stimulate initial ATR signalling activity but may not be enough to maintain the signal. In line with this, one study has demonstrated that in *Schizosaccharomyces pombe* the AAD domain of TOPBP1 homologue Rad4 is not required for initial Rad3 (ATR homologue) activation, but is rather required for checkpoint amplification (Lin et al. 2012).

Interestingly, it has been demonstrated that CHK1-S345 is dephosphorylated by protein phosphatase 2A (PP2A), suggesting that during unchallenged conditions this dephosphorisation ensures a low basal level of phosphorylated CHK1 in cells (Leung-Pineda et al. 2006). The loss of CHK1 phosphorylation seen in BLM-S251A cells in this experiment could therefore be explained by initial ATR activation through a secondary ATR-activation mechanism. The phosphorylation resulting from this initial ATR activation is depleted over time by PP2A, and as BLM-S251A cells are unable to activate ATR through TOPBP1 the pool of phosphorylated CHK1 is not replenished, resulting in loss of phosphorylation of CHK1 over time.

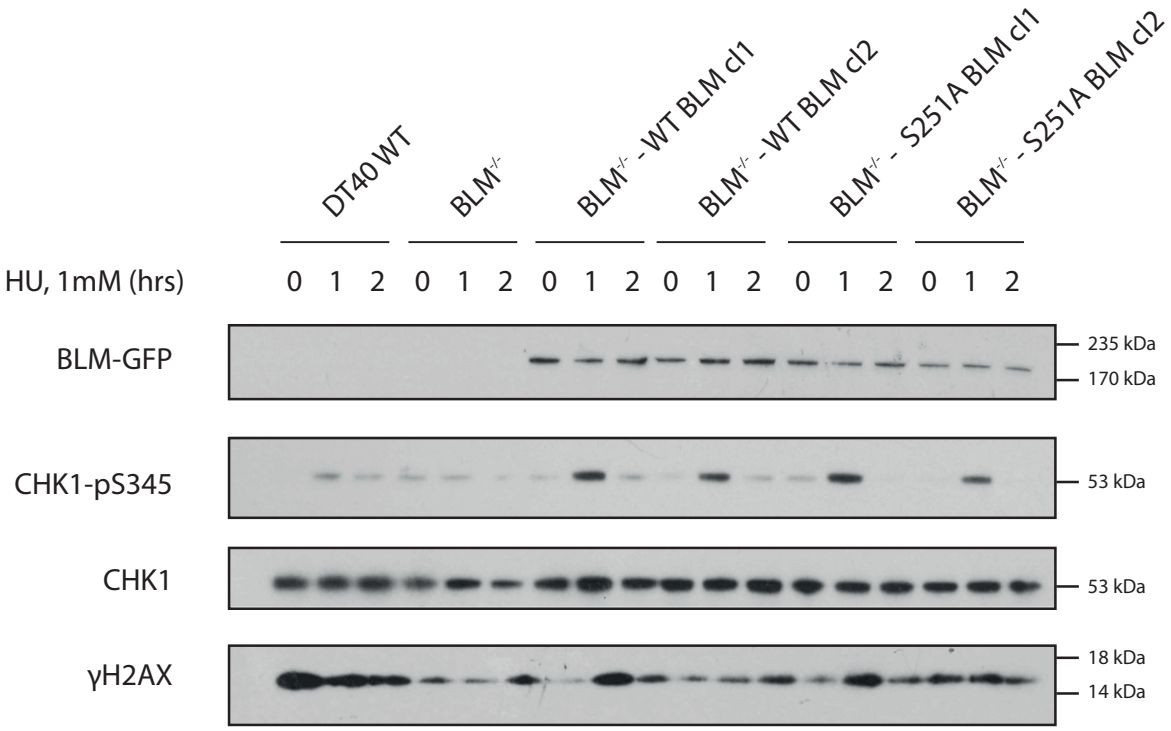


Figure 20. BLM$^{-/-}$ and BLM-S251A cells are less able to activate ATR signalling in response to HU challenge. DT40 WT, BLM$^{-/-}$, BLM$^{-/-}$+BLM WT and BLM$^{-/-}$ + BLM S251A cell lines were treated with 1mM HU for the indicated times before harvesting for SDS-PAGE and western blotting with the antibodies as indicated.

3.3.2 Assessing DNA replication in response to HU

To investigate the effect of HU treatment on DNA replication, cells were labelled consecutively with IdU and CldU for 20 minutes. 200 μM HU was added alongside the second label. This allows for the analysis of continued replication when cells are subjected to replication stress.

Initially, the tract length ratio was used to assess the ability of cells to continue replication in the presence of HU. In this setup both labels are added to cells for the same amount of time. If no replication stress was present it would be expected that the ratio between the first and second label would be approximately 1. With the addition of HU in the second label, replication may stall or slow in order to deal with any potential lesions or stresses arising from the challenge. Addition of HU may therefore result in a tract length ratio of <1 (**Figure 21**).

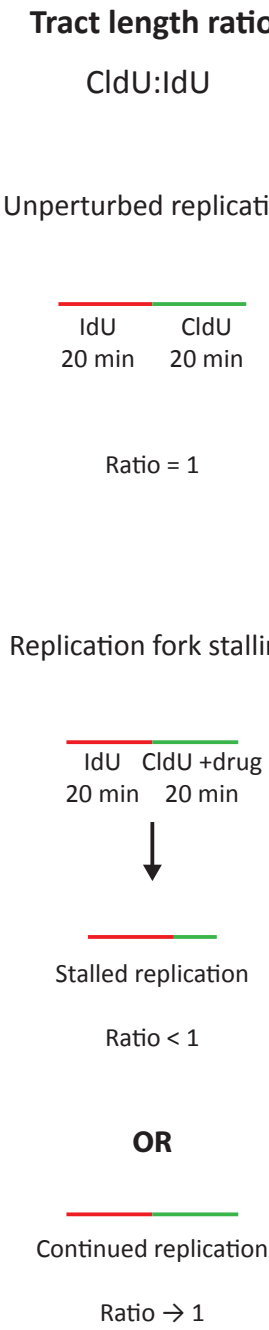


Figure 21. Schematic illustrating the changes tract length ratio as predicted following replication fork stalling.

As expected, analysis of tract length in WT cells resulted in a ratio <1, indicating that replication has slowed due to the replication stress (**Figure 22**). Conversely, results from $BLM^{-/-}$ and BLM-S251A cell lines give a higher average tract length ratio, indicating that BLM mutant cells are continuing replication, despite the presence of replication stress.

Next, the frequency of replication structures in the cells lines was assessed. HU treatment resulted in a reduction in fork stalling and an increase of origin firing in BLM-S251A cells compared to WT cells (**Figure 23**). However, assessment of fork symmetry uncovered that bi-directional forks in $BLM^{-/-}$ and BLM-S251A cell lines are more asymmetrical than those in WT cells (**Figure 24**), suggesting that mutant cell lines are stalling more frequently than WT cells, contrasting with observations from the quantification of the frequency of replication structures. These findings support the notion that TOPBP1-BLM interaction is required for the efficient control of the replication programme under the conditions of diverse replication stress, but the observations regarding fork stalling are not fully explained by these experiments.

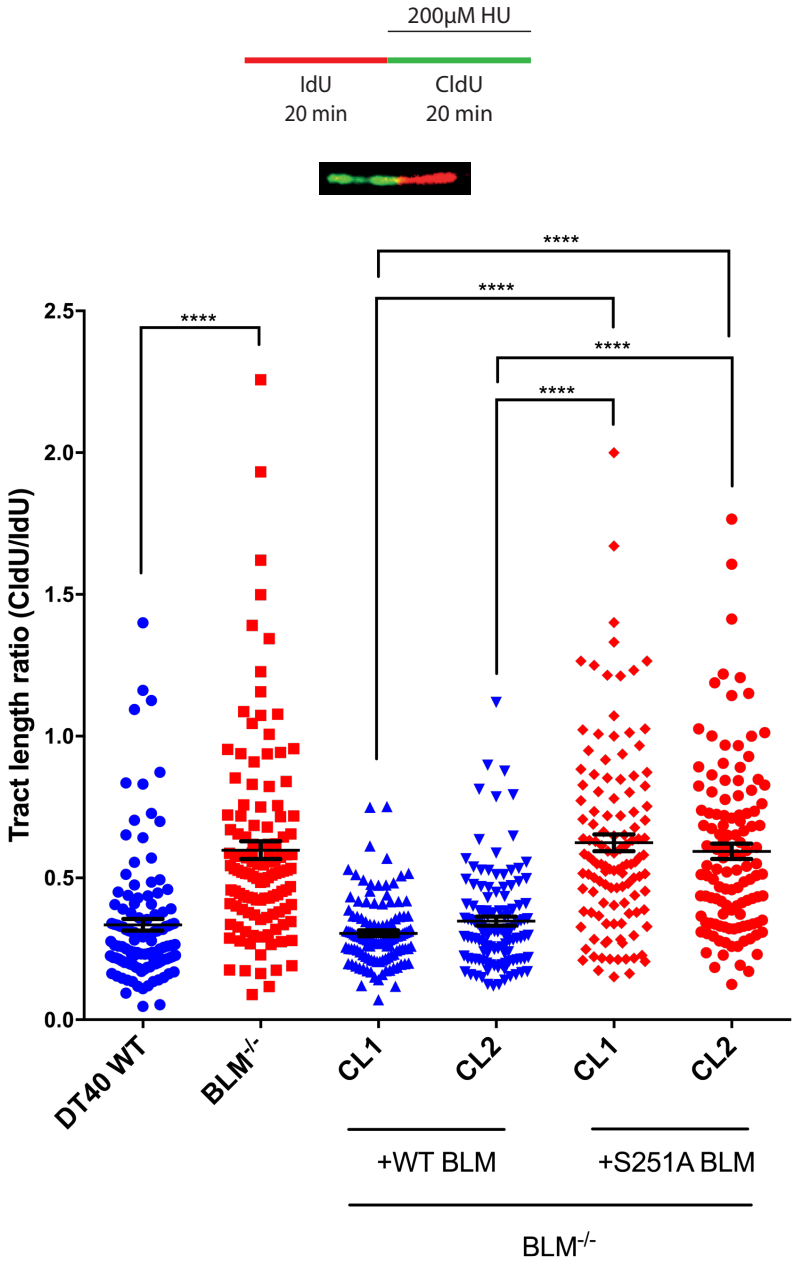


Figure 22. Top – schematic of the DNA fibre labelling experiment investigating continued DNA replication in response to challenge. Below – dot blot showing the ratio between the first and second labels of elongating forks in DT40 WT, $BLM^{-/-}$, $BLM^{-/-}$+BLM WT and $BLM^{-/-}$ + BLM S251A cell lines following challenge with 200 μM HU (**** $P \leq 0.0001$, Mann-Whitney test, calculated from 3 independent experimental repeats with a minimum of 30 elongating forks measured per cell line, per repeat). The bars represent ± s.e.m.

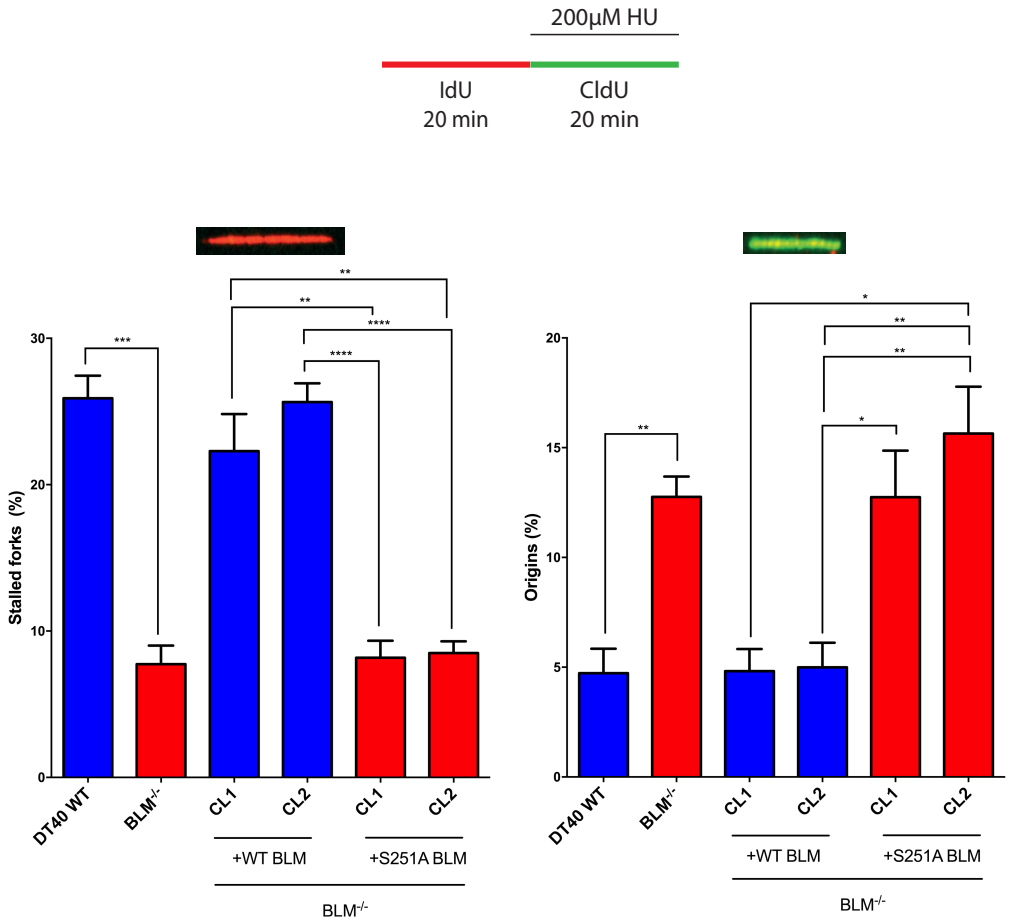


Figure 23. Top – schematic of the DNA fibre labelling experiment investigating continued DNA replication in response to challenge. Below – quantification of the frequency of new origin firing and stalled replication forks in DT40 WT, $BLM^{-/-}$, $BLM^{-/-}$+BLM WT and $BLM^{-/-}$ + BLM S251A cell lines following treatment with 200 μM HU (* $P \leq 0.05$, ** $P \leq 0.01$, *** $P \leq 0.001$, **** $P \leq 0.0001$, Student's t-test, , calculated from 3 independent experimental repeats with a minimum of 100 replication structures per cell line, per repeat). The bars represent ± s.e.m.

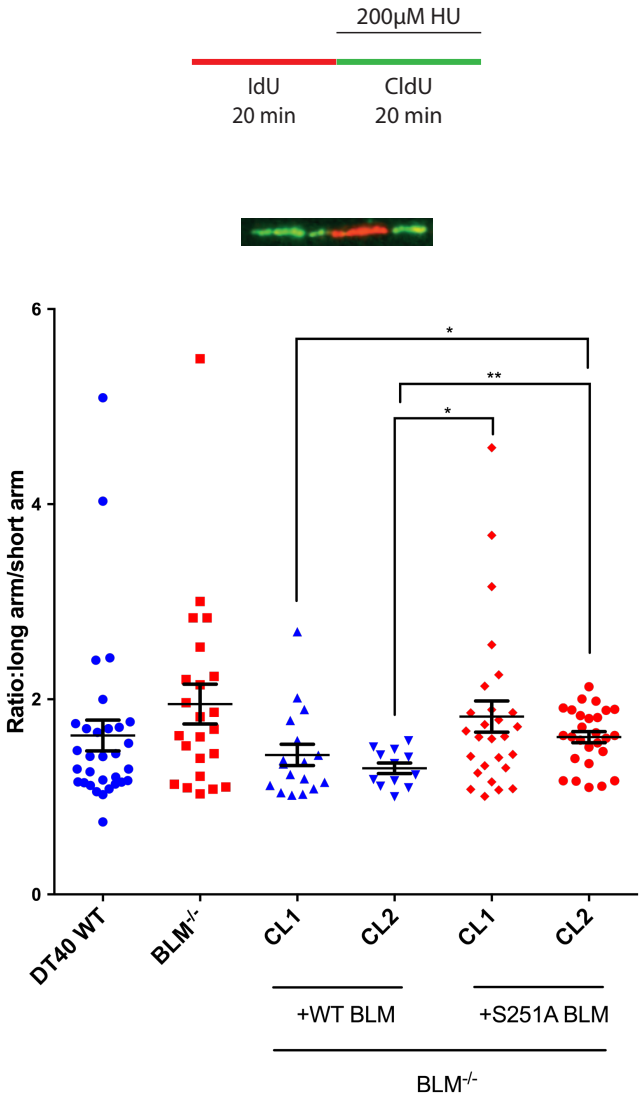


Figure 24. Top – schematic of the DNA fibre labelling experiment investigating continued DNA replication in response to challenge. Below – dot blot showing the distribution of CldU tract length ratios of bi-directional forks in DT40 WT, $BLM^{-/-}$, $BLM^{-/-}$+BLM WT and $BLM^{-/-}$ + BLM S251A cell lines during challenge with 200µM HU (** $P \leq 0.01$, ** $P \leq 0.01$, Mann-Whitney test, calculated from 3 independent experimental repeats with a minimum of 20 bi-directional forks measured per cell line). The bars represent ± s.e.m.

3.4 BLM-S251A cells complete replication through dormant origin firing

The data presented so far suggest that BLM-S251A cells are unable to properly activate the S-phase checkpoint and continue to carry out DNA replication despite the presence of a variety of DNA replication stress factors. However, it is not clear how replication is completed in these cells. Two possible scenarios were proposed; BLM-S251A cells could be more able to recover stalled replication forks, hence completing replication. Alternatively, mutant BLM cell lines could be relying on firing dormant origins to conclude replication. Both scenarios could explain the increased tract length ratio observed in BLM-S251A cells. The result could arise from efficient recovery of stalled forks, or a new origin may fire in close proximity to the original fork, that is now stalled due to replication stress. If a new origin fires in close proximity of the original fork, this would also result in a red and green tract following labelling, giving the impression that it is an elongating fork. As increased origin firing was observed with replication challenge, it is hypothesised that BLM mutant cells are likely to be relying on origin firing to complete replication.

To test this hypothesis and differentiate between these two possibilities, cells were treated with roscovitine, a cyclin-dependent kinase targeting CDK2, CDK7, CDK9 and others (Meijer et al. 1997). The addition of the inhibitor blocks the firing of new origins, whereas forks that are already progressing are unaffected by the treatment (**Figure 25**). If mutant cells are more able to recover stalled forks then the addition of roscovitine to this setup should reduce origin firing in BLM-S251A and BLM-deficient cells to a level comparable to that observed in WT cells, however, the tract length ratio would remain the same. If mutant cells are dependent on origin firing to complete replication both

origin firing, and tract length ratio levels should revert to wildtype levels with the addition of roscovitine.

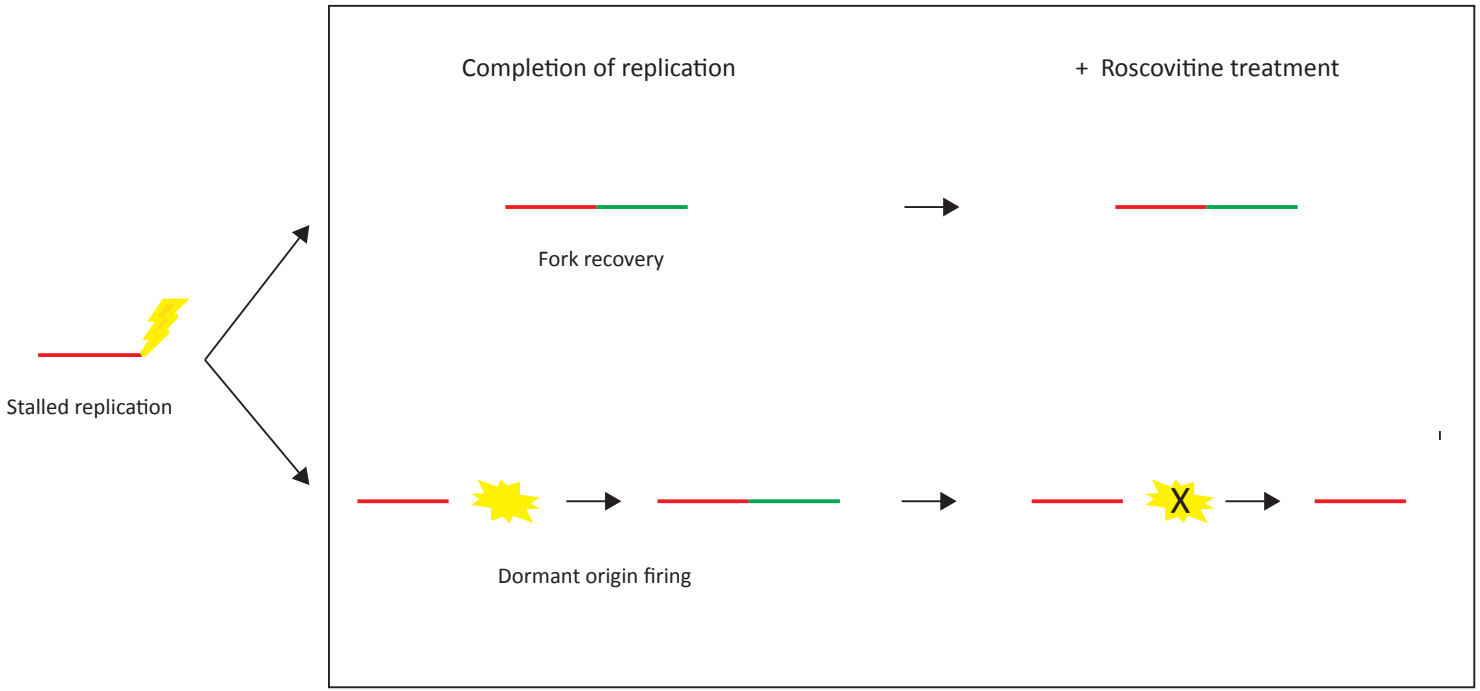


Figure 25. Schematic illustrating, middle – the proposed scenarios for completion of replication, and right – the effect of the addition of roscovitine in differentiating between these scenarios.

The setup for this experiment was the sequential addition of IdU and CldU for 20 minutes, with the addition of 200 μM HU with the second label. Roscovitine was present throughout the labelling process at a concentration of 100 μM. The assessment of the frequency of replication structures demonstrated that the level of origin firing in $BLM^{-/-}$ and $BLM^{-/-}$-S251A cells had been reduced to a level equivalent to that of WT cells following roscovitine treatment (**Figure 26**). The calculation of the tract length ratio in $BLM^{-/-}$ and $BLM^{-/-}$-S251A cells revealed that the ratio was reduced to levels indistinguishable from BLM-WT cell lines following roscovitine treatment (**Figure 27**). These results provide evidence that BLM-S251A cells complete replication by the firing of new origins in conditions of replication stress.

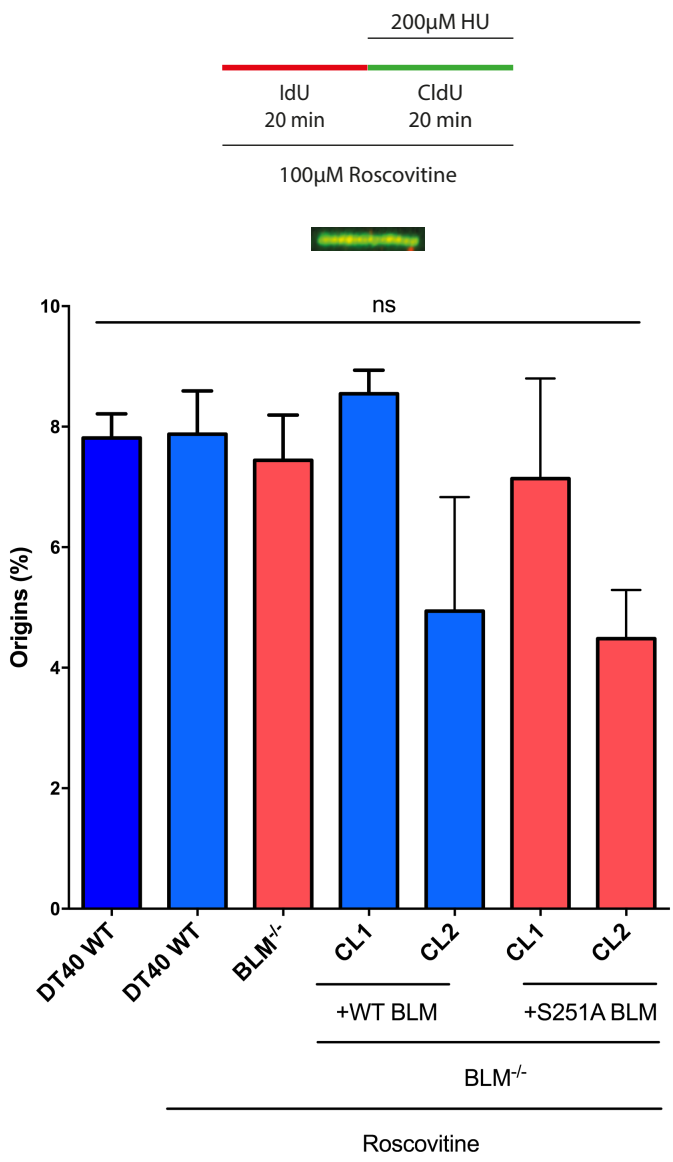


Figure 26. Top – schematic of the DNA fibre labelling experiment investigating the mechanism for completing DNA replication in response to challenge. Below – quantification of the frequency of new origin firing in DT40 WT, $BLM^{-/-}$, $BLM^{-/-}$+BLM WT and $BLM^{-/-}$ + BLM S251A cell lines following treatment with 200 µM HU in the presence of 100 µM roscovitine. The leftmost bar labelled DT40 WT signifies WT cells treated with HU, but without roscovitine (ns. P> 0.05, Student's t-test, calculated from 3 independent experimental repeats with a minimum of 100 replication structures per cell line, per repeat).). The bars represent ± s.e.m

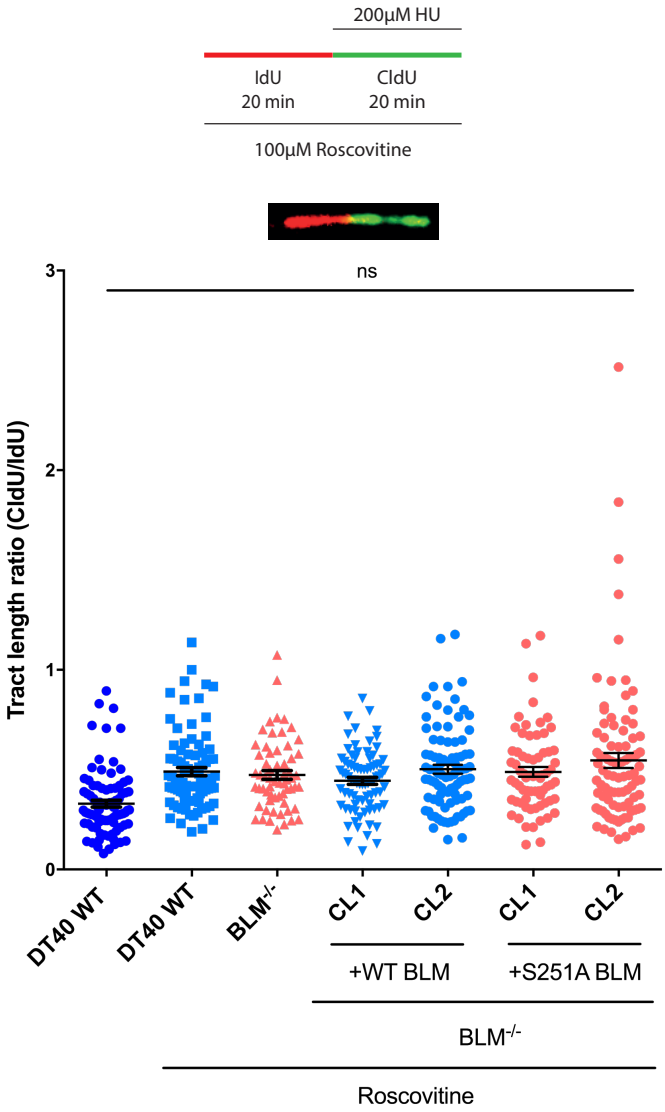


Figure 27. Top – schematic of the DNA fibre labelling experiment investigating the mechanism for completing DNA replication in response to challenge. Below – dot blot showing the ratio between the first and second labels of elongating forks in DT40 WT, $BLM^{-/-}$, $BLM^{-/-}$+BLM WT and $BLM^{-/-}$ + BLM S251A cell lines following challenge with 200 μM HU in the presence of 100 μM roscovitine. The leftmost data points labelled DT40 WT signifies WT cells treated with HU, but without roscovitine (ns. P> 0.05, Mann-Whitney test, calculated from 3 independent experimental repeats with a minimum of 30 elongating forks measured per cell line, per repeat). The bars represent ± s.e.m

3.5 Rescuing checkpoint and replication phenotypes by the fusion of TOPBP1 ATR activating domain to BLM-S251A

Results so far have demonstrated that there is a clear checkpoint and DNA replication defect in DT40 cells when the interaction between TOPBP1 and BLM has been abrogated. Previous findings from others have established that the TOPBP1 ATR activating domain (AAD) is required to stimulate ATR activity and a single mutation within this domain is sufficient to abrogate this stimulation(Kumagai et al. 2006). To investigate if the defects observed when the TOPBP1-BLM interaction was disrupted could be rescued by the presence of the minimal TOPBP1 fragment required for ATR activation, expression plasmids containing BLM-S251A fused with either the WT TOPBP1-AAD domain or TOPBP1-AAD-W1145R, which is unable to activated ATR were generated by Jadwiga Nieminuszczy and the resulting constructs used to complement $BLM^{-/-}$ cells (Kumagai et al. 2006).

3.5.1 Restoring replication phenotypes with the addition of TOPBP1-AAD to BLM-S251A

The experimental setup with HU was used to assess the tract length ratio in BLM-S251A-AAD fusion cells. The addition of TOPBP1-ADD reduced the tract length ratio to a level indistinguishable from WT cell lines, whereas the addition of the mutant AAD resulted in a tract length ratio similar to that observed in $BLM^{-/-}$ cells (**Figure 28**).

Evaluation of the frequency of replication structures revealed that the fusion of the AAD to BLM-S251A was sufficient to return levels of origin firing and stalled forks to WT levels. Cells expressing the AAD-mutant mimicked the levels of origin firing and fork stalling observed in $BLM^{-/-}$ cells (**Figure 29**). Together, these results confirm that the

phenotypes observed in BLM-S251A cells can be rescued by re-activating the ATR kinase. Thus, the inability of BLM to interact with TOPBP1 prevents proper control of the replication programme.

To investigate if the fusion of the TOPBP1-AAD to BLM-S251A also restores ATR signalling the BLM-S251A-AAD fusion cell lines were exposed to replication stress, and the phosphorylation of CHK1-S345 was monitored. This experiment was carried out by Jadwiga Nieminuszczy and is presented here with her permission. In this experiment cells were exposed to 1μM of aphidicolin for 24 hours to induce replication stress. Aphidicolin inhibits DNA polymerase α by preventing the binding of dCTP to the DNA polymerase α binding site, thus preventing replication progression (Baranovskiy et al. 2014; Krokan et al. 1981). The result of this experiment demonstrated that the fusion of BLM-S251A to TOPBP1-AAD can rescue the ATR signalling defect previously observed in $BLM^{-/-}$ and BLM-S251A cells, whereas the fusion with TOPBP1-AAD-W1145R could not restore ATR signalling. This experiment provides evidence that BLM interacts with TOPBP1 to stimulate ATR signalling.

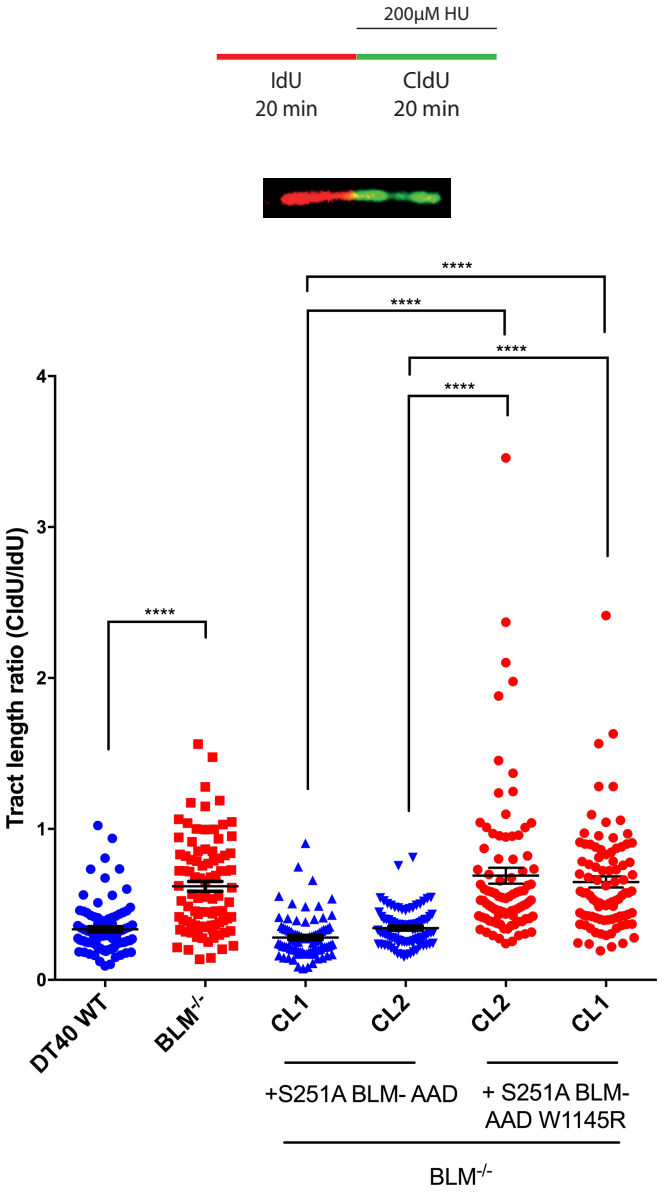


Figure 28. Top – schematic of the DNA fibre labelling experiment investigating DNA replication in response to challenge. Below – dot blot showing the ratio between the first and second labels of elongating forks in DT40 WT, $BLM^{-/-}$, $BLM^{-/-}$ - S251A – AAD and $BLM^{-/-}$ - S251A – AAD W1145R cell lines following challenge with 200 μM HU (**** $P \leq 0.0001$, Mann-Whitney test, calculated from 3 independent experimental repeats with a minimum of 30 elongating forks measured per cell line per repeat). The bars represent ± s.e.m

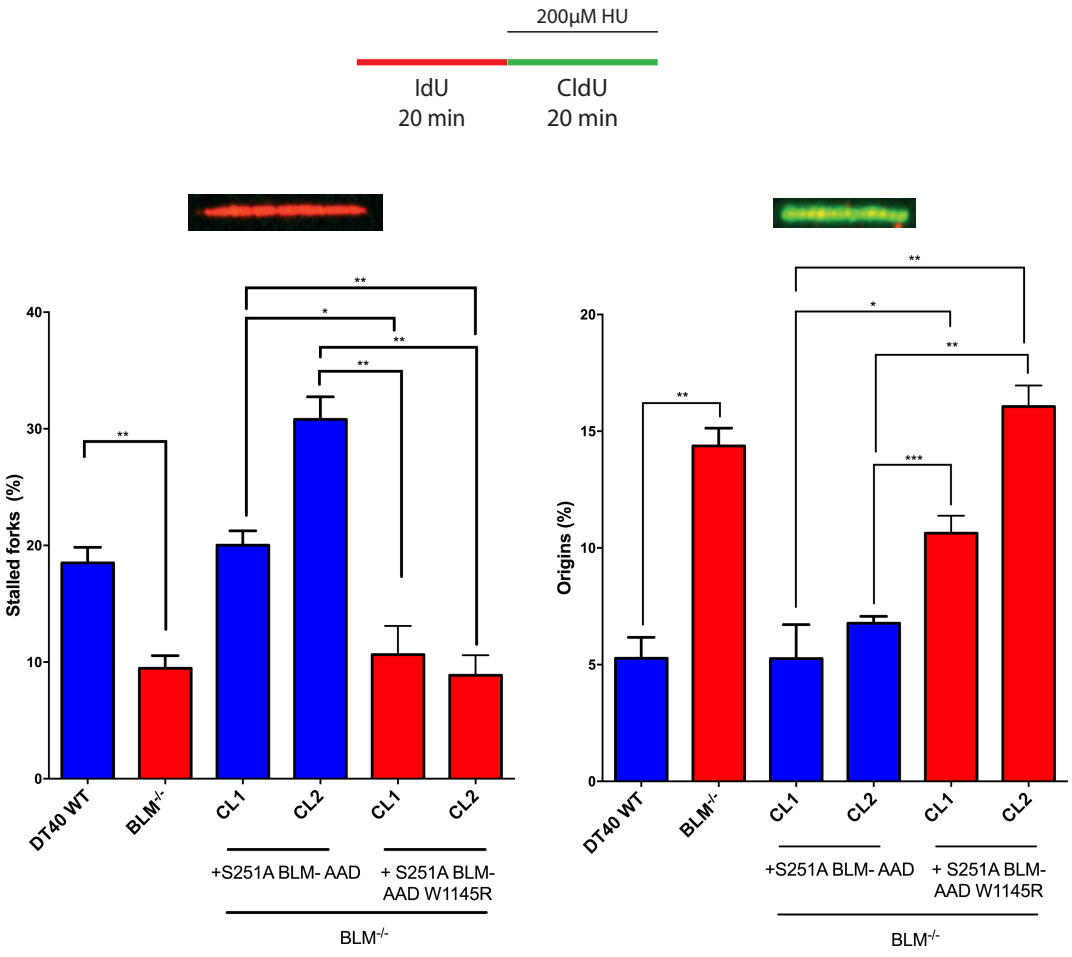


Figure 29. Top – schematic of the DNA fibre labelling experiment investigating continued DNA replication in response to challenge. Below – quantification of the frequency of new origin firing and stalled replication forks in DT40 WT, $BLM^{-/-}$, $BLM^{-/-}$ - S251A – AAD and $BLM^{-/-}$ - S251A – AAD W1145R cell lines following treatment with 200 μM HU (* $P \leq 0.05$, ** $P \leq 0.01$, *** $P \leq 0.001$, Student's t-test, calculated from 3 independent experimental repeats with a minimum of 100 replication structures per cell line per repeat). The bars represent ± s.e.m.

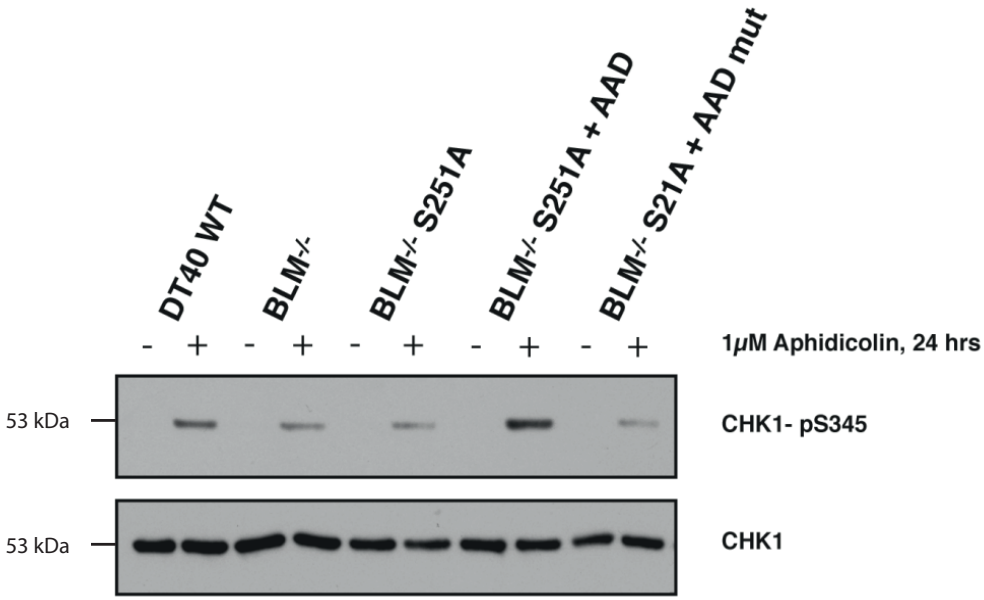


Figure 30. The ATR signalling defect observed in BLM-S251A cells can be rescued by fusing BLM-S251A to TOPBP1-AAD. The phenotype cannot be rescued by fusion to the mutated TOPBP1-AAD. DT40 WT, $BLM^{-/-}$, $BLM^{-/-}$ + BLM S251A, $BLM^{-/-}$ + BLM S251A + AAD and $BLM^{-/-}$ + BLM S251A + AAD – W1145R cell lines were treated with 1μM aphidicolin for the indicated times before harvesting for SDS-PAGE and western blotting with the antibodies as indicated. Western blot curtesy of Jadwiga Nieminuszczy.

4. Introducing the BLM-S304A mutation into human cell lines

One of the objectives of this project was to investigate the role of BLM in ATR activation, thus contributing towards the understanding of the development of disease phenotypes in Bloom syndrome patients. To achieve this, attempts were made to generate a human cell line carrying the BLM-S304A mutation.

4.1 Generating a BLM-S304A human cell line by CRISPR/Cas9

To establish a human cell line with the BLM S304A mutation the CRISPR/Cas9 system was utilised. The strategy to introduce the point mutation relied upon repairing the DSB introduced by Cas9 by HR. A template oligo containing the BLM-S304A mutation was introduced alongside the nuclease to act as a repair template (**Figure 31**). The strategy, designed by Dr Andrew Blackford, also introduced a Acu1 restriction enzyme site to allow for rapid screening of clones.

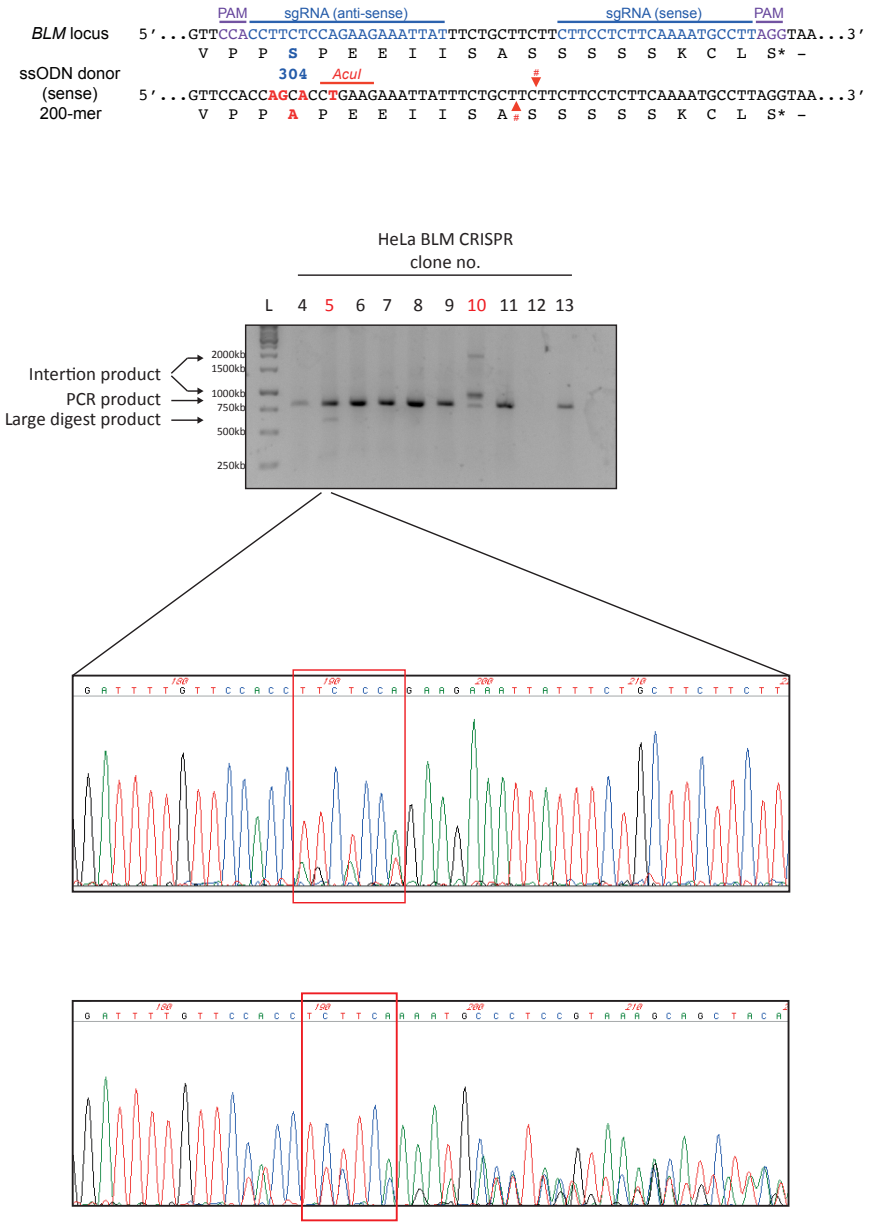


Figure 31. Top – CRISPR/Cas9 targeting strategy for introducing BLM-S304A mutation to human cells (red) and a restriction enzyme recognition site (red). The restriction enzyme cut site is indicated with red arrows. Second – restriction enzyme digest of PCR product from BLM-S304A targeted HeLa cells. Third – sequencing result from HeLa BLM CRISPR cl 5, the targeted residues highlighted within the red box. Fourth - sequencing result from HeLa BLM CRISPR cl 10, the targeted residues highlighted within the red box.

The CRISPR/Cas9 construct was transfected into cells, and single clones expanded. To test if the point mutation had been introduced into cells, genomic DNA was extracted and PCR carried out, generating a product of 805 base pairs. The PCR product was screened by restriction enzyme digest for the incorporation of the restriction enzyme site, which would be indicative of the integration of the BLM-S304A mutation. Successful digestion would generate two products, one of 593 base pairs and the second of 212 base pairs following PCR. This strategy was applied to both HeLa and RPE1 cell lines and over 100 clones were screened. No RPE1 BLM-S304A clones screened by this strategy were recovered, suggesting that the point mutation had not been successfully introduced.

Following screening of BLM-S304A CRISPR clones in HeLa cell lines, one potentially positive clone was identified, referred to as clone 5 (**Figure 31**). From the restriction enzyme digest, there are two clear bands visible in the agarose gel. The upper band corresponds to the full-length PCR product, the second to the larger of the two digest fragments. The smaller fragment is not visible in the image. This result could have arisen in two ways; the first possibility was that the BLM-S304A has been successfully introduced but the digest was incomplete, explaining the residual full-length PCR product. The second possibility was that the BLM-S304A mutation had been introduced at one allele only, giving a heterozygote cell line with both the mutant and wildtype alleles present. In order to determine if clone 5 was homo- or heterozygous for the BLM-S304A mutation the PCR product was sequenced. The sequencing data showed a double sequencing read at the positions that would have been mutated by the introduction of the BLM-S304A mutation and the restriction enzyme site (**Figure 31**). This result

suggests that the cell line is heterozygous at the BLM locus, with one copy of the WT BLM locus still being present. This cell line can therefore not be used to study the effect of the BLM-S304A on checkpoint signalling in human cells.

4.2 Identifying a BLM deficient human cell line

The second strategy to obtain a human cell line to investigate BLM-S304A was to identify a BLM knockout cell line and complement this cell line with BLM-WT or BLM-S304A cDNA, generating a system similar to the DT40 system already used. The CRISPR approach used to generate the point mutant could also give rise to BLM knockout cell lines due to other genetic alterations. The restriction enzyme digest of BLM CRISPR cl10 in HeLa suggested that some genetic changes, including insertions, were likely to have taken place in this clone (**Figure 31**, cl10). The PCR product from this cell line was therefore sequenced. The results of the sequencing showed that although some genetic changes had arisen as a result of the cutting activity of CRISPR/Cas9, the wildtype allele was still present at at least one of the alleles in this cell line, and the cell line was therefore not a full knockout (**Figure 31**, bottom panel).

To further screen the HeLa clones to identify a knockout, the cell lines generated by the CRISPR/Cas9 targeting of BLM were screened by western blot to evaluate the BLM protein levels expressed in each cell line (**Figure 32**). Although some clones were expressing a lower level of BLM, all cell lines were expressing WT BLM at some level. **Figure 32** shows cl10, discussed above. It is clear from the higher exposure of the blot, marked with an asterisk, that there is a very low level of BLM still expressed in cl10, in addition to a larger protein product probably resulting from an insertion. Several other

clones, cl1, cl12, cl21 (**Figure 32**) appear to express lower levels of BLM and could be used for later targeting to generate the point mutant or a full knockout.

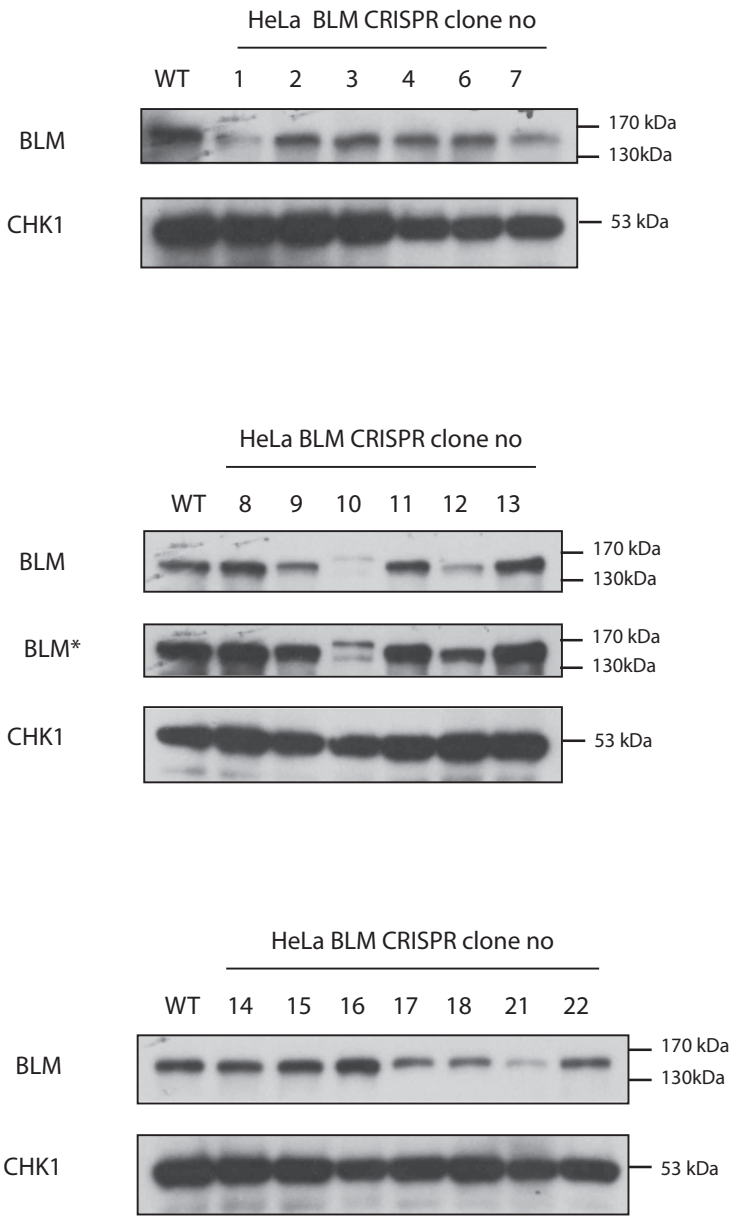


Figure 32. Investigation of BLM expression levels in HeLa clones resulting from BLM-S304A CRISPR targeting. Clones were harvested for SDS-PGE and western blotting with the antibodies as indicated.

The same strategy as above was adopted to screen clones generated by CRISPR-Cas9 targeting of BLM in RPE1. From this screen three potential BLM knockout cell lines were identified in collaboration with Drs Carl Morrow and Samuel Jones (**Figure 33**). In order to verify the clones as true BLM knockouts the clones, referred to as C7, D3 and E7, were tested for sister chromatid exchanges. An increased level of sister chromatid exchanges is a hallmark of Bloom syndrome and is used as a diagnostic tool for the disease (German et al. 1965). Therefore, if one or more of the cell lines displays increased SCEs this would be classed as a BLM knockout cell line. Cells from each of the potential BLM knockout cell lines and the wildtype parent cell line were labelled with BrdU and stained for SCEs. The results of the SCE analysis showed that of the three cell lines analysed, only D3 displayed a distinctive increase in SCEs when compared to the WT cells. Chromosomes from this cell line were riddled with crossover events, characteristic of the Bloom syndrome phenotype (**Figure 34**). The cell line RPE1-D3 was therefore classed as BLM deficient cell line and used in further experiments.

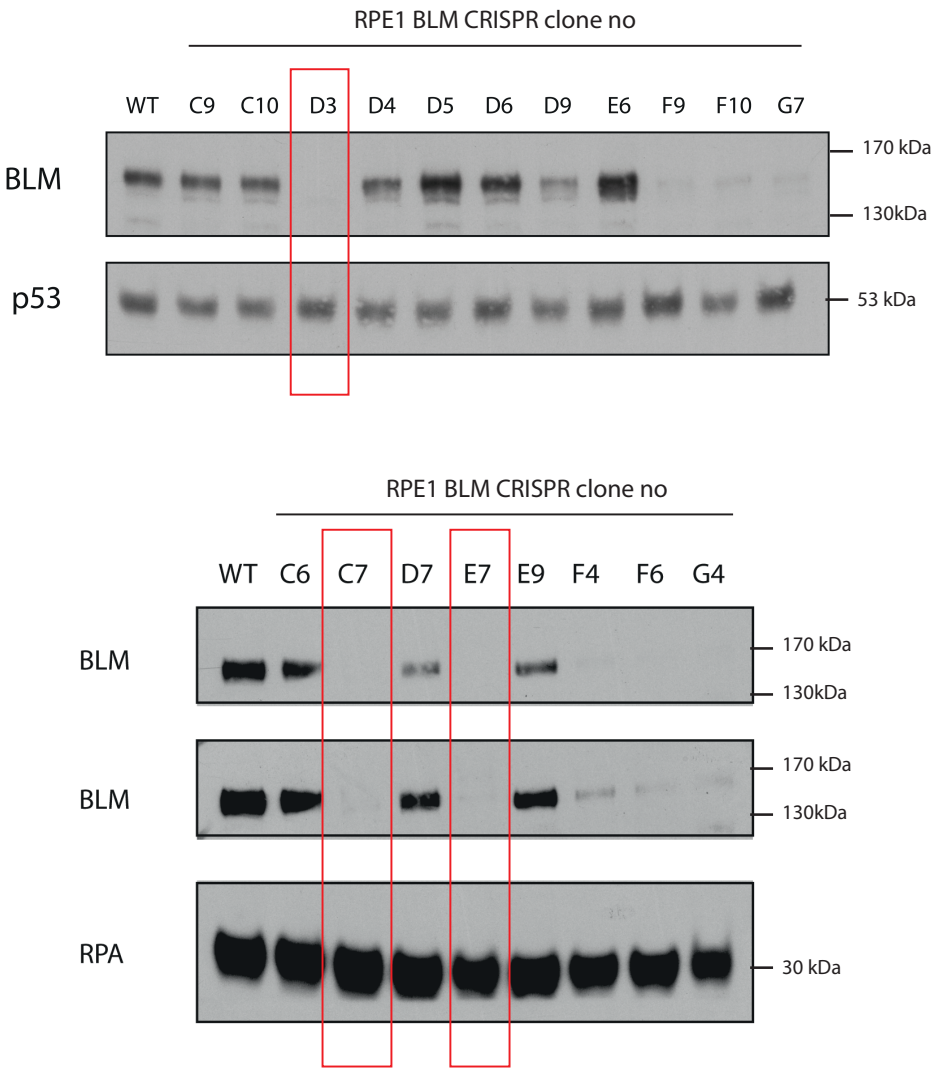


Figure 33. Investigation of BLM expression levels in RPE1 clones resulting from BLM-S304A CRISPR targeting. Clones were harvested for SDS-PGE and western blotting with the antibodies as indicated.

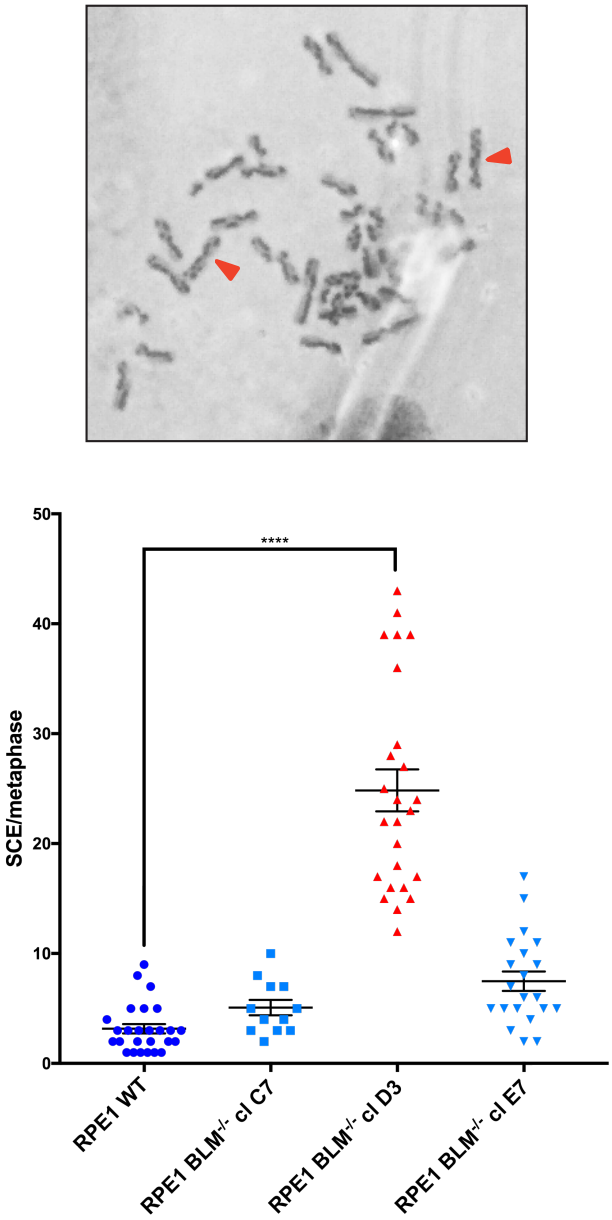


Figure 34. Top – representative image of SCEs in RPE1-D3, below – quantification of SCEs in three potential BLM-deficient RPE1 cell lines (**** $P \leq 0.0001$, Mann-Whitney test, calculated from 2 independent repeats, a minimum of 15 metaphases quantified per cell line, per repeat). The bars represent ± s.e.m.

4.3 Complementing human cell lines with BLM-WT or BLM-S304A cDNA

To generate a system allowing for the study of the role of TOPBP1-BLM interaction in human cells both the BLM deficient RPE1-D3 cell line and wildtype HeLa cells were transfected with either BLM-WT-GFP or BLM-S304A-GFP cDNA, with the aim of establishing stable cell lines expressing these constructs. As endogenous BLM is not expressed in the RPE1-D3 clone, this clone could be used for experiments if complementation was successful. As a backup strategy, wildtype HeLa cells were also complemented. If successful, this strategy would require the endogenous BLM to be knocked down with siRNA targeting the BLM 5' untranslated region (UTR) prior to experiments being carried out.

RPE1-D3 and HeLa cells were transfected with either BLM-WT-GFP or BLM-S304A-GFP cDNA and expanded whilst under selection. Once expanded, cells were sorted to single clones based on expression of GFP and left to grow on. Clones were harvested, and protein expression tested by western blot.

The western blot analysis of RPE1-D3 complemented clones identified four clones that had been successfully complemented with the BLM-WT-GFP construct. However, there was no immediately identifiable clone that had been successfully complemented with BLM-S304A-GFP (**Figure 35**). Following blotting for GFP, a faint band was seen in the BLM-S304A-GFP cl2 sample, and the total protein level in this sample, determined by CHK1 levels, was substantially lower compared to WT complemented samples. In order to determine if this clone was indeed expressing the transgene, the cell line was assessed by FACS analysis with the help of Mr Kevin Clark (WIMM FACS facility). D3-

S304A cl2 was assessed alongside RPE1-D3 as well as D3-WT cl2. This WT complemented cell line was selected as it was the clone with the lowest expression of the transgene, and therefore most likely to be suitable as a pair for BLM-S304A cl2. FACS analysis of the cell lines showed that although BLM-WT cl2 was expressing the transgene, a large number of the cells were not (**Figure 36**). Furthermore, the sample prepared from D3-S304A cl2 was only weakly positive for GFP, and not expressing the transgene at a level that was usable for experiments. One possible option to improve this would be to sort for and expand GFP-positive cells from both transfected cell lines, then testing for expression of the transgene.

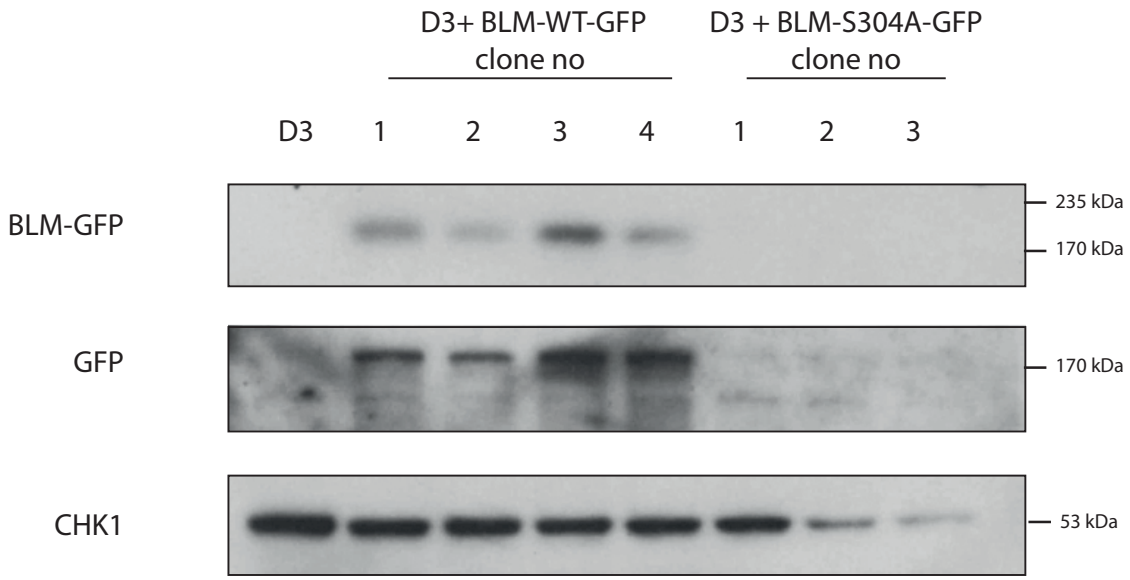


Figure 35. Investigation of BLM-WT-GFP or BLM-S304A-GFP expression levels in BLM-deficient RPE1 D3 cell line following transfection with BLM-WT-GFP or BLM-S304A-GFP cDNA. Clones were harvested for SDS-PGE and western blotting with the antibodies as indicated.

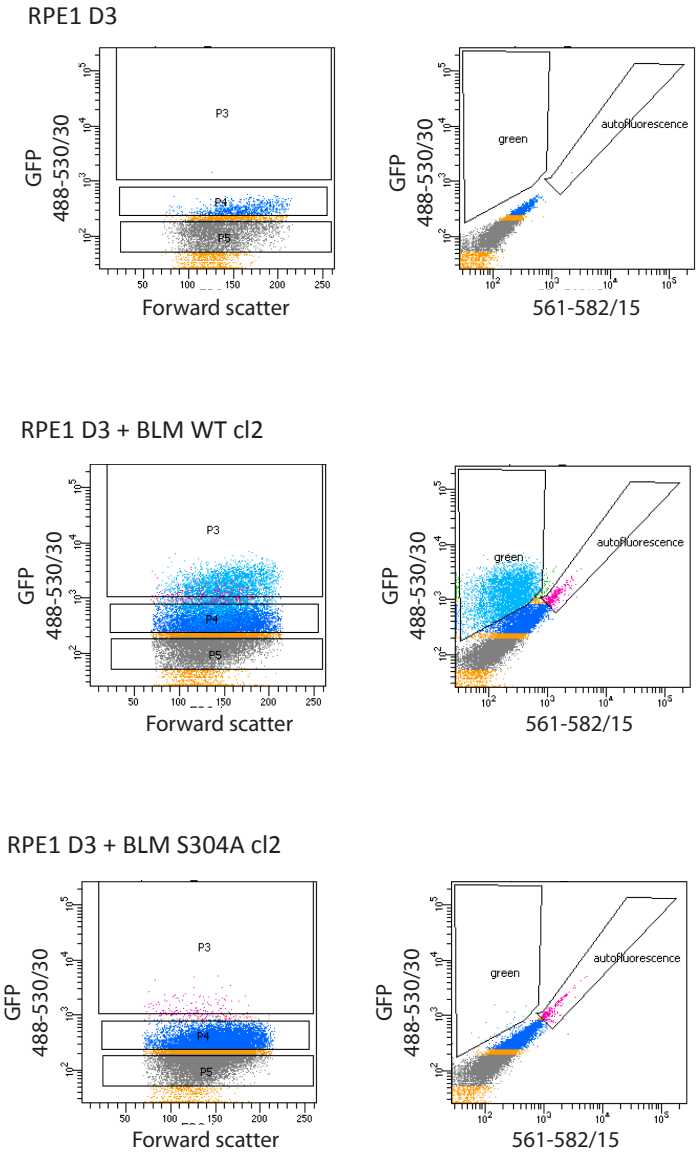


Figure 36. FACS analysis of BLM-WT-GFP or BLM-S304A-GFP expression levels in BLM-deficient RPE1 D3 cell line following transfection with BLM-WT-GFP or BLM-S304A-GFP cDNA.

When analysing the HeLa complemented clones, three clones expressing BLM-S304A-GFP were identified by the presence of a double band by western blot. The lower band signifies the endogenous BLM and the higher band the GFP-tagged transgene (**Figure 37**). However, no clones expressing a similar level of BLM-WT was found. Therefore, no usable pair of BLM-WT-GFP and BLM-S304A-GFP expressing cell lines was identified using this strategy.

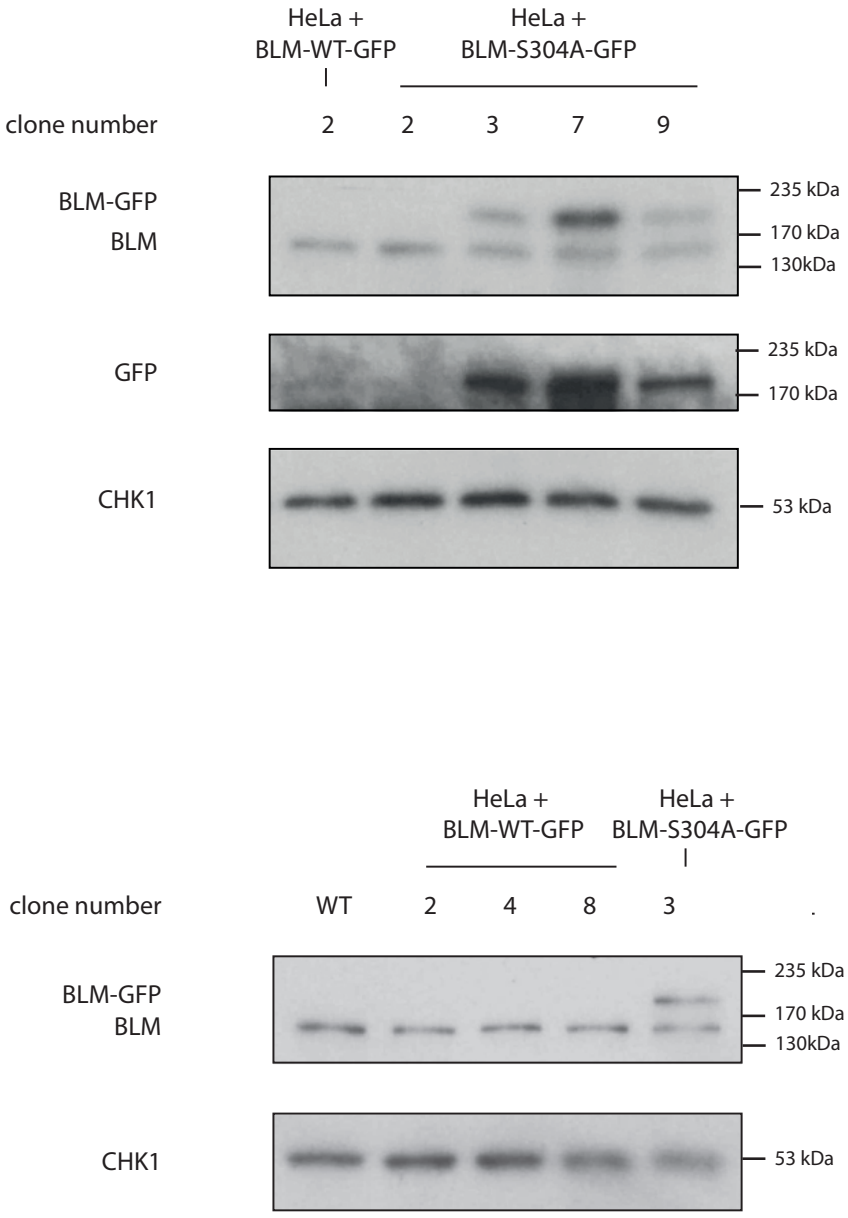


Figure 37. Complementation of HeLa cells with either BLM-S304A or BLM-WT cDNA. The lower band signifies endogenous BLM, the upper band is expression of the transgene.

5. Investigating the checkpoint response in BLM-deficient human cells

5.1 The checkpoint response in BLM-deficient RPE1 cells

In order to establish whether the phenotypes seen in DT40 cells can also be detected in BLM deficient human cells, RPE1-D3 cells were used to assess the checkpoint response in human cells. WT RPE1 and $BLM^{-/-}$ RPE1-D3 cells were treated with CPT or HU to induce replication stress and harvested for western blot. As in DT40 experiments, the phosphorylation of ATR target CHK1-S345 was used as a readout of checkpoint activity. ATR has a large number of additional targets, that are not conserved in chicken, but can be assessed in human cells. These targets include ATR-Thr1989, an auto-phosphorylation event, MCM2-S102, NBS1-S343, RPA-S33 and SMC1-S966 (Cortez et al. 2001; Nam et al. 2011; A. Y. L. Lee et al. 2007; Olson et al. 2006; Wang & Qin 2003). Assessment of additional ATR downstream targets could reveal whether BLM contributes to the direction of ATR kinase activity towards all or a subset of its targets. This may uncover if BLM is involved in ATR activation in certain circumstances, or in response to particular lesions. As a further control, the ATR inhibitor AZ20 was used to assess phosphorylation levels in the absence of ATR.

To investigate the ability of BLM deficient RPE1 cells to respond to DSBs, D3 and WT cells were treated with 100 nM CPT for 20 or 60 minutes and the phosphorylation of ATR targets assessed (**Figure 38**). Under these conditions the ATR inhibitor AZ20

reduced the level of phosphorylation of all ATR targets investigated. A reduction in the level of MCM2 S102 and CHK1 S345 phosphorylation was seen in D3 cells, comparable to what was observed in WT cells treated with the ATR inhibitor.

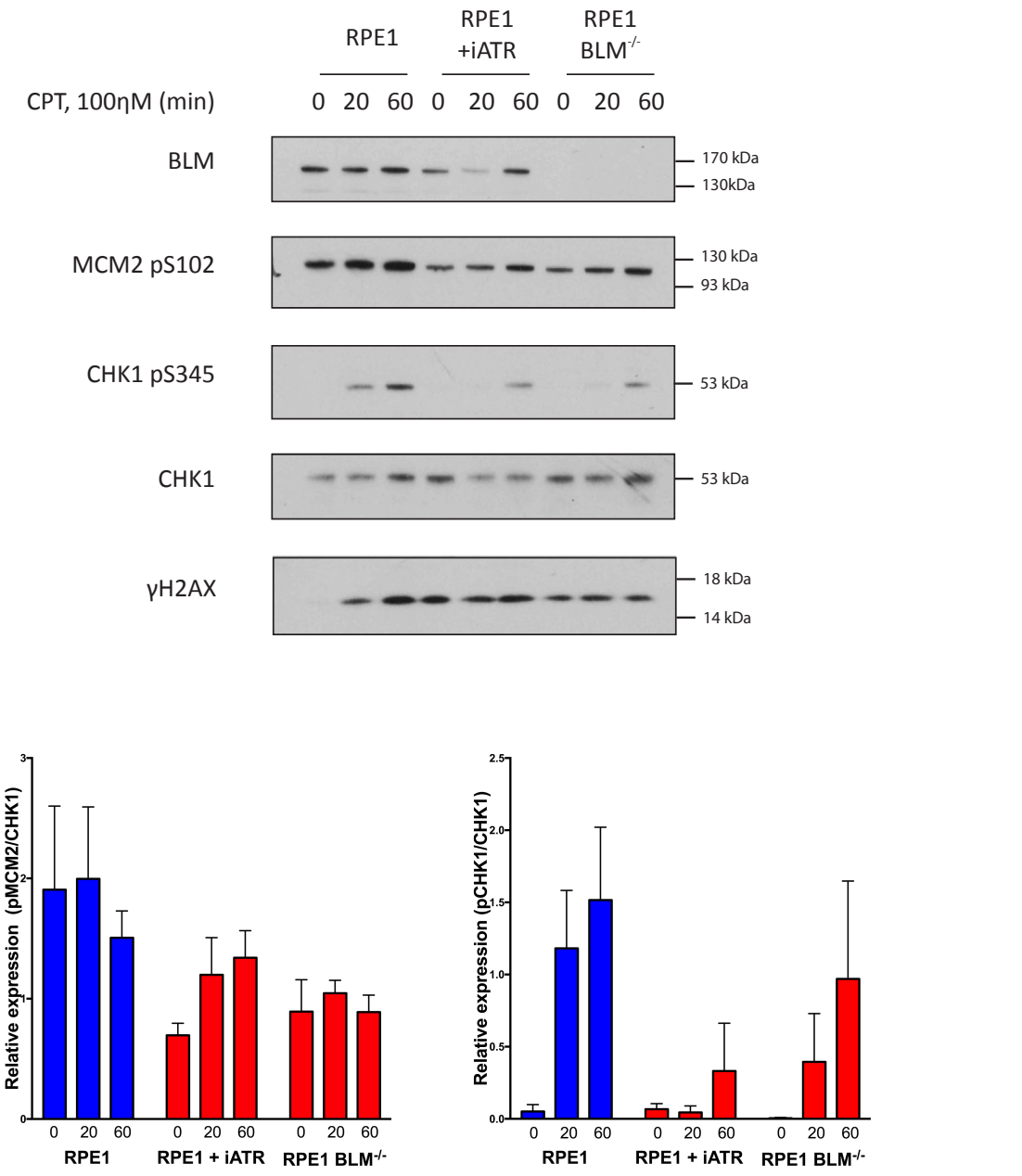


Figure 38. Top – RPE1 and RPE1-BLM$^{-/-}$ cell lines were treated with 100 nM CPT for the indicated times before harvesting for SDS-PGE and western blotting with the antibodies as specified. Acting as a control, the ATR inhibitor AZ20 at a final concentration of 3 μM was added to WT RPE1 cells 30 minutes prior to HU treatment. Below – quantification of the phosphorylation of MCM2 pS102 and CHK1 pS345 as a ratio with total CHK1 (quantified from two independent experimental repeats, error bars represent s.e.m.).

Next, WT and D3 RPE1 cells were treated with 1 mM HU for 1 or 2 hours. Following HU treatment both MCM2 S102 and CHK1 S345 had been phosphorylated in WT cells (**Figure 39**). The addition of the ATR inhibitor dramatically reduced the phosphorylation of these sites. The loss of BLM in D3 cells results in reduced phosphorylation of ATR targets MCM2 S102 and CHK1 S345.

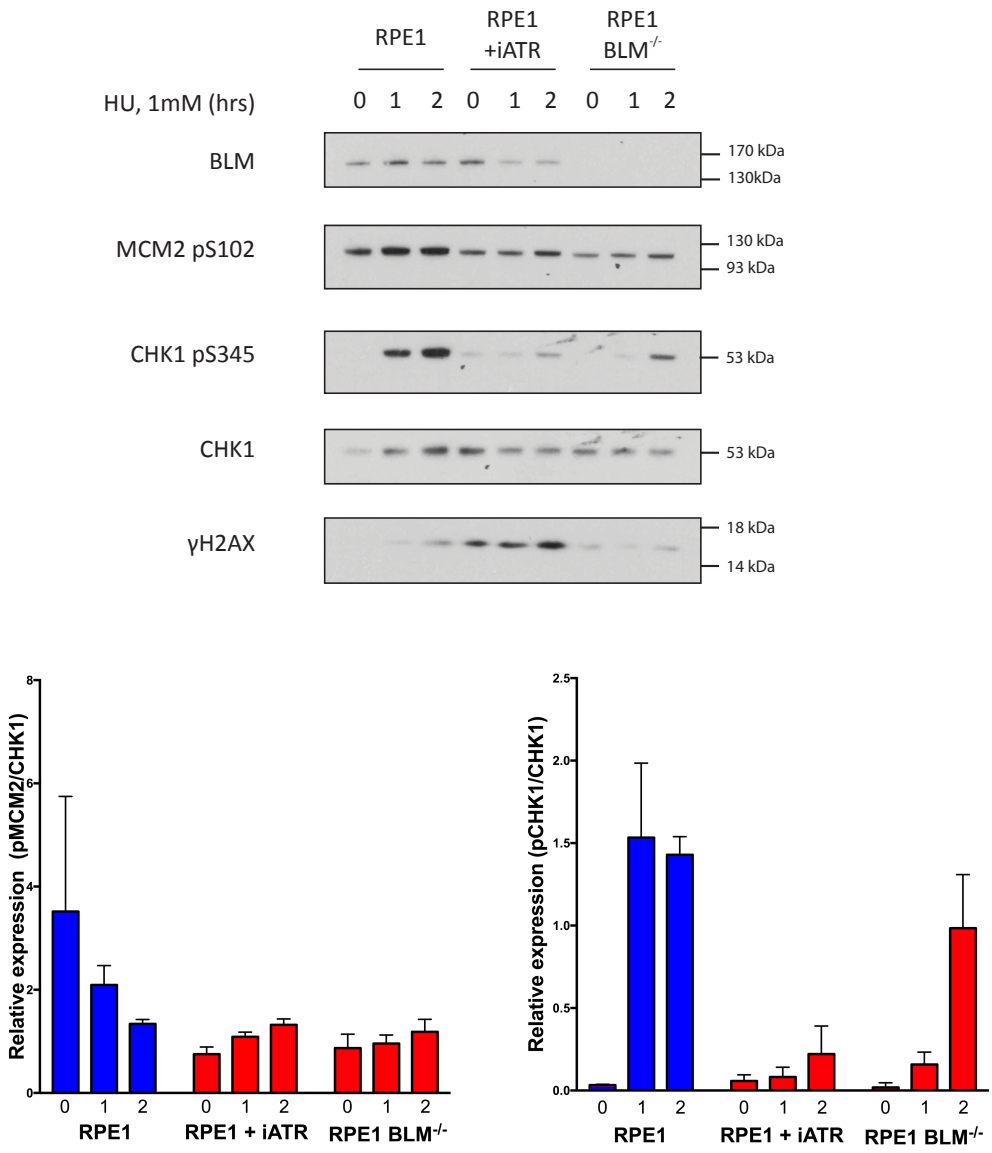


Figure 39. Top – RPE1 and RPE1-BLM$^{-/-}$ cell lines were treated with 1 mM HU for the indicated times before harvesting for SDS-PGE and western blotting with the antibodies as specified. Acting as a control, the ATR inhibitor AZ20 at a final concentration of 3 μM was added to WT RPE1 cells 30 minutes prior to HU treatment. Below – quantification of the phosphorylation of MCM2 pS102 and CHK1 pS345 as a ratio with total CHK1 (quantified from two independent experimental repeats, error bars represent s.e.m.)..

The findings presented here suggest that BLM does play a role in the activation ATR in response to replication stress induced by both HU and CPT treatment, supporting results from DT40 $BLM^{-/-}$ and BLM-S251A cells. Overall, these results demonstrate a defect in the checkpoint response due to BLM depletion in human cells, which is in support of findings from Bloom syndrome patient lines (Davies et al. 2004).

5.2 Assessing the checkpoint response in human cell lines using siRNA against BLM

To further investigate if the role of BLM in checkpoint activation, HeLa and U2OS cells were depleted of BLM using siRNA targeting the BLM 5' UTR. This avenue of investigation could reveal if the ATR-activation defect observed in BLM-deficient RPE1 cells can be observed in other human cell lines.

HeLa WT and BLM depleted HeLa cells were treated with HU in the same way as RPE1-D3 clones, allowing for comparison of the response of the cell lines to replication stress. HeLa WT cells are able to phosphorylate all ATR targets examined (**Figure 40**). BLM depletion in HeLa cells results in the reduced ability to phosphorylate MCM2 S102 and CHK1 S345 in response to HU. Similarly, the phosphorylation of ATR targets is induced in WT U2OS following replication challenge, however, the depletion of BLM in these cells resulted in the reduced ability of ATR to phosphorylate the same targets (**Figure 41**).

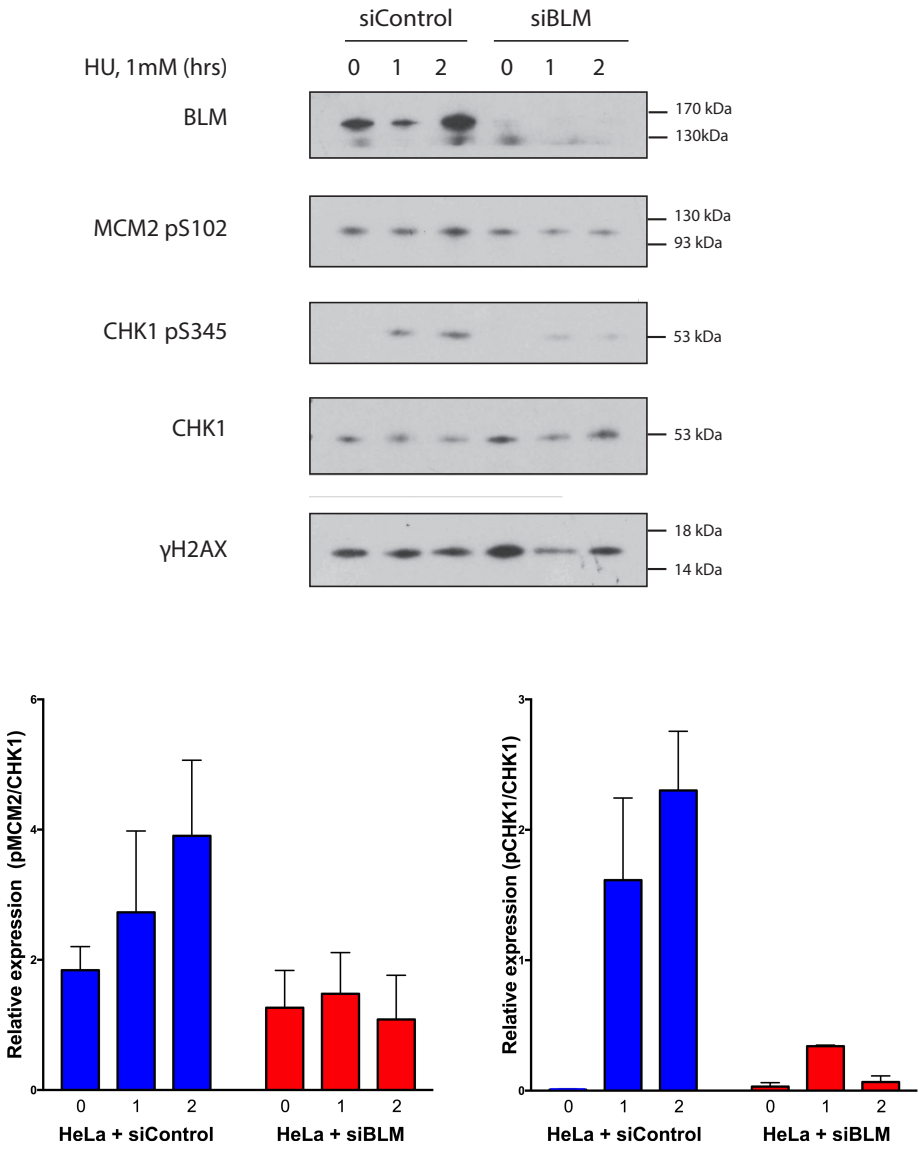


Figure 40. HeLa cells were transfected with either siControl or siBLM 72 hrs prior to treatment with 1 mM HU for the indicated times. Cells were harvested for SDS-PGE and western blotting with the antibodies as specified. Below – quantification of the phosphorylation of MCM2 pS102 and CHK1 pS345 as a ratio with total CHK1 (quantified from two independent experimental repeats, error bars represent s.e.m.).

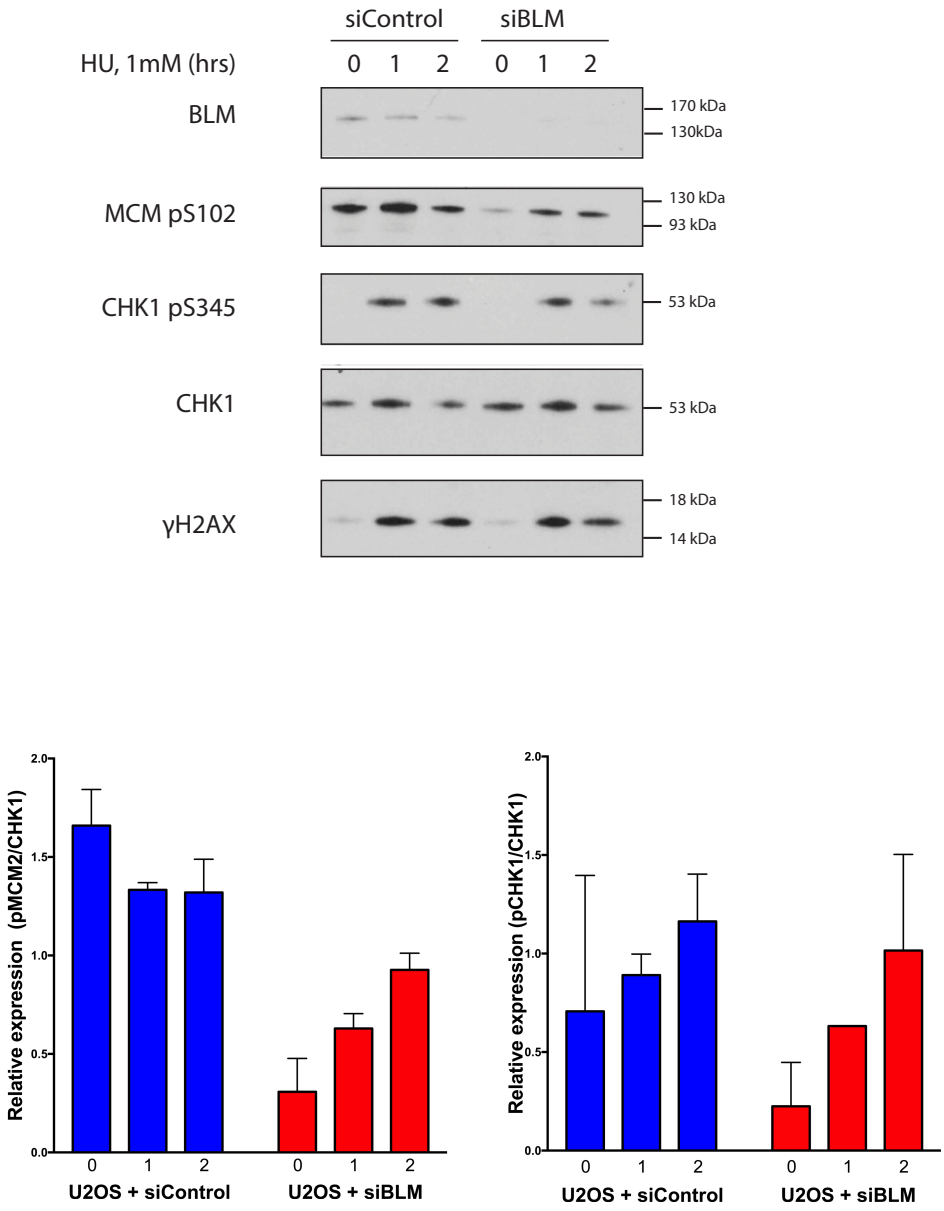


Figure 41. U2OS cells were transfected with either siControl or siBLM 72 hrs prior to treatment with 1 mM HU for the indicated times. Cells were harvested for SDS-PGE and western blotting with the antibodies as specified. Below – quantification of the phosphorylation of MCM2 pS102 and CHK1 pS345 as a ratio with total CHK1 (quantified from two independent experimental repeats, error bars represent s.e.m.).

The results obtained using siRNA knockdown of BLM in U2OS and HeLa are in support of results gained from the investigation of RPE1-D3 BLM-deficient cells.

The findings presented in this chapter demonstrate that depletion of BLM in human cell lines results in reduced ATR activity towards some of its targets following replication stress, causing an S-phase checkpoint defect. This indicates that the findings from DT40 are also conserved in human cells. However, the results do not provide information about the contribution of the TOPBP1-BLM interaction to the defect. Confirmation of the importance of this interaction in checkpoint activation would require establishing a human cell line with the point mutation, either through CRISPR/Cas9 or complementation of BLM-deficient cell lines.

It would also be necessary to extend the investigation of the replication phenotype displayed by BLM-S251A DT40 cells using DNA fibre in human cells to assess the evolutionary conservation of this mutation. To do this it would be essential to establish a robust DNA fibre technique in human cell lines. Wildtype RPE1 cells were utilised when attempting to set up the DNA fibre technique in human cells. Cells were labelled with IdU and CldU consecutively for 20 minutes, with or without HU added alongside the second label in the same way as in the DT40 experiments (**Figure 42**). Results from this trial experiment established a protocol for visualising DNA replication in RPE1 cells. These data that the DNA fibre technique can be used to investigate the replication dynamics in human RPE1 cells.

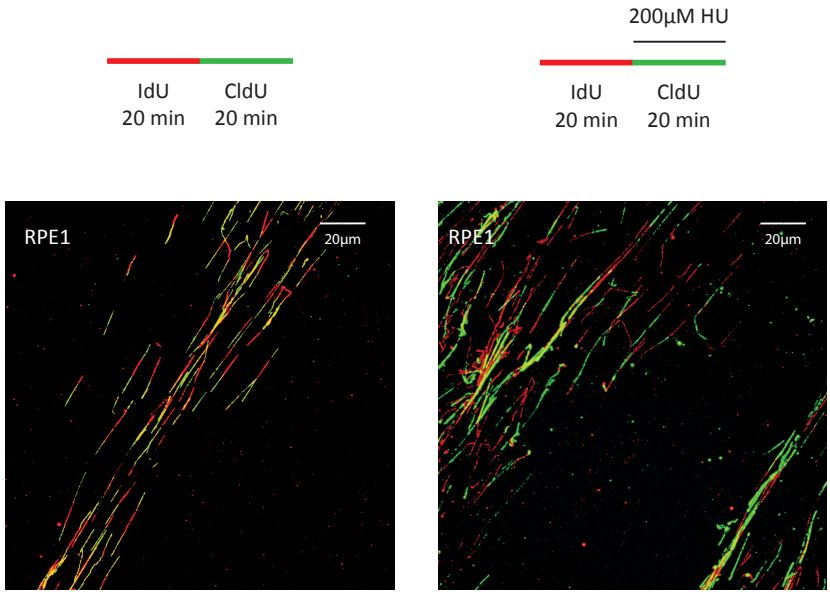


Figure 42. Top – schematic of the DNA fibre labelling experiment investigating DNA replication in unchallenged conditions (left) or investigating DNA replication during ongoing challenge (right). Below - representative images of actual DNA fibres from RPE1 cells during unchallenged replication (left) and during ongoing replication challenge (right).

6. Establishing novel DNA fibre technique variants in human cells

The final objective of this project was to establish and build upon existing techniques to further investigate the role of BLM-TOPBP1 interaction in DNA end-resection and processing of collapsed replication forks. To establish these techniques, experiments were carried out in wildtype HeLa cells and HeLa cells deficient for the nuclease EXD2.

EXD2 deficient cell lines display resection defects, spontaneous chromosomal instability and sensitivity to agents introducing replication stress (Broderick et al. 2016). Similarly, BLM has been demonstrated to promote resection of DBSs and genome instability is a hallmark of BLM-deficient cells (Gravel et al. 2008; Chaganti et al. 1974). In addition, work presented here has demonstrated that BLM-deficient cells, as well as cells with abrogated TOPBP1-BLM interaction are sensitive to a variety of DNA damaging agents. The EXD2 deficient cells were therefore used as a positive control to establish DNA fibre techniques, which can then be implemented to study the impact of BLM-S304A mutation on the processing of stressed replication forks.

6.1 Introduction

6.1.1 EXD2 in homologous recombination

Up until recently HR was been described to be initiated by the endonuclease activity of MRN complex with the support of CTIP, allowing for the initial incision into DNA and initiation of HR (Cannavo & Cejka 2014; Sartori et al. 2007). MRE11 can then facilitate

short-range resection, generating short stretches of ssDNA (Huertas & Jackson 2009; Mimitou & Symington 2008; Nicolette et al. 2010). These stretches are further extended by long-range resection carried out by EXO1 or DNA2 nucleases, supported by the helicases BLM and WRN (Zhu et al. 2008; Cejka, Cannavo, et al. 2010; Nimonkar et al. 2011; Sturzenegger et al. 2014). The ssDNA generated through resection is then coated with RPA, which is subsequently displaced by BRCA2, facilitating Rad51 filament generation and strand invasion, necessary for HR (San Filippo et al. 2008).

EXD2 was first identified as a putative 3' – 5' exonuclease through a screen for proteins involved in supressing sensitivity to mitomycin C (Smogorzewska et al. 2010). Previous observations have provided some indication that MRE11 required one or more interactions with other proteins to stimulate its nuclease activity and allow for efficient resection, which is otherwise limited (Paull & Gellert 1998; Sartori et al. 2007). New findings from Broderick and colleagues have established EXD2 as a novel HR factor. EXD2 functionally interacts with the MRN complex, utilising its exonuclease activity to accelerate resection of DSBs and facilitate HR (Broderick et al. 2016). However, EXD2 was not found to be involved in the initial sensing of the break and is therefore likely to function downstream of MRE11. The authors go on to hypothesise that EXD2 may promote initial short -range resection to generate short 3'overhangs, which in turn may promote long-range resection by acting as a substrate for BLM-EXO1 or BLM-DNA2 thus promoting HR.

Earlier this year a second study identified EXD2 as predominantly localising to the mitochondria and is required for mitoribosome integrity and efficient mitochondrial

mRNA translation (Silva et al. 2018). The authors of this study demonstrate that EXD2 depleted cells displayed multiple metabolic defects, decreased respiration and increased reactive oxygen species (ROS). Although Silva and colleagues confirm the 3' - 5' exonuclease activity of EXD2, they contradict that EXD2 is a nuclear protein and did not find that loss of EXD2 conveys sensitivity for DNA damaging agents. However, the author and others have noted that a possible role of EXD2 in DDR cannot be eliminated, as differences in experimental approaches may have prevented the detection of this role (Silva et al. 2018; Zid & Kapahi 2018). Work is ongoing to establish if EXD2 does have a dual role, one in the mitochondria and a separate function in the nucleus. A dual function for DDR proteins in the nucleus and the mitochondria is not a novel idea. Previously published work has established a role for ATR in the mitochondria, suggesting that ATR localises to the mitochondria following UV damage (Hilton et al. 2015). This study suggests that ATR localisation to the mitochondria could prolong the cell survival rate, thus allowing DNA repair to take place. It is possible that EXD2 also has a dual role similar to this.

6.2 DNA fibre analysis of untreated HeLa and EXD2 deficient cells

To further probe into the resection phenotype observed by Broderick et al, the DNA fibre technique was employed in HeLa and two EXD2 deficient clones. Firstly, untreated cells were used to investigate if EXD2 plays a role in unchallenged replication. To this end, cells were labelled sequentially with IdU and CldU for 20 minutes. There was no significant difference in the frequency of replication structures between WT and EXD2-

deficient cells (**Figure 43**), suggesting that overall DNA replication is not affected by EXD2 depletion. However, the analysis of bi-directional forks revealed that EXD2$^{-/-}$ cells were more asymmetric than wildtype cells, suggesting that individual forks are more prone to stalling in these cells (**Figure 44**). This could indicate that EXD2 plays a role in repair of endogenous lesions arising during normal DNA replication.

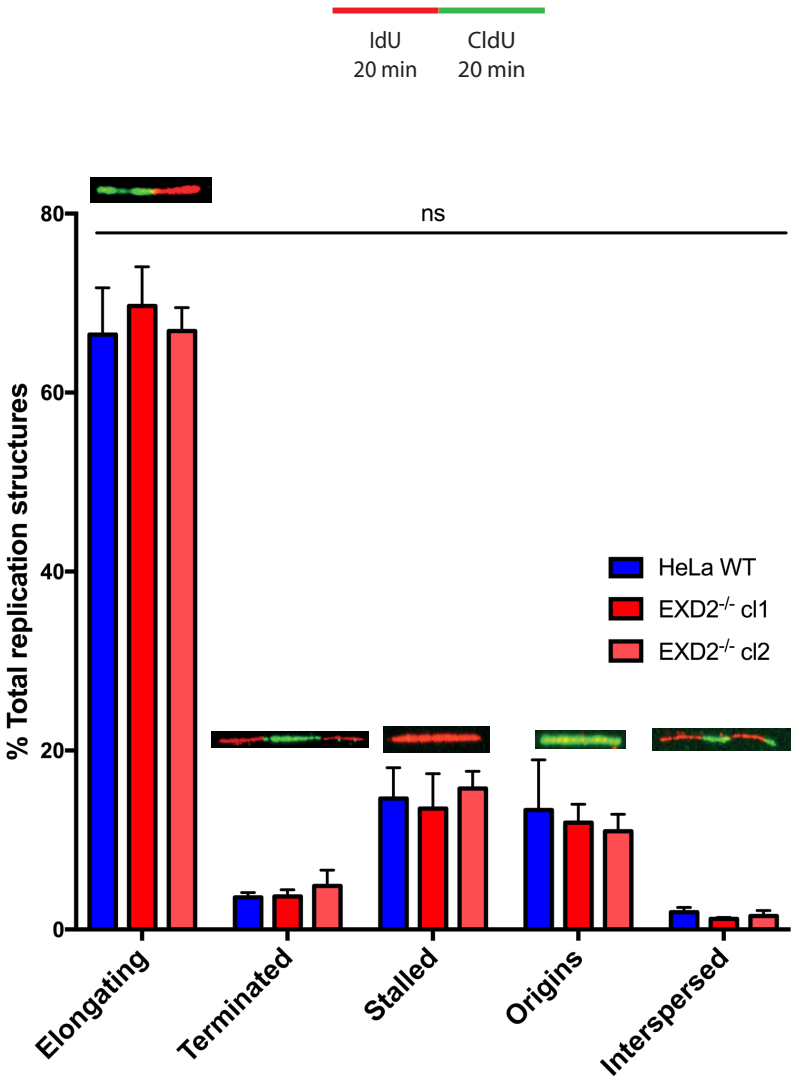


Figure 43. Top – schematic of the DNA fibre labelling experiment unchallenged continued DNA replication. Below – quantification of the frequency of occurrence of replication structures in unchallenged HeLa WT and HeLa EXD2$^{-/-}$ cell lines (ns. P> 0.05, Student's t-test, calculated based on 3 independent experimental repeats, a minimum of 100 structures counted per cell line, per repeat). The bars represent ± s.e.m

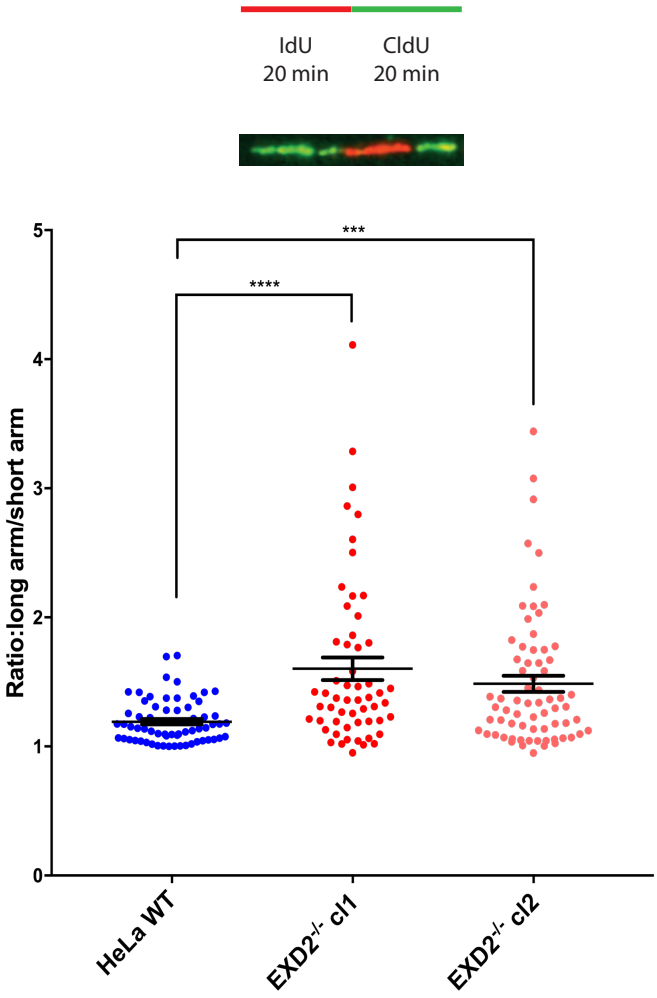


Figure 44. Top – schematic of the DNA fibre labelling experiment investigating DNA replication in unchallenged conditions. Below – dot blot showing the distribution of CldU tract length ratios of bi-directional forks in unchallenged HeLa WT and HeLa EXD2$^{-/-}$ cell lines (*** $P \leq 0.001$, **** $P \leq 0.0001$, Mann-Whitney test, calculated based on 3 independent experimental repeats, a minimum of 20 bi-directional forks measured per cell line, per repeat). The bars represent ± s.e.m.

6.3 Investigating the DNA replication phenotypes of EXD2-deficient cells following replication fork collapse

EXD2 depleted cells have been demonstrated to be sensitive to a number of DNA damaging agents, including MMC, CPT and phleomycin, which induces both single and double strand breaks in DNA (Sleigh 1976; Belenguer et al. 1995; Smogorzewska et al. 2010; Broderick et al. 2016). Cells were treated with 4 mM HU for four hours, in order to replication fork collapse in order to gain understanding the involvement of EXD2 in response to replication fork collapse (Sirbu et al. 2013). Under these conditions EXD2 deficient cell lines were found to have a decreased percentage of elongating forks and increased percentage of stalled forks compared to WT HeLa cells (**Figure 45**). In fact, the percentage decrease in elongating forks of approximately 10% in EXD2$^{-/-}$ cells when compared to WT, corresponds to the 10% increase of stalled forks seen in EXD2 deficient cells. Consistent with replication forks stalling more frequently in unchallenged EXD2$^{-/-}$, these results suggest that EXD2$^{-/-}$ cells are less able to recover collapsed forks.

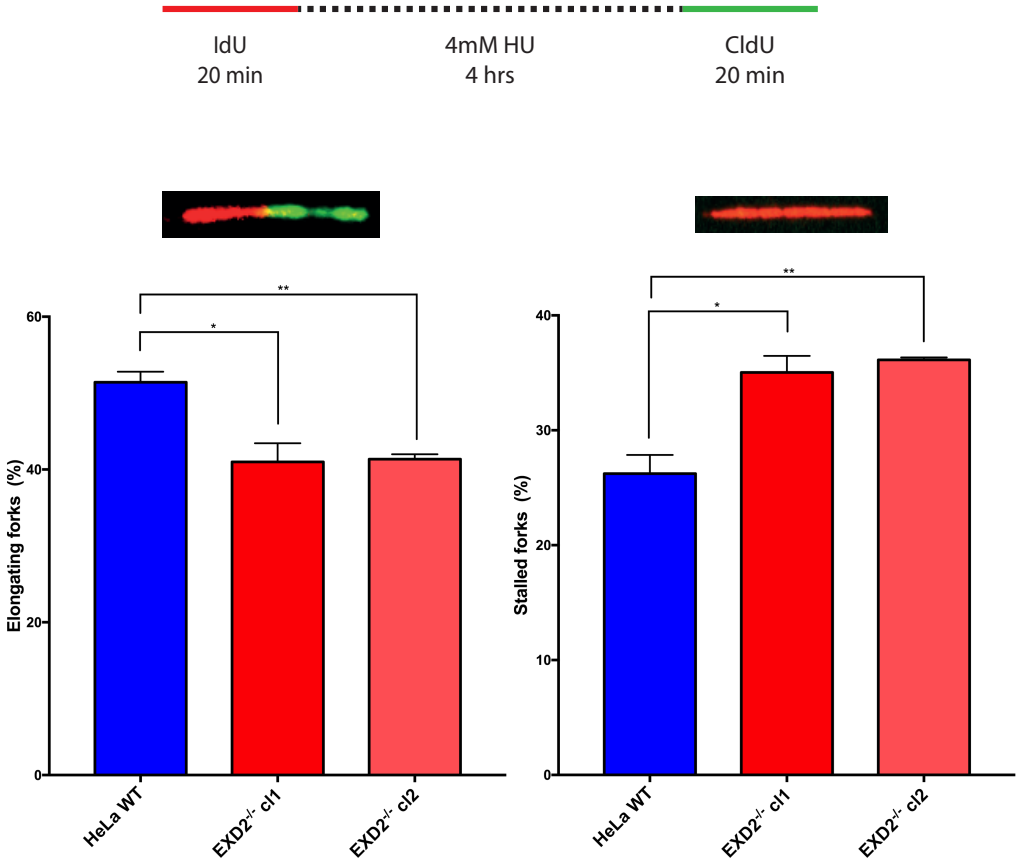


Figure 45. Top – schematic of the DNA fibre labelling experiment investigating the cellular response to replication fork collapse. Below – quantification of the frequency of elongating and stalled replication forks HeLa WT and HeLa EXD2$^{-/-}$ cell lines following replication fork collapse (* $P \leq 0.05$, ** $P \leq 0.01$, Student's t-test, calculated based on 3 independent experimental repeats, a minimum of 100 structures counted per cell line, per repeat). The bars represent ± s.e.m

When assessing fork symmetry in cells treated with HU it was clear that there were very few bi-directional forks which could be quantified following fork collapse. It is possible that this could be attributed to the high overall level of fork stalling in EXD2-deficient cells with this dose of HU, as demonstrated in **Figure 45**. Thus, the likelihood of two forks restarting following the treatment may be very small, resulting in a small number of these structures to be visualised. Although the small number of bi-directional forks investigated in these experiments indicate a trend of increased fork stalling in the two mutant HeLa cell lines, the insufficient data set precludes from drawing a firm conclusion (**Figure 46**).

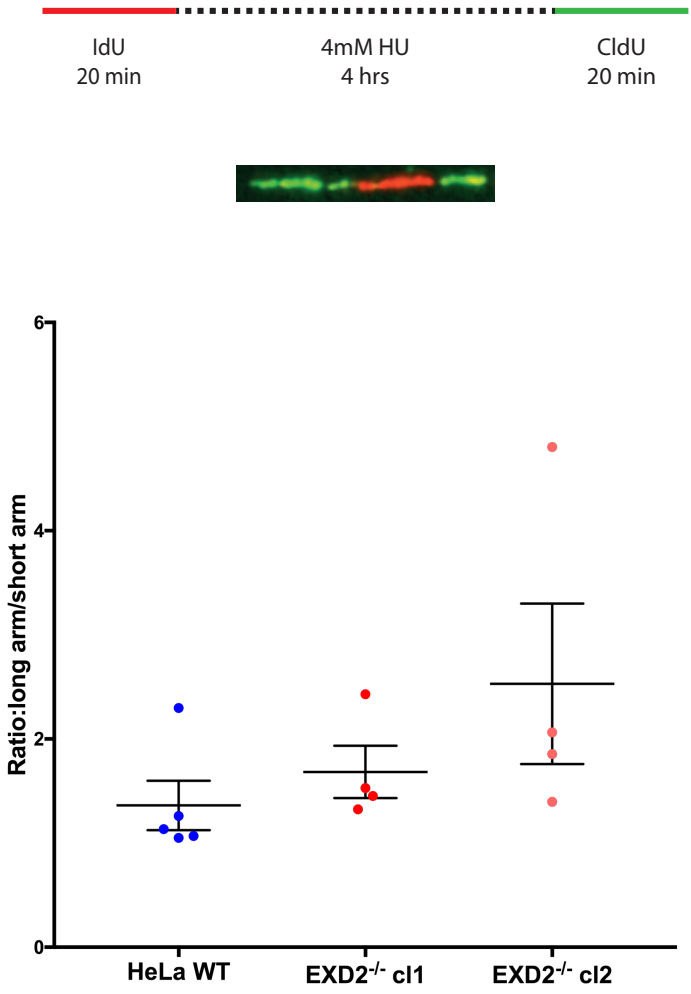


Figure 46. Top – schematic of the DNA fibre labelling experiment investigating the cellular response to replication fork collapse. Below – dot blot showing the distribution of CldU tract length ratios of bi-directional forks in HeLa WT and HeLa EXD2$^{-/-}$ cell lines following replication fork collapse. (based on 3 independent experimental repeats) The bars represent ± s.e.m.

6.4 Evaluating DNA resection of stressed replication forks in HeLa and EXD2 deficient cells

As EXD2 has been found to be involved in efficient DNA end resection and proposed to support the MRN complex to generate the initial stretches of ssDNA to initiate HR, the DNA fibre technique was used to further assess the resection in EXD2 deficient cells (Broderick et al. 2016). To allow for the evaluation of DNA resection of stressed replication forks, the cells were labelled consecutively with each IdU and CldU for 20 minutes. Cells were subsequently treated with 4 mM of HU for 4 hours, causing replication fork collapse and allowing resection to take place.

The ratio between the red and green track was used to assess the extent of resection taking place. In this case the length of the first label (IdU) is divided by the length of the second (CldU). The track from the first label, in this case red, is unaffected by the treatment and resection. The red track therefore signifies unperturbed replication and acts as the control track in the calculation. The second label, in green, will vary in length depending on the extent of resection taking place (**Figure 47**) (Nieminuszczy et al. 2016). If resection is taking place, the green track will become shorter during the HU treatment, leaving only a short green label after the treatment, resulting in a ratio larger than 1. In the case where replication stalls and the fork is not restarted the ratio would remain at 1. Finally, if the replication is unaffected by the drug treatment or replication is recovered during treatment then the green track will be longer than the red, giving a ratio lower than one.

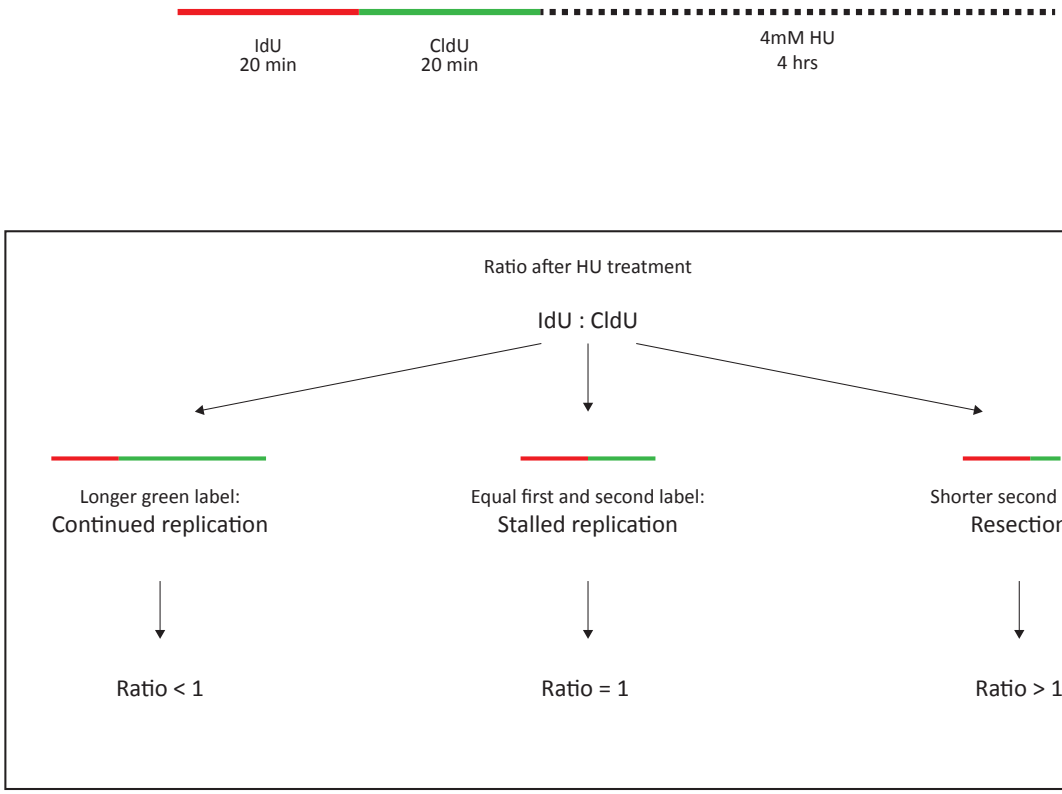


Figure 47. Top – schematic of the DNA fibre labelling experiment investigating DNA end-resection. Below – schematic illustrating the predicted change in the ratio between the first and second label of elongating forks following treatment with HU and possible resection.

When this setup was used and visualised in wildtype and EXD2-deficient HeLa cells, the results showed that the ratio between IdU and CldU was higher in both EXD2$^{-/-}$ mutants when compared to WT HeLa (**Figure 48**). These results suggest that there is increased fork resection in EXD2-deficient cell lines compared to WT HeLa cells. As EXD2 was hypothesised to contribute to the efficient resection of DNA breaks, it is surprising that loss of EXD2 results in increased resection under these conditions. One possible explanation for this is that EXD2 also plays a role in preventing excessive resection by other nucleases, and its depletion therefore results in extensive resection. Long-range resection may not be initiated efficiently in EXD2 deficient cells; thus, the over-resection phenotype may have been missing in earlier studies where resection was monitored after a shorter interval of time. This could be further investigated by looking at resection at shorter time points.

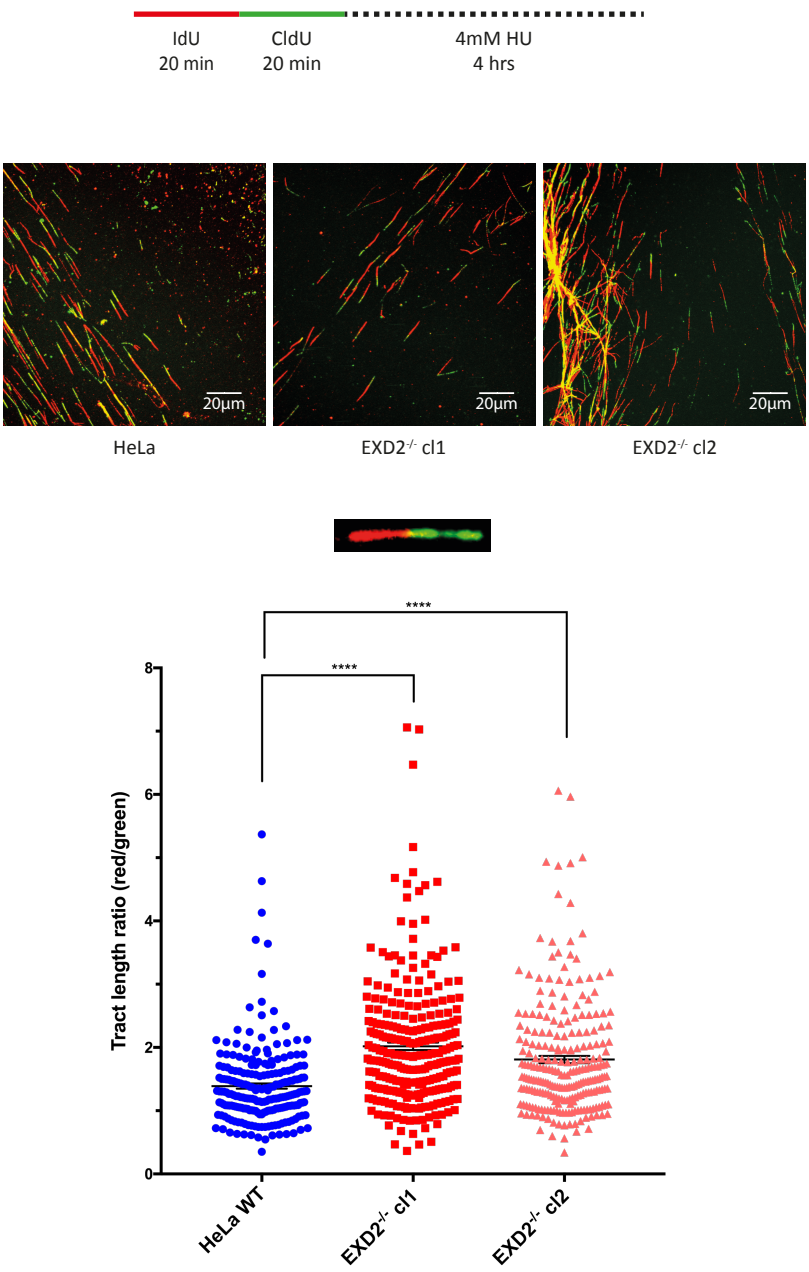


Figure 48. Top – schematic of the DNA fibre labelling experiment investigating DNA end-resection. Middle – representative images of HeLa WT and HeLa EXD2$^{-/-}$ cell lines following labelling and HU treatment as above. Bottom – dot blot showing the ratio between the first and second labels of elongating forks in HeLa and HeLa-EXD2$^{-/-}$ cell lines following challenge with 4 mM HU (**** $P \leq 0.0001$, Mann-Whitney test, calculated based on 3 independent experimental repeats, a minimum of 30 elongating forks measured per cell line, per repeat). The bars represent ± s.e.m

6.5 Investigating DNA resection in EXD2$^{-/-}$ cells co-depleted with BRCA2 or MRE11

As EXD2 has been tied to initiation of HR, the next objective was to establish if simultaneous loss of EXD2 and depletion of known HR factors MRE11 or BRCA2 would further affect the resection phenotype observed in EXD2$^{-/-}$ cells. EXD2 has been demonstrated to interact with the MRN complex and thus accelerate resection, therefore the co-depletion of EXD2 and MRE11 could provide further insight into the mechanism of efficient resection. Considering the increased resection observed in EXD2$^{-/-}$ cells, the aim was to investigate whether the depletion of MRE11 in EXD2$^{-/-}$ would reverse this phenotype, preventing resection all together.

BRCA2 is essential in regulating RAD51 function during HR, and acts downstream of EXD2 in the HR pathway, as well as being required to protect of stressed forks against unscheduled, pathological resection (Davies et al. 2001; Schlacher et al. 2011; Chaudhuri et al. 2016). It has been demonstrated that BRCA2 is involved in blocking the degradation of stalled replication forks from MRE11-dependent degradation (Schlacher et al. 2011; Lomonosov et al. 2003). This raises the question if depletion of BRCA2 alongside loss of EXD2 could lead to further resection.

Firstly, HeLa and EXD2$^{-/-}$ cell lines treated with control siRNA were compared. The same increase in resection was observed in HeLa and EXD2$^{-/-}$ cells lines treated with siRNA as when evaluating the cells without siRNA. This result demonstrated that the siRNA treatment in itself did not affect the experimental result (**Figure 49**). Next, HeLa

wildtype cells treated with siControl, siBRCA2 or siMRE11 were compared. Findings demonstrated that depletion of BRCA2, but not MRE11, resulted in an increased level of resection compared to the control (**Figure 50**). Considering the known role of MRE11 in the initiation of resection, it is unsurprising that depletion of MRE11 does not increase resection (Cejka 2015). Furthermore, the loss of BRCA2 resulting in increased resection could be due to a putative role in preventing DNA degradation at the fork (Schlacher et al. 2011; Lomonosov et al. 2003).

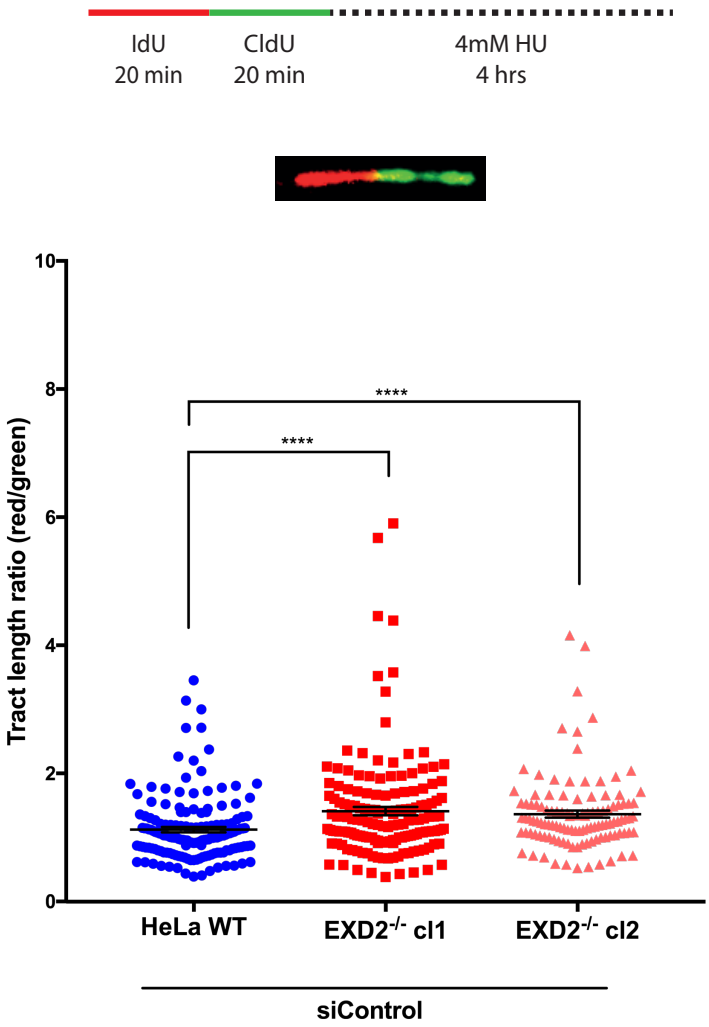


Figure 49. Top – schematic of the DNA fibre labelling experiment investigating DNA end-resection. Below – HeLa and HeLa-EXD2$^{-/-}$ cell lines were transfected with siControl 72 hrs prior to labelling and treatment as indicated above. The dot blot shows the ratio between the first and second labels of elongating forks in HeLa and HeLa-EXD2$^{-/-}$ cell lines (**** $P \leq 0.0001$, Mann-Whitney test, calculated based on 3 independent experimental repeats, a minimum of 30 elongating forks measured per cell line, per repeat). The bars represent ± s.e.m

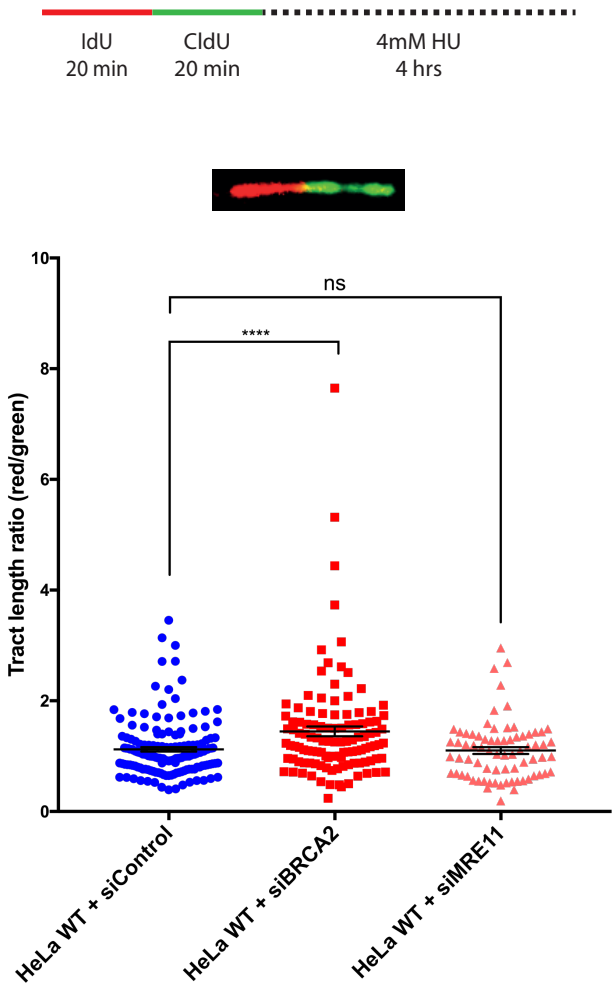


Figure 50. Top – schematic of the DNA fibre labelling experiment investigating DNA end-resection. Below – HeLa cells were transfected with siControl, siBRCA2 or siMRE11 72 hrs prior to labelling and treatment as indicated above. The dot blot shows the ratio between the first and second labels of elongating forks in HeLa cells depleted for either BRCA2 or MRE11 (**** P $\leq$ 0.0001, Mann-Whitney test, calculated based on 3 independent experimental repeats with a minimum of 30 elongating forks measured per cell line, per repeat) The bars represent $\pm$ s.e.m.

When EXD2$^{-/-}$ cell lines were depleted for BRCA2, the resection phenotype seen due to EXD2 deficiency alone was not further enhanced (**Figure 51**). In fact, the level of resection in EXD2$^{-/-}$, HeLa-siBRCA2 and EXD2$^{-/-}$-siBRCA2 cells were indistinguishable, supportive of BRCA2 and EXD2 acting in the same pathway, and loss of BRCA2 does not allow for further resection beyond what is seen in EXD2$^{-/-}$ cells. Another possible explanation may be that there is a limit to the amount of resection that is permitted within a collapsed fork as part of HR. Therefore, the abolition of a parallel pathway may not increase resection, but perhaps affect the ability of cells to recover resected forks and thus further compromising genome stability.

Depletion of MRE11 nuclease has been shown to rescue the pathological resection observed in BRCA1/2 deficient cells (Schlacher et al. 2011; Chaudhuri et al. 2016). To assess if MRE11 is also driving resection of stressed replication forks in the EXD2$^{-/-}$ cells, siRNA targeting MRE11 was employed. Depleting HeLa WT cells of MRE11 did not affect the resection profile of the cells. Depletion of MRE11 in EXD2$^{-/-}$ cells did not result in increased resection in cells beyond what was seen in EXD2$^{-/-}$ cells (**Figure 52**). These results suggest that resection seen in EXD2$^{-/-}$ cells is not dependent on the activity of the MRE11 nuclease and is most likely driven by other nucleases. A good candidate for this activity would be the DNA2 nuclease and/or EXO1 (Thangavel et al. 2015).

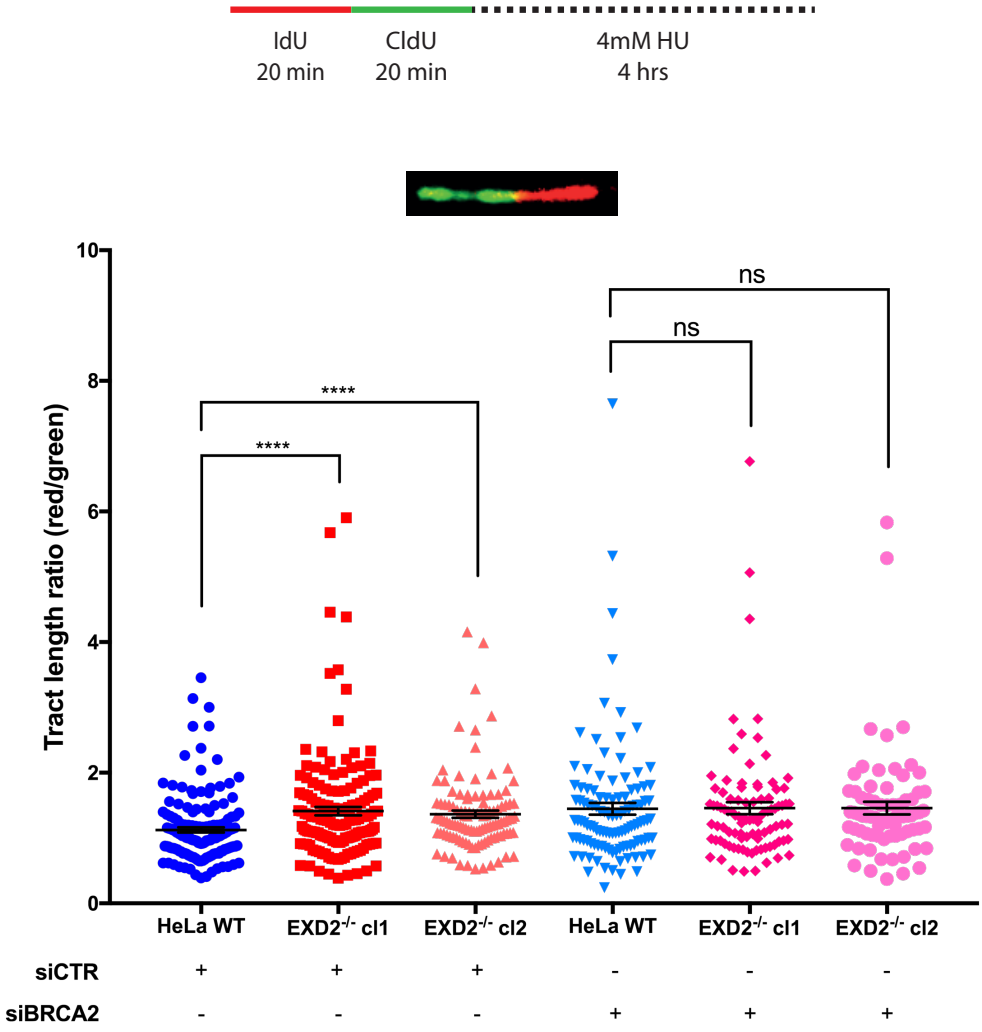


Figure 51. Top – schematic of the DNA fibre labelling experiment investigating DNA end-resection. Below – HeLa cells were transfected with siControl or siBRCA2 72 hrs prior to labelling and treatment as indicated above. The dot blot shows the ratio between the first and second labels of elongating forks in HeLa WT and HeLa-EXD2$^{-/-}$ cell lines depleted for BRCA2 (ns $P > 0.05$, **** $P \leq 0.0001$, Mann-Whitney test, calculated from 3 independent experimental repeats with a minimum of 25 elongating forks measured per cell line and condition, per repeat). The bars represent ± s.e.m

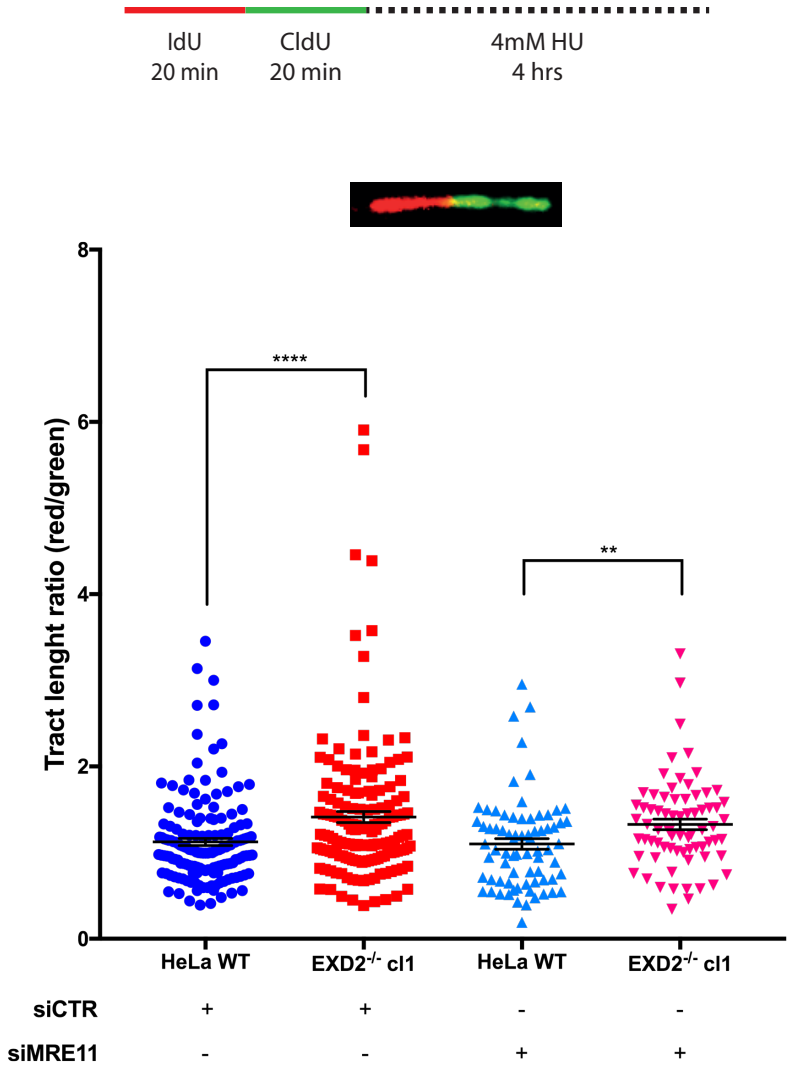


Figure 52. Top – schematic of the DNA fibre labelling experiment investigating DNA end-resection. Below – HeLa cells were transfected with siControl or siMRE11 72 hrs prior to labelling and treatment as indicated above. The dot blot shows the ratio between the first and second labels of elongating forks in HeLa WT and HeLa-EXD2$^{-/-}$ cell lines depleted for MRE11 (** $P \leq 0.01$**** $P \leq 0.0001$, Mann-Whitney test, calculated from 3 independent experimental repeats with a minimum of 25 measured events per cell line and condition, per repeat). The bars represent ± s.e.m

6.6 Concluding remarks

The results presented in this chapter demonstrate that EXD2-deficient cells are more prone to replication stalling following replication fork collapse. Furthermore, EXD2$^{-/-}$ cells exhibit an over-resection phenotype following replication fork collapse caused by prolonged exposure to a high dose of HU. Together these results suggest that EXD2 has a role in the control of resection and preventing fork stalling. The long stretches of ssDNA resulting from over-resection have been suggested to be susceptible to clustered mutations that can underlie cancer development, suggesting EXD2 could have a role in preventing cancer development (Roberts et al. 2012; Karanja et al. 2014). It is possible that the increased resection in EXD2$^{-/-}$ cells could make it problematic to restart replication, hence accounting for the increased levels of fork stalling observed in the work presented here.

The results shown here contrast publish results suggesting that EXD2 loss results in reduced resection following irradiation (Broderick et al. 2016). It is however possible that EXD2 can play a dual role in resection by encouraging efficient initiation or resection, and secondly preventing excessive resection by other nucleases through a yet unknown mechanism. It is possible that such a preventative role of EXD2 in resection only becomes apparent after the long stretches of ssDNA that are required for efficient HR have been generated (Rubnitz & Subramani 1984). Furthermore, the depletion of MRE11 did not further increase resection as seen in EXD2$^{-/-}$ cells, suggesting that the resection seen in these cells is carried out by other nucleases, possibly EXO1 of DNA2. Further investigations into the resection phenotype would be required to address

questions arising from this work, possibly including the knockdown of additional nucleases in parallel to EXD2 to investigate if this could rescue the resection phenotype seen in EXD2$^{-/-}$ cells.

6.6.1 Use in the further investigations of the TOPBP1-BLM interaction

The results presented in this chapter demonstrate that the DNA fibre technique can be efficiently implemented in human cells to evaluate a multitude of DNA replication phenotypes, including resection of stressed replication forks. Furthermore, these applications of the technique can be used in cells following knockdown of genes using siRNA.

As BLM has a known function in DNA resection, it would be interesting to investigate if the TOPBP1-BLM interaction affects this role of BLM. There is some evidence suggesting that EXO1 and BLM work in parallel pathways in DNA resection, and the depletion of both factors together resulted in a distinct resection defect (Gravel et al. 2008). By utilising the techniques outlined in this chapter, it would be possible to gain further insight into how BLM cooperates with other proteins to facilitate DNA end resection and if its interaction with TOPBP1 is involved in this.

7. Discussion and concluding remarks

Work presented in this thesis further expands on work published by Blackford et al 2015, where the interaction between TOPBP1 BRCT 4-5 and the phosphorylated BLM S304 was first identified and outlined. Here, findings confirm and expands upon the function of the interaction between TOPBP1 and BLM in the suppression of chromosomal instability. In particular, this work demonstrates the importance of TOPBP1-BLM interaction in promoting ATR checkpoint signalling and hence supporting faithful DNA replication and the maintenance of genome stability.

Previous work from our lab and others identified the interaction between TOPBP1 and BLM as required for genome stability (Blackford et al. 2015; Wang et al. 2013). However, the S338 of BLM suggested by Wang and colleagues to be important in mediating this interaction and regulating BLM protein levels is poorly conserved and in fact, not required to facilitate the interaction (Blackford et al. 2015; Sun et al. 2017). Accordingly, the crystal structure of a BLM peptide encompassing the BLM-S304 residue interacts with BRCT4-5 of TOPBP1 when phosphorylated, consistent with the known mode of function of BRCT domains (Sun et al. 2017). The evidence presented here provides further support of the role of TOPBP1-BLM interaction mediated by BLM-S304 in promoting efficient genome duplication.

7.1 BLM is required for full checkpoint activation and faithful DNA replication in DT40 cells

It has previously been shown that BLM localised to sites of DNA damage following irradiation (Bischof et al. 2001). Additionally, there are a multitude of papers presenting evidence supporting a role for BLM in S-phase checkpoint activation(Frei & Gasser 2000; Gravel et al. 2008; Davies et al. 2004; Davies et al. 2007). However, the molecular mechanism underpinning this phenotype remains unclear. Moreover, these results have been generated using BLM-depleted cells, thus not distinguishing between the enzymatic (helicase) function of BLM from other potential functions (i.e. structural). Therefore, the molecular mechanism behind this phenomenon has not been defined. Results presented here establish a possible non-enzymatic function of BLM in promoting the intra-S-phase checkpoint by facilitating full ATR activity through its interaction with TOPBP1.

7.1.1 TOPBP1-BLM interaction is required for efficient ATR signalling in DT40 cells

The data presented here show that interaction between BLM and TOPBP1 is crucial in the efficient signalling through ATR. In DT40 cells the disruption of the TOPBP1-BLM interaction through the mutation of BLM S251 resulted in the reduced ability of cells to phosphorylate ATR downstream targets in response to genotoxic stress. In particular, the phosphorylation of ATR target CHK1 was severely impaired by BLM-S251A mutation, supporting the notion that BLM is required in TOPBP1 dependent stimulation of ATR kinase activity. This finding would be further strengthened by the addition of analysis of the cell cycle profile of the $BLM^{-/-}$ and BLM-S251A mutant cells lines. Such analysis would

reveal if the ATR signalling defect observed is indeed caused by the loss of the interaction between TOPBP1 and BLM and not due to cells accumulating in other cell cycle phases. However, in support of findings presented here, previously published work utilising $BLM^{-/-}$ DT40 cells demonstrated only a slight increase in cells in G_2-M phase when compared to wild type, suggesting that the cell cycle is not dramatically affected by the loss of BLM (Wang et al. 2000).

7.1.2 Faithful DNA replication requires BLM interaction with TOPBP1

ATR has been shown to play a role in DNA replication control (Shechter et al. 2004). In particular, the S-phase checkpoint has been demonstrated to supress dormant origin firing, hence ensuring that replication only progresses once repair of DNA damage is completed (Maya-Mendoza et al. 2007). Furthermore, the interaction between TOPBP1 and ATR is required to promote the recovery of replication forks in response to replication stress (Mordes et al. 2008).

Results generated through the use of the DNA fibre technique revealed that BLM plays a key role in controlling DNA replication in response to replication stresses. The investigation of the ability of replication to progress in the presence of DNA damaging agents, either by studying fork recovery or ongoing replication during replication stress, demonstrated that BLM-S251A cells were more able to recover or continue replication when challenged. Analysis of the frequency of replication structures further revealed that BLM-S251A cells are firing more dormant origins and are stalling less than wildtype cells, indicating that both $BLM^{-/-}$ and BLM-S251A can continue replication despite replication stress, at the expense of genome stability. These phenotypes could be

reversed by the fusion of the TOPBP1-AAD to BLM-S251A but not the TOPBP1-AAD mutant that is unable to activate ATR. This confirmed that the phenotypes observed were caused by the failure of BLM to interact with TOPBP1, hence disrupting ATR signalling. Furthermore, these findings suggest that replication in the absence of ATR signalling is completed by increasing origin firing. These results are consistent with studies investigating the effect of ATR and CHK1 on checkpoint activation. These studies demonstrated that depletion of CHK1 or ATR resulted in reduced replication velocity and increased origin firing or reduced distance between origins (Petermann et al. 2006; Maya-Mendoza et al. 2007; Petermann, Woodcock, et al. 2010; Técher et al. 2016; Sanjiv et al. 2016). Interestingly, the abrogation of TOPBP1-BLM interaction did not affect fork progression or origin firing in untreated cells, suggesting that BLM is not required for maintenance of DNA replication under normal conditions. This finding is inconsistent with results from Bloom syndrome patient cell lines, where the loss of BLM resulted in reduced replication fork speed and inter-origin distances, as was observed in CHK1 and ATR deficient cells (Rao et al. 2007). This inconsistency may be caused by the differences in experimental systems and emphasises the importance of generating a human cell line that contains the BLM-S304A mutation to further investigate the replication phenotypes observed in chicken cells.

Analysis of fork symmetry following replication challenge revealed that BLM-S251A cells are increasingly asymmetric compared to WT cells. Contrary to the investigation of overall replication structures, this result suggested that individual replication forks in $BLM^{-/-}$ and BLM-S251A cells are more prone to stalling than forks in WT cells. Although these results appear contradictory, the likely explanation is that the assay investigating

fork symmetry is a more sensitive measure of fork stress than analysis of replication structures. Accordingly, investigation of the mechanism of completion of replication in BLM-S251A cells provided some explanation to this apparent conflict. The treatment of cells with the broad-spectrum cyclin-dependent kinase inhibitor roscovitine revealed that both $BLM^{-/-}$ and BLM-S251A cells were relying upon the firing of dormant origins to complete replication. This result is supported by the increase of origin firing seen in $BLM^{-/-}$ and BLM-S251A cells. Furthermore, as more origins are firing, it is possible that some stalled forks are masked by the firing of a new origin proximal to the stalled fork, resulting in what appears to be an elongating fork, thus reducing the number of observable stalled forks. It is therefore possible that $BLM^{-/-}$ and BLM-S251A are in fact less able to recover stressed replication forks. It follows, that replication in this genetic background is therefore completed through the firing of dormant origins.

These results provide evidence for a non-enzymatic role of BLM in genome stability via the activation of ATR signalling and DNA replication control. This is consistent with work by others, linking BLM deficiency to increased replication origin firing and reduced fork stability and restart, and again are consistent with findings from experiments investigating DNA replication in CHK1 and ATR deficient of depleted cells (Rao et al. 2007; Davies et al. 2007; Petermann et al. 2006; Petermann, Woodcock, et al. 2010; Sanjiv et al. 2016; Técher et al. 2017). Furthermore, results presented here suggest that the abrogation of TOPBP1-BLM interaction results in cells being less able to respond to replication stress. Previous work has demonstrated that loss of interaction between TOPBP1 and ATR also results in this phenotype (Mordes et al. 2008). This further

strengthens the hypothesis that BLM contributes to the stimulation of ATR activity through its interaction with TOPBP1.

As mentioned above, the fusion of BLM-S251A to TOPBP1 AAD was sufficient to rescue ATR signalling in DT40 cells, providing additional confirmation that BLM is involved in stimulating ATR activity through its interaction with TOPBP1. To further add to this work, it would be imperative to establish if the TOPBP1-AAD on its own could stimulate ATR signalling activity. It is noteworthy that a previous study has utilised the TOPBP1-AAD fused to the oestrogen receptor in a screen for ATR inhibitor. When this construct was translocated to the nucleus it resulted in the generalised activation of ATR, allowing for easy identification of potent ATR inhibitors (Toledo et al. 2011). To draw a firm conclusion and rule out the possibility that the use of the TOPBP1-AAD alone could stimulate ATR in the experiments presented here, it would be necessary to include a further control cell line expressing TOPBP1-AAD alone. However, the results presented here suggest that the BLM-S251A-AAD fusion does not constitutively activate ATR, as was seen in the system used by Toledo and colleagues. No ATR activation through the phosphorylation of CHK1 was seen in untreated DT40 cells expressing the BLM-S251A-AAD construct, providing evidence that the construct only activates ATR in response to replication stress and does not constitutively activate ATR.

To establish if the ATR signalling defects and replication phenotypes observed here are conclusively due to the abrogation of the interaction between TOPBP1 and BLM, further investigations into the possible contribution of the BLM helicase would be necessary. By carrying out these experiments with additional control cell lines, including a BLM

helicase mutant and a BLM-S251A/BLM helicase double mutant, it would be possible to establish how the BLM-S251A mutation affect the helicase function of BLM. This is particularly interesting as the BLM-S251A cells display an intermediate level of SCEs, a phenotype commonly attributed to the loss of BLM helicase activity in HR (Blackford et al. 2015; Bizard & Hickson 2014). It is therefore possible that the mutation of the S251 residue of BLM affects the helicase domain of BLM, preventing its normal function, and that this could account of some of the phenotypes observed here. However, it is noteworthy that the mutation of TOPBP1-K704, a residue critical for the function of the BRCT5 domain and interaction with BLM, also results in increased levels of SCEs, suggesting that this phenotype could be attributed to the abrogated interaction between TOPBP1 and BLM, and thus defective ATR activity (Blackford et al. 2015).

7.2 BLM deficiency in human cells results in an S-phase checkpoint defect

The results from BLM DT40 cell lines provide evidence that BLM plays a non-enzymatic role in S-phase checkpoint activation and replication control through its interaction with TOPBP1. However, the DT40 system has limitations; the availability of antibodies recognising phosphorylated ATR targets is limited, resulting in a restricted insight into the possible role of BLM in ATR signalling. Furthermore, given the role of replicative stress in driving tumourigenesis and the high incidence of cancer observed amongst Bloom syndrome patients, it would be of great benefit to determine the significance of BLM-TOPBP1 interaction in a mammalian system.

7.2.1 Identification of a BLM-deficient RPE1 cell line

Although CRISPR/Cas9 targeting of the BLM-S304 residue did not yield clones with the BLM-S304A mutation, it did result in the identification of the potential BLM knockout cell lines. Investigation of the level of SCEs in these three cell lines revealed that one of the three clones displayed elevated levels of SCEs, a feature characteristic of Bloom syndrome (German et al. 1965; Chaganti et al. 1974). Given that BLM protein was not detected in the other two clones by western blot analysis, but the level of SCEs in these clones was normal, it is possible that only a very low level of BLM is sufficient to suppress the SCE phenotype. A second explanation could be that some off-target effect of the CRISPR strategy has resulted in a mutation of a second gene, compensating for the SCE phenotype seen in $BLM^{-/-}$ cells. These two options could explain why although the two clones appeared to be deficient for BLM by western blot, levels of SCEs were not elevated. Sequencing of the clones could reveal if either of these two scenarios could explain the result obtained here.

7.2.2 BLM-deficient RPE1 cells exhibit an ATR signalling defect

A striking observation is that the $BLM^{-/-}$ RPE1 cells displayed a defect in ATR signalling following replication challenge. This defect was found to be similar to that observed when ATR was inhibited, suggesting that BLM, likely through its interaction with TOPBP1, plays an important role in checkpoint activation. To further expand on this analysis, it would be beneficial to examine if the TOPBP1-BLM interaction is required to direct ATR activity to additional targets, including NBS1-S343, RPA-S33 or even BLM itself (Davies et al. 2004). This would further address the question if TOPBP1-BLM interaction is required to stimulate ATR activity towards all or a subset of its substrates.

7.2.3 BLM function in ATR signalling is conserved in other human systems

The results obtained from the RPE1 BLM$^{-/-}$ cell line, discussed above, support a role for BLM in ATR activation. This finding is further reinforced by comparable results using siRNA to knockdown the expression of BLM in HeLa and U2OS cell lines. Again, depletion of BLM in these cells resulted in the decreased phosphorylation of ATR targets following replication stress. Furthermore, these results demonstrate that the role for BLM in the activation of the S-phase checkpoint is evolutionarily conserved, at least from chickens to humans.

Interestingly, a previous study of depletion of BLM in U2OS cells identified no impairment of the phosphorylation of CHK1-S345 following treatment with 1 μM CPT for 1 hour (Gravel et al. 2008). Only upon co-depletion of BLM and EXO1 was a defect observed. It is however conceivable that the difference in experimental setup and drug does used could account for the differing results. The above-mentioned study utilised a CPT at a dose that would readily induce DSBs, whereas the results presented here rely upon HU, which does not lead to an immediate collapse of replication forks following treatment (Zellweger et al. 2015). It is likely that the two drug treatments would result in the generation of different replication structures at the fork, which in turn could result in different checkpoint responses. Notably, evidence suggests that low doses of HU induce replication fork stalling and only at higher doses would result in fork collapse (Ray Chaudhuri et al. 2012; Zellweger et al. 2015). The dose of CPT used by Gravel and colleagues will generate double strand breaks (Zellweger et al. 2015). The different treatment conditions are likely to result in different amounts of RPA-coated ssDNA,

required for ATR activation, thus the ATR activation in response to lesions generated could be expected to distinct (Recolin et al. 2014). It is therefore tempting to speculate that the interaction between TOPBP1 and BLM is needed only in response to certain types of replication stresses, and that other mechanisms could trigger ATR activity in other situations. It is possible that the newly discovered ETAA1 could respond to certain types of DNA damage, either instead of or in parallel to TOPBP1, to give a robust checkpoint response (Haahr et al. 2016).

The results presented here are consistent with findings from Bloom syndrome patient cell lines, where the Bloom syndrome patient cells were found to be hypersensitive to HU (Davies et al. 2004). Furthermore, work in yeast has demonstrated that the BLM homologue Sgs1 stimulates the checkpoint kinase Rad53p upon depletion of the nucleotide pool by HU (Bjergbaek et al. 2005). Consistent with the findings of this thesis, this role of Sgs1 in Rad53 activation did not require the function of the helicase domain. This supports the notion of a non-catalytic role for BLM in S-phase checkpoint and opens up the possibility that mechanistically, this non-enzymatic function of BLM in promoting efficient activation of the replication checkpoint, is conserved from yeast to humans. Further experiments, including DNA fibre analysis of BLM depleted cell lines and experiments using a BLM-S304A mutant cell line would give additional insight into the mechanism of the structural role of BLM in ATR activation.

7.3 Developing tools to further study the involvement of BLM in checkpoint signalling and DNA replication in human cells

BLM has well-defined functions in HR, including in resection and dHJ dissolution. However, the role of the TOPBP1-BLM interaction in HR remains mostly unexplored. Previous work from the lab has demonstrated that the BLM-S251A mutation results in an intermediate increase in SCEs, between WT and $BLM^{-/-}$ cells, suggesting that TOPBP1-BLM interaction contributes to the role of BLM in genome stability maintenance and HR (Blackford et al. 2015).

To explore the contribution of TOPBP1-BLM interaction in resection of DSBs resulting from collapsed replication forks, the DNA fibre resection assay was successfully set up in human cells. Additionally, a technique of assessing replication fork collapse was implemented in HeLa cells. These techniques allow for the investigation of replication phenotypes beyond replication structures traditionally used and would provide additional insight into the contribution of TOPBP1-BLM interaction in the maintenance of genome stability.

7.4 Questions arising from this work

Work presented in this thesis has uncovered a structural, non-enzymatic role for BLM in the activation of the S-phase checkpoint and genome stability. BLM is involved in the stimulation of ATR activity via an interaction with TOPBP1, hence ensuring faithful DNA replication and suppression of genome instability. However, to gain further mechanistic

insight into this novel role of BLM in this process, a number of outstanding issues need to be addressed in future studies.

7.4.1 The contribution of TOPBP1-BLM interaction in Bloom syndrome phenotypes

The work presented here has provided new insight into the role of BLM maintaining genome integrity. However, it remains unclear how the interaction between BLM and TOPBP1 contributes towards the development of disease phenotypes in Bloom syndrome sufferers.

It is well established that inactivation of *BLM* causes cancer, and cancer is the most serious medical complication observed in sufferers of Bloom syndrome and is the most common cause of death amongst affected individuals (Cunniff et al. 2017). The majority of Bloom syndrome patients have homozygous mutations in *BLM* suggested to inactivate the *BLM* gene, either in the form of nonsense mutation or small insertion/deletion resulting in a premature stop codon within or in advance of the helicase core of the protein (Ellis et al. 1994; Li et al. 1998; Ellis et al. 1998; Straughen et al. 1998). It is therefore not surprising that the majority of mutations of *BLM* in cancer are found within the helicase domains, spanning the residues 658-1197 (Bennett & Keck 2004; Hickson 2003; Cunniff et al. 2017). However, the cancer predisposition phenotype in individuals with Bloom syndrome has mainly been attributed to BLM as a helicase and its role in multiple steps of recombination-targeted repair (Watt & Hickson 1996; Mohaghegh & Hickson 2001; Croteau et al. 2014). Interestingly, a recent study suggested that heterozygous carriers of certain germline *BLM* mutations were at increased risk of early-onset colorectal cancer emphasising the role of BLM in cancer

development in the general population (De Voer et al. 2015). Furthermore, somatic mutations in *BLM* have been identified in some cancers, confirming that BLM can play a part in tumorigenesis and tumour progression. No mutations of the S304 residue of BLM, investigated in this thesis, have been observed in sporadic cancers (data from the COSMIC catalogue, made available by Wellcome Trust Sanger Institute, http://cancer.sanger.ac.uk/cosmic). This observation raises the question if the role of BLM in ATR activation does contribute to the cancer predisposition seen in Bloom syndrome sufferers. Although BLM-S304 mutation has not been observed in cancers so far, mutations have been found in the region surrounding S304 (+/- 20bp), and it is possible that these mutations could disrupt the binding of TOPBP1 to BLM by changing the confirmation of this region of the protein. A further interesting line of investigation would be to look into if the BLM mutations found in cancers affects TOPBP1-BLM interaction and can capitulate phenotypes seen in cells where the TOPBP1-BLM interaction has been disrupted.

In addition to work in human cells, it would be valuable to investigate the role of TOPBP1-BLM interaction on an organismal level. Work is currently underway to develop a mouse model where the TOPBP1-BLM interaction has been disrupted to further investigate the potential disease phenotypes tied to the disruption of this interaction. Considering the ATR signalling defect demonstrated in the work presented here it is tempting to draw parallels between Bloom and Seckel syndromes. The two syndromes have some overlapping phenotypes, including growth defects, which could suggest some overlap in disease development (Ciccia & Elledge 2010). However, in contrast to Bloom syndrome, Seckel syndrome is not characterised by a predisposition to cancer,

suggesting that the disruption of ATR signalling could in some instances protect against cancer development (Brown & Baltimore 2000; Murga et al. 2009). This, together with the observation that BLM S304 has yet to be found to be mutated in human cancers, puts into question if the role of BLM in ATR signalling established here contributes to the cancer incidence in Bloom syndrome. Investigation of a mouse with a disrupted TOPBP1-BLM interaction could go some way in addressing the contribution of the role of BLM in ATR signalling on Bloom syndrome phenotypes, including the broad cancer incidence. It is tempting to speculate that the BLM-S309A (mouse equivalent to the human BLM S304 residue) mice may not develop cancer, similarly to Seckel mice (Brown & Baltimore 2000; Murga et al. 2009). Interestingly, attempts to generate a mouse model carrying the TOPBP1-AAD W1147R mutant that is unable to activate ATR revealed that this mutation is embryonically lethal (Zhou et al. 2013). This work went on to demonstrate that inactivation of TOPBP1-AAD in MEFs resulted in compromised CHK1 signalling following UV irradiation. These findings demonstrate a critical role for TOPBP1-dependent ATR activation in mice, and it follows from this that if BLM is involved in activation of ATR through TOPBP1 this may lead to critical phenotypes in mice. However, as BLM-deficient mice are viable, it is not likely that abrogating TOPBP1-BLM interaction in mice will be lethal (Warren et al. 2010). This mouse line would also provide insight into the role of TOPBP1-BLM in the development of other phenotypes of Bloom syndrome. In particular, it is possible that the abrogation of the interaction could affect the development of the mice, resulting in phenotypes such as growth retardation also seen in Seckel syndrome (Zeman & Cimprich 2014).

Some published work has suggested that the level of ATR signalling is crucial in protecting against cancer development, with heterozygous ATR mice display a slight increase in tumorigenesis (Brown & Baltimore 2000). Results presented here suggest that the disruption of the interaction between TOPBP1 and BLM does not completely abolish ATR signalling. In addition, previous work concerning the disruption of this mutation demonstrated that the disruption of the TOPBP1-BLM interaction resulted in increased numbers of SCEs and chromosomal aberrations (Blackford et al. 2015). These findings could be linked to a predisposition to cancer, and it is therefore possible that the mice could develop cancer.

7.4.2 BLM may interact with ETAA1 to activate ATR

Recently ETAA1 was discovered as a novel activator of ATR, providing a second mechanism for ATR activation and adding another layer of complexity to the network (Bass et al. 2016; Haahr et al. 2016; Feng et al. 2016). Interestingly, ETAA1 and TOPBP1 co-deficiency is synthetically lethal, demonstrating that ETAA1 and TOPBP1 underpin parallel pathways to ATR activation and together ensure a robust response to replication challenges (Haahr et al. 2016). It has been shown that TOPBP1 and ETAA1 are recruited to DNA damage through different mechanisms to activate ATR, suggesting that ETAA1 and TOPBP1could activate ATR in response to different types of challenges (Bass et al. 2016). It is also therefore a possibility that the remaining ATR signalling seen in the experiments here are due to activation through from ETAA1 rather than TOPBP1.

Interestingly, ETAA1 has also been shown to interact with BLM and the other components of the Bloom complex, and ETAA1-depleted cells display a 2.5 fold increase

in SCE levels compared to the 10-fold increase seen in BLM-depleted cells (Bass et al. 2016). It is therefore clear that ETAA1 interacts with BLM, however the mechanism for this interaction is not yet know. It would be interesting to establish if BLM is also involved in ATR activation through ETAA1, perhaps through a different mechanism than its interaction with TOPBP1.

7.4.2 The phosphorylation BLM and its recruitment to chromatin

To gain further insight into the regulation of TOPBP1-BLM interaction it would also be crucial to uncover the kinase responsible for phosphorylating BLM at S304. The residue sits within a potential CDK consensus motif, suggesting that the phosphorylation may be a cell-cycle dependent event.

In addition, it remains unclear how BLM and TOPBP1 would be recruited to chromatin, in order to facilitate ATR activation. A potential candidate to facilitate BLM recruitment to chromatin is FANCM. FANCM has been found to interact with BLM binding partner TOP3A, and has been linked to the maintenance of replication fork stability, ATR activation and conservation of genome integrity (Deans & West 2009; Schwab et al. 2010; Blackford et al. 2012). TOPBP1 is known to interact with a number of proteins present at chromatin following DNA damage, including Rad9 and MDC1 (Wang et al. 2011; Blackford et al. 2015; Burtelow et al. 2000; Yan & Michael 2009). It is therefore possible that TOPBP1 is recruited to chromatin by one of these proteins.

Concluding remarks

Work carried out and presented in this thesis has identified the first non-catalytic role of BLM in the maintenance of genome stability. Furthermore, findings demonstrate the importance of maintaining the interaction between TOPBP1 and BLM in order to facilitate a checkpoint response to genotoxic stress (**Figure 53**). It is tempting to speculate that this previously undocumented role of BLM could contribute towards the phenotypes observed in Bloom syndrome patients, including the developmental abnormalities and broad cancer incidence seen in these patients. In addition, this study has provided novel insight into the molecular mechanism by which cells protect their genome in the face of replicative stress. The findings presented here advance our understanding of how cells maintain genome stability, thus providing insight into tumourigenesis in the human population. In the future, such knowledge has the potential to contribute to the discovery and development of new cancer treatment strategies.

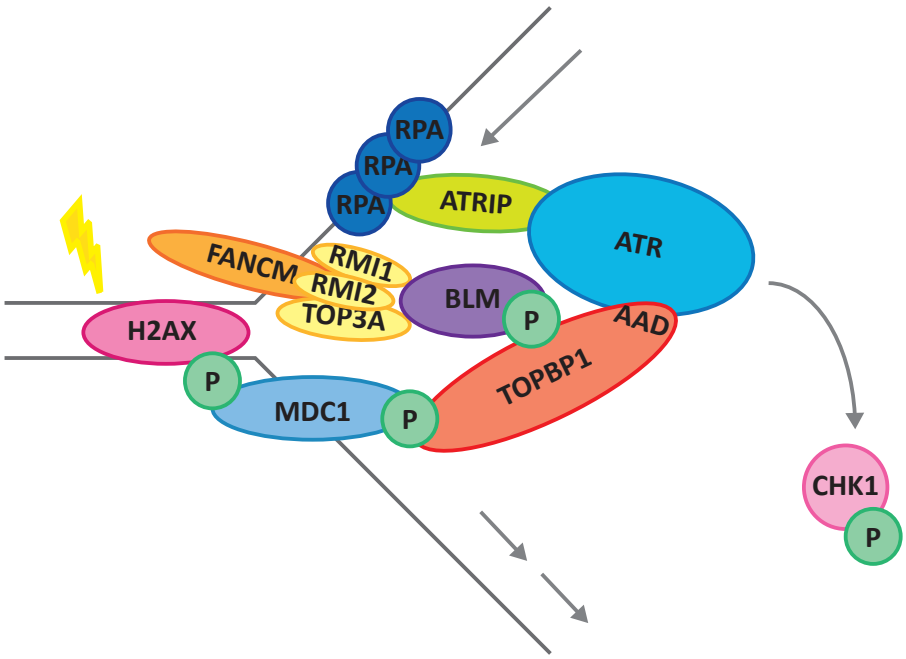


Figure 53. Model of the activation of ATR kinase activity. BLM and TOPBP1 are independently recruited to chromatin, possibly through interactions with FANCM and MDC1 respectively. This brings TOPBP1 and BLM together, interacting via TOPBP1 BRCT4-5 and the phosphorylated BLM-S304 residue. Thus, allowing for efficient ATR stimulation and S-phase checkpoint activation.

References

Bachrati, C.Z. & Hickson, I.D., 2008. RecQ helicases: Guardian angels of the DNA replication fork. *Chromosoma*, 117(3), pp.219–233.

Ball, H.L. et al., 2007. Function of a Conserved Checkpoint Recruitment Domain in ATRIP Proteins. *Molecular and Cellular Biology*, 27(9), pp.3367–3377. Available at: http://mcb.asm.org/cgi/doi/10.1128/MCB.02238-06.

Ball, H.L., Myers, J.S. & Cortez, D., 2005. ATRIP Binding to Replication Protein A-Single-stranded DNA Promotes ATR-ATRIP Localization but Is Dispensable for Chk1 Phosphorylation. *Molecular Biology of the Cell*, 16(5), pp.2372–2381. Available at: http://www.molbiolcell.org/cgi/doi/10.1091/mbc.E04-11-1006.

Baranovskiy, A.G. et al., 2014. Structural basis for inhibition of DNA replication by aphidicolin. *Nucleic Acids Research*, 42(22), pp.14013–14021.

Bartek, J., Bartkova, J. & Lukas, J., 2007. DNA damage signalling guards against activated oncogenes and tumour progression. *Oncogene*, 26(56), pp.7773–9. Available at: http://www.ncbi.nlm.nih.gov/pubmed/18066090 [Accessed January 5, 2015].

Bartkova, J. et al., 2005. DNA damage response as a candidate anti-cancer barrier in early human tumorigenesis. *Nature*, 434(April). Available at: http://www.nature.com/nature/journal/v434/n7035/abs/nature03482.html [Accessed October 24, 2014].

Bass, T.E. et al., 2016. ETAA1 acts at stalled replication forks to maintain genome integrity. *Nature Cell Biology*, 18(11), pp.1185–1195. Available at: http://www.nature.com/doifinder/10.1038/ncb3415.

Belenguer, P. et al., 1995. Effects of Phleomycin-induced DNA Damage on the Fission Yeast Schizosaccharomyces pombe Cell Cycle. , 11, pp.225–231.

Bell, S.P. & Stillman, B., 1992. ATP-dependent recognition of eukaryotic origins of DNA replication by a multiprotein complex. *Nature*, 357(6374), pp.128–134. Available at: http://www.nature.com/doifinder/10.1038/357128a0.

Bennett, R.J. & Keck, J.L., 2004. Structure and Function of RecQ DNA Helicases. *Critical Reviews in Biochemistry and Molecular Biology*, 39(2), pp.79–97. Available at: http://www.ncbi.nlm.nih.gov/pubmed/15217989.

Bermudez, V.P. et al., 2003. Loading of the human 9-1-1 checkpoint complex onto DNA by the checkpoint clamp loader hRad17-replication factor C complex in vitro. *Proceedings of the National Academy of Sciences of the United States of America*, 100(4), pp.1633–1638.

Bernstein, D.A. & Keck, J.L., 2005. Conferring substrate specificity to DNA helicases: Role of the RecQ HRDC domain. *Structure*, 13(8), pp.1173–1182.

Bischof, O. et al., 2001. Regulation and localization of the Bloom syndrome protein in response to DNA damage. *The Journal of cell biology*, 153(2), pp.367–80. Available at: http://www.pubmedcentral.nih.gov/articlerender.fcgi?artid=2169463&tool=pmc

entrez&rendertype=abstract.
Bizard, A.H. & Hickson, I.D., 2014. The dissolution of double Holliday junctions. *Cold Spring Harbor perspectives in biology*, 6(7), p.a016477. Available at: http://www.ncbi.nlm.nih.gov/pubmed/24984776 [Accessed November 2, 2014].
Bjergbaek, L. et al., 2005. Mechanistically distinct roles for Sgs1p in checkpoint activation and replication fork maintenance. *The EMBO journal*, 24(2), pp.405–17. Available at: http://www.pubmedcentral.nih.gov/articlerender.fcgi?artid=545806&tool=pmcentrez&rendertype=abstract [Accessed October 21, 2013].
Blackford, A.N. et al., 2012. The DNA translocase activity of FANCM protects stalled replication forks. *Human molecular genetics*, 21(9), pp.2005–16. Available at: http://www.ncbi.nlm.nih.gov/pubmed/22279085 [Accessed September 10, 2014].
Blackford, A.N. et al., 2015. TopBP1 Interacts with BLM to Maintain Genome Stability but Is Dispensable for Preventing BLM Degradation. *Molecular Cell*, 57(6), pp.1133–1141. Available at: http://linkinghub.elsevier.com/retrieve/pii/S1097276515001045.
Blackford, A.N. & Jackson, S.P., 2017. ATM, ATR, and DNA-PK: The Trinity at the Heart of the DNA Damage Response. *Molecular Cell*, 66(6), pp.801–817. Available at: http://dx.doi.org/10.1016/j.molcel.2017.05.015.
Bloom, L.B., 2009. Loading clamps for DNA replication and repair. *DNA Repair*, 8(5), pp.570–578.
Bosotti, R., Isacchi, A. & Sonnhammer, E.L., 2000. FAT: a novel domain in PIK-related kinases. *Trends in biochemical sciences*, 25(5), pp.225–7. Available at: http://www.ncbi.nlm.nih.gov/pubmed/10782091.
Broderick, R. et al., 2016. EXD2 promotes homologous recombination by facilitating DNA end resection. *Nature cell biology*, 18(3), pp.271–280.
Brosh, R.M. et al., 1999. Functional and physical interaction between WRN helicase and human replication protein A. *The Journal of biological chemistry*, 274(26), pp.18341–50. Available at: http://www.ncbi.nlm.nih.gov/pubmed/10373438.
Brosh, R.M. et al., 2000. Replication protein A physically interacts with the Bloom's syndrome protein and stimulates its helicase activity. *The Journal of biological chemistry*, 275(31), pp.23500–8. Available at: http://www.ncbi.nlm.nih.gov/pubmed/10825162 [Accessed November 13, 2013].
Brown, E.J. & Baltimore, D., 2000. ATR disruption leads to chromosomal fragmentation and early embryonic lethality service ATR disruption leads to chromosomal fragmentation and early embryonic lethality. *Genes & Development*, 14(626), pp.397–402.
Buerstedde, J.M. & Takeda, S., 1991. Increased ratio of targeted to random integration after transfection of chicken B cell lines. *Cell*, 67(1), pp.179–188.
Bulavin, D. V et al., 2003. Dual phosphorylation controls Cdc25 phosphatases and mitotic entry. *Nature cell biology*, 5(6), pp.545–551.
Burtelow, M.A., Kaufmann, S.H. & Karnitz, L.M., 2000. Retention of the human Rad9 checkpoint complex in extraction-resistant nuclear complexes after DNA damage. *Journal of Biological Chemistry*, 275(34), pp.26343–26348.
Byun, T.S. et al., 2005. Functional uncoupling of MCM helicase and DNA polymerase activities activates the ATR-dependent checkpoint. *Genes and Development*,

19(9), pp.1040–1052.
Caldecott, K.W., 2008. Single-strand break repair and genetic disease. *Nature reviews. Genetics*, 9(8), pp.619–31. Available at: http://www.nature.com/doifinder/10.1038/nrg2380.
Calos, M.P., Krysan, P.J. & Smith, J.G., 1993. Autonomous Replication in Human Cells of Multimers of Specific Human and Bacterial DNA Sequences. , 13(5), pp.2688–2696.
Cannavo, E. & Cejka, P., 2014. Sae2 promotes dsDNA endonuclease activity within Mre11-Rad50-Xrs2 to resect DNA breaks. *Nature*, 514(7520), pp.122–125. Available at: http://dx.doi.org/10.1038/nature13771.
Capasso, H. et al., 2002. Phosphorylation activates Chk1 and is required for checkpoint-mediated cell cycle arrest. *Journal of cell science*, 115(Pt 23), pp.4555–64. Available at: http://jcs.biologists.org/cgi/doi/10.1242/jcs.00133.
Cejka, P. et al., 2012. Decatenation of DNA by the S. cerevisiae Sgs1-Top3-Rmi1 and RPA Complex: A Mechanism for Disentangling Chromosomes. *Molecular Cell*, 47(6), pp.886–896. Available at: http://dx.doi.org/10.1016/j.molcel.2012.06.032.
Cejka, P., 2015. DNA End Resection: Nucleases Team Up with the Right Partners to Initiate Homologous Recombination. *The Journal of biological chemistry*, 290(38), pp.22931–8. Available at: http://www.ncbi.nlm.nih.gov/pubmed/26231213.
Cejka, P., Cannavo, E., et al., 2010. DNA end resection by Dna2–Sgs1–RPA and its stimulation by Top3–Rmi1 and Mre11–Rad50–Xrs2. *Nature*, 467(7311), pp.112–116. Available at: http://www.nature.com/doifinder/10.1038/nature09355.
Cejka, P., Plank, J.L., et al., 2010. Rmi1 stimulates decatenation of double Holliday junctions during dissolution by Sgs1–Top3. *Nature Structural & Molecular Biology*, 17(11), pp.1377–1382. Available at: http://www.nature.com/doifinder/10.1038/nsmb.1919.
Cescutti, R. et al., 2010. TopBP1 functions with 53BP1 in the G1 DNA damage checkpoint. *The EMBO journal*, 29(21), pp.3723–32. Available at: http://www.pubmedcentral.nih.gov/articlerender.fcgi?artid=2982761&tool=pmcentrez&rendertype=abstract [Accessed November 10, 2014].
Chaganti, R.S., Schonberg, S. & German, J., 1974. A manyfold increase in sister chromatid exchanges in Bloom's syndrome lymphocytes. *Proceedings of the National Academy of Sciences of the United States of America*, 71(11), pp.4508–12. Available at: http://www.pubmedcentral.nih.gov/articlerender.fcgi?artid=433916&tool=pmcentrez&rendertype=abstract.
Chaudhuri, A.R. et al., 2016. Replication fork stability confers chemoresistance in BRCA-deficient cells. *Nature*, 535(7612), pp.382–7. Available at: http://www.ncbi.nlm.nih.gov/pubmed/27443740.
Chen, C.F. & Brill, S.J., 2007. Binding and activation of DNA topoisomerase III by the Rmi1 subunit. *Journal of Biological Chemistry*, 282(39), pp.28971–28979.
Chen, M.-S., Ryan, C.E. & Piwnica-Worms, H., 2003. Chk1 Kinase Negatively Regulates Mitotic Function of Cdc25A Phosphatase through 14-3-3 Binding. *Molecular and Cellular Biology*, 23(21), pp.7488–7497. Available at: http://mcb.asm.org/cgi/doi/10.1128/MCB.23.21.7488-7497.2003.
Chen, S. et al., 2009. Mechanism of ATP-Driven PCNA Clamp Loading by S. cerevisiae RFC. *Journal of Molecular Biology*, 388(3), pp.431–442. Available at:

http://dx.doi.org/10.1016/j.jmb.2009.03.014.
Ciccia, A. & Elledge, S.J., 2010. The DNA Damage Response: Making It Safe to Play with Knives. *Molecular Cell*, 40(2), pp.179–204. Available at: http://dx.doi.org/10.1016/j.molcel.2010.09.019.
Conti, C. et al., 2007. Replication Fork Velocities at Adjacent Replication Origins Are Coordinately Modified during DNA Replication in Human Cells. *Molecular Biology of the Cell*, 18(8), pp.3059–3067. Available at: http://www.ncbi.nlm.nih.gov/pubmed/20941375.
Cortez, D. et al., 2001. ATR and ATRIP: Partners in Checkpoint Signaling. *Science*, 294(5547), pp.1713–1716. Available at: http://www.ncbi.nlm.nih.gov/pubmed/11721054.
Cortez, D., Glick, G. & Elledge, S.J., 2004. Minichromosome maintenance proteins are direct targets of the ATM and ATR checkpoint kinases. *Proceedings of the National Academy of Sciences*, 101(27), pp.10078–10083. Available at: http://www.pnas.org/cgi/doi/10.1073/pnas.0403410101.
Cotta-Ramusino, C. et al., 2011. A DNA damage response screen identifies RHINO, a 9-1-1 and TopBP1 interacting protein required for ATR signaling. *Science (New York, N.Y.)*, 332(6035), pp.1313–7. Available at: http://www.ncbi.nlm.nih.gov/pubmed/21659603.
Cottarel, J. et al., 2013. A noncatalytic function of the ligation complex during nonhomologous end joining. *Journal of Cell Biology*, 200(2), pp.173–186.
Couch, F.B. et al., 2013. ATR phosphorylates SMARCAL1 to prevent replication fork collapse. *Genes and Development*, 27(14), pp.1610–1623.
Croteau, D.L. et al., 2014. Human RecQ Helicases in DNA Repair, Recombination, and Replication. *Annual Review of Biochemistry*, 83(1), pp.519–552. Available at: http://www.annualreviews.org/doi/10.1146/annurev-biochem-060713-035428.
Cunniff, C., Bassetti, J.A. & Ellis, N.A., 2017. Bloom's syndrome: Clinical spectrum, molecular pathogenesis, and cancer predisposition. *Molecular Syndromology*, 8(1), pp.4–23.
Dalal, S.N. et al., 1999. Cytoplasmic localization of human cdc25C during interphase requires an intact 14-3-3 binding site. *Molecular and Cellular Biology*, 19(6), pp.4465–79.
Davies, A.A. et al., 2001. Role of BRCA2 in control of the RAD51 recombination and DNA repair protein. *Molecular Cell*, 7(2), pp.273–282.
Davies, S.L. et al., 2004. Phosphorylation of the Bloom ' s Syndrome Helicase and Its Role in Recovery from S-Phase Arrest. *Molecular and cellular biology*, 24(3), pp.1279–91.
Davies, S.L., North, P.S. & Hickson, I.D., 2007. Role for BLM in replication-fork restart and suppression of origin firing after replicative stress. *Nature structural & molecular biology*, 14(7), pp.677–9. Available at: http://www.ncbi.nlm.nih.gov/pubmed/17603497 [Accessed October 21, 2013].
Deans, A.J. & West, S.C., 2009. FANCM connects the genome instability disorders Bloom's Syndrome and Fanconi Anemia. *Molecular cell*, 36(6), pp.943–53. Available at: http://www.ncbi.nlm.nih.gov/pubmed/20064461 [Accessed October 20, 2013].
Delacroix, S. et al., 2007. The Rad9-Hus1-Rad1 (9-1-1) clamp activates checkpoint signaling via TopBP1. *Genes and Development*, 21(12), pp.1472–1477.

Dewar, J.M. & Walter, J.C., 2017. Mechanisms of DNA replication termination. *Nature reviews. Molecular cell biology*, 18(8), pp.507–516. Available at: http://dx.doi.org/10.1038/nrm.2017.42.

Duursma, A.M. et al., 2013. A role for the MRN complex in ATR activation via TOPBP1 recruitment. *Molecular cell*, 50(1), pp.116–22. Available at: http://www.ncbi.nlm.nih.gov/pubmed/23582259 [Accessed October 21, 2013].

Ellis, N.A. et al., 1994. Linkage disequilibrium between the FES, D15S127, and BLM loci in Ashkenazi Jews with Bloom syndrome. *Am J Hum Genet*, 55(3), pp.453–460. Available at: http://www.ncbi.nlm.nih.gov/pubmed/8079989.

Ellis, N. a et al., 1998. The Ashkenazic Jewish Bloom syndrome mutation blmAsh is present in non-Jewish Americans of Spanish ancestry. *American journal of human genetics*, 63(6), pp.1685–1693.

Ellis, N. a. et al., 1995. The Bloom's syndrome gene product is homologous to RecQ helicases. *Cell*, 83(4), pp.655–666. Available at: http://linkinghub.elsevier.com/retrieve/pii/0092867495901051.

Eykelenboom, J. et al., 2013. ATR Activates the S-M Checkpoint during Unperturbed Growth to Ensure Sufficient Replication Prior to Mitotic Onset. *Cell Reports*, 5(4), pp.1095–1107. Available at: http://dx.doi.org/10.1016/j.celrep.2013.10.027.

Feijoo, C. et al., 2001. Activation of mammalian Chk1 during DNA replication arrest: A role for Chk1 in the intra-S phase checkpoint monitoring replication origin firing. *Journal of Cell Biology*, 154(5), pp.913–923.

Feng, S. et al., 2016. Ewing tumor-associated antigen 1 interacts with replication protein A to promote restart of stalled replication forks. *Journal of Biological Chemistry*, 291(42), pp.21956–21962.

Ferguson, A.M. et al., 2005. Normal Cell Cycle and Checkpoint Responses in Mice and Cells Lacking Cdc25B and Cdc25C Protein Phosphatases. *Society*, 25(7), pp.2853–2860.

Fragkos, M. et al., 2015. DNA replication origin activation in space and time. *Nature Reviews Molecular Cell Biology*, 16(6), pp.360–374. Available at: http://www.nature.com/doifinder/10.1038/nrm4002.

Frei, C. & Gasser, S.M., 2000. The yeast Sgs1p helicase acts upstream of Rad53p in the DNA replication checkpoint and colocalizes with Rad53p in S-phase-specific foci. *Genes & development*, 14, pp.81–96.

Frick, D.N. & Richardson, C.C., 2001. DNA primases. *Annual review of biochemistry*, 70, pp.39–80. Available at: http://www.ncbi.nlm.nih.gov/pubmed/11395402.

Fukuda, K. et al., 1995. Structure-function relationship of the eukaryotic DNA replication factor, proliferating cell nuclear antigen. *The Journal of biological chemistry*, 270(38), pp.22527–34. Available at: http://www.ncbi.nlm.nih.gov/pubmed/7673244.

Furnari, B., Rhind, N. & Russell, P., 1997. Cdc25 mitotic inducer targeted by chk1 DNA damage checkpoint kinase. *Science (New York, NY)*, 277(5331), pp.1495–1497. Available at: http://www.sciencemag.org/cgi/content/full/277/5331/1495%5Cnpapers3://publication/uuid/4B499A31-1A37-49F8-A482-C350621EDDB1.

Gambus, A. et al., 2011. MCM2-7 form double hexamers at licensed origins in Xenopus egg extract. *Journal of Biological Chemistry*, 286(13), pp.11855–11864.

Gatei, M. et al., 2003. Ataxia-telangiectasia-mutated (ATM) and NBS1-dependent

phosphorylation of Chk1 on Ser-317 in response to ionizing radiation. *The Journal of biological chemistry*, 278(17), pp.14806–11. Available at: http://www.ncbi.nlm.nih.gov/pubmed/12588868 [Accessed January 7, 2015].

Ge, X.Q., Jackson, D.A. & Blow, J.J., 2007. Dormant origins licensed by excess Mcm2-7 are required for human cells to survive replicative stress. *Genes and Development*, 21(24), pp.3331–3341.

German, J., 1993. Bloom syndrome: a mendelian prototype of somatic mutational disease. *Medicine*, 72(6), pp.393–406. Available at: http://www.ncbi.nlm.nih.gov/pubmed/8231788.

German, J., Archibald, R. & Bloom, D., 1965. Chromosomal Breakage in a Rare and Probably Genetically Determined Syndrome of Man. *Science (New York, N.Y.)*, 148, pp.506–507.

Giannattasio, M. & Branzei, D., 2017. S-phase checkpoint regulations that preserve replication and chromosome integrity upon dNTP depletion. *Cellular and Molecular Life Sciences*, 74(13), pp.2361–2380.

Giono, L.E. et al., 2017. Mdm2 promotes Cdc25C protein degradation and delays cell cycle progression through the G2/M phase. *Oncogene*, 36(49), pp.6762–6773. Available at: http://dx.doi.org/10.1038/onc.2017.254.

Gong, Z. et al., 2010. BACH1/FANCJ Acts with TopBP1 and Participates Early in DNA Replication Checkpoint Control. *Molecular Cell*, 37(3), pp.438–446. Available at: http://dx.doi.org/10.1016/j.molcel.2010.01.002.

Gorgoulis, V.G. et al., 2005. Activation of the DNA damage checkpoint and genomic instability in human precancerous lesions. *Nature*, pp.907–913.

Gottlieb, T.M. & Jackson, S.P., 1993. The DNA-dependent protein kinase: Requirement for DNA ends and association with Ku antigen. *Cell*, 72(1), pp.131–142. Available at: http://linkinghub.elsevier.com/retrieve/pii/009286749390057W.

Graham, T.G.W., Walter, J.C. & Loparo, J.J., 2016. Two-Stage Synapsis of DNA Ends during Non-homologous End Joining. *Molecular Cell*, 61(6), pp.850–858. Available at: http://dx.doi.org/10.1016/j.molcel.2016.02.010.

Gravel, S. et al., 2008. DNA helicases Sgs1 and BLM promote DNA double-strand break resection. *Genes and Development*, 22(20), pp.2767–2772.

Guo, Z. et al., 2000. Requirement for Atr in phosphorylation of Chk1 and cell cycle regulation in response to DNA replication blocks and UV-damaged DNA in Xenopus egg extracts. *Genes & development*, 14(21), pp.2745–56. Available at: http://www.ncbi.nlm.nih.gov/pubmed/11069891.

Haahr, P. et al., 2016. Activation of the ATR kinase by the RPA-binding protein ETAA1. *Nature Cell Biology*, 18(11), pp.1196–1207. Available at: http://www.nature.com/doifinder/10.1038/ncb3422.

Halazonetis, T.D., 2004. Constitutively active DNA damage checkpoint pathways as the driving force for the high frequency of p53 mutations in human cancer. *DNA Repair*, 3(8–9), pp.1057–1062.

Heinzel, S.S. et al., 1991. Autonomous DNA replication in human cells is affected by the size and the source of the DNA. *Molecular and cellular biology*, 11(4), pp.2263–72. Available at: /Volumes/Work/Vishnu/Study Drive/PhD/Library/other/Mol. Cell. Biol.-1991-Heinzel-2263-72-jabo1.pdf%5Cnhttp://www.pubmedcentral.nih.gov/articlerender.fcgi?artid=359926&tool=pmcentrez&rendertype=abstract.

Helleday, T., 2011. The underlying mechanism for the PARP and BRCA synthetic lethality: Clearing up the misunderstandings. *Molecular Oncology*, 5(4), pp.387–393. Available at: http://dx.doi.org/10.1016/j.molonc.2011.07.001.

Hickson, I.D., 2003. RecQ helicases: caretakers of the genome. *Nature reviews. Cancer*, 3(3), pp.169–78. Available at: http://dx.doi.org/10.1038/nrc1012.

Hilton, B.A. et al., 2015. ATR Plays a Direct Antiapoptotic Role at Mitochondria, which Is Regulated by Prolyl Isomerase Pin1. *Molecular cell*, 60(1), pp.35–46. Available at: http://www.ncbi.nlm.nih.gov/pubmed/26387736.

Hollstein, M. et al., 1991. p53 mutations in human cancers. *Science*, 253(5015), pp.49–53. Available at: http://www.sciencemag.org/cgi/doi/10.1126/science.1905840.

Houtgraaf, J.H., Versmissen, J. & van der Giessen, W.J., 2006. A concise review of DNA damage checkpoints and repair in mammalian cells. *Cardiovascular Revascularization Medicine*, 7(3), pp.165–172.

Hu, P. et al., 2001. Evidence for BLM and Topoisomerase IIIalpha interaction in genomic stability. *Human molecular genetics*, 10(12), pp.1287–98. Available at: http://www.ncbi.nlm.nih.gov/pubmed/11406610.

Huertas, P. & Jackson, S.P., 2009. Human CtIP Mediates Cell Cycle Control of DNA End Resection and Double Strand Break Repair. *Journal of Biological Chemistry*, 284(14), pp.9558–9565. Available at: http://www.jbc.org/lookup/doi/10.1074/jbc.M808906200.

Ilves, I. et al., 2010. Activation of the MCM2-7 Helicase by Association with Cdc45 and GINS Proteins. *Molecular Cell*, 37(2), pp.247–258. Available at: http://dx.doi.org/10.1016/j.molcel.2009.12.030.

Jackson, D.A. & Pombo, A., 1998. Replicon clustes are stable units of chromosome structure: evidence that nuclear organization contributes to the efficient activation and propagation of S phase in human cells. *Journal of Cell Biology*, 140(6), pp.1285–1295.

Jackson, S.P. & Bartek, J., 2009. The DNA-damage response in human biology and disease. *Nature*, 461(7267), pp.1071–1078. Available at: http://www.pubmedcentral.nih.gov/articlerender.fcgi?artid=2906700&tool=pmcentrez&rendertype=abstract.

Jazayeri, A. et al., 2006. ATM- and cell cycle-dependent regulation of ATR in response to DNA double-strand breaks. *Nature cell biology*, 8(1), pp.37–45.

Jeggo, P.A., Pearl, L.H. & Carr, A.M., 2016. DNA repair, genome stability and cancer: a historical perspective. *Nature reviews. Cancer*, 16(1), pp.35–42. Available at: http://www.nature.com/doifinder/10.1038/nrc.2015.4.

Jiang, X. et al., 2006. The FATC Domains of PIKK Proteins Are Functionally Equivalent and Participate in the Tip60-dependent Activation of DNA-PKcs and ATM. *Journal of Biological Chemistry*, 281(23), pp.15741–15746. Available at: http://www.jbc.org/lookup/doi/10.1074/jbc.M513172200.

Kaneko, H., Orii, K.O., et al., 1997. BLM (the causative gene of Bloom syndrome) protein translocation into the nucleus by a nuclear localization signal. *Biochemical and biophysical research communications*, 240(2), pp.348–53. Available at: http://www.ncbi.nlm.nih.gov/pubmed/9388480.

Kaneko, H., Inoue, R., et al., 1997. Two Japanese Siblings with Bloom Syndrome Gene Mutation and B-Cell Lymphoma. *Leukemia & Lymphoma*, 27(5–6), pp.539–542. Available at:

http://informahealthcare.com/doi/abs/10.3109/10428199709058322 [Accessed October 27, 2014].
Karanja, K.K. et al., 2014. Preventing over-resection by DNA2 helicase/nuclease suppresses repair defects in Fanconi anemia cells. *Cell Cycle*, 13(10), pp.1540–1550.
Karow, J.K. et al., 2000. The Bloom's syndrome gene product promotes branch migration of holliday junctions. *Proceedings of the National Academy of Sciences of the United States of America*, 97(12), pp.6504–8. Available at: http://www.ncbi.nlm.nih.gov/pubmed/10823897%5Cnhttp://www.pubmedcentral.nih.gov/articlerender.fcgi?artid=PMC18638%5Cnhttp://www.pubmedcentral.nih.gov/articlerender.fcgi?artid=18638&tool=pmcentrez&rendertype=abstract.
Kaykov, A. & Nurse, P., 2015. The spatial and temporal organization of origin firing during the S-phase of fission yeast. *Genome research*, 25(3), pp.391–401. Available at: http://www.ncbi.nlm.nih.gov/pubmed/25650245.
Kelman, Z., 1997. PCNA: structure, functions and interactions. *Oncogene*, 14(6), pp.629–640. Available at: http://www.ncbi.nlm.nih.gov/pubmed/9038370%5Cnhttp://www.nature.com/onc/journal/v14/n6/pdf/1200886a.pdf.
Kerzendorfer, C. & O'Driscoll, M., 2009. Human DNA damage response and repair deficiency syndromes: Linking genomic instability and cell cycle checkpoint proficiency. *DNA Repair*, 8(9), pp.1139–1152.
Kilkenny, M.L. et al., 2013. Structures of human primase reveal design of nucleotide elongation site and mode of Pol tethering. *Proceedings of the National Academy of Sciences*, 110(40), pp.15961–15966. Available at: http://www.pnas.org/cgi/doi/10.1073/pnas.1311185110.
Kim, S. et al., 1999. Substrate Specificities and Identification of Putative Substrates of ATM Kinase Family Members Substrate Specificities and Identification of Putative Substrates of ATM Kinase Family Members *. *The Journal of Biological Chemistry*, 274(53), pp.37538–37543.
De Klein, A. et al., 2000. Targeted disruption of the cell-cycle checkpoint gene ATR leads to early embryonic lethality in mice. *Current Biology*, 10(8), pp.479–482.
Kondo, T. et al., 2001. Recruitment of Mec1 and Ddc1 Checkpoint Proteins to Double-Strand Breaks Through Distinct Mechanisms. *Science*, 294(5543), pp.867–870. Available at: http://www.sciencemag.org/cgi/doi/10.1126/science.1063827.
Krokan, H., Wist, E. & Krokan, R.H., 1981. Aphidicolin inhibits DNA synthesis by DNA polymerase alpha and isolated nuclei by a similar mechanism. *Nucleic acids research*, 9(18), pp.4709–4719.
Kumagai, A. et al., 2006. TopBP1 activates the ATR-ATRIP complex. *Cell*, 124(5), pp.943–55. Available at: http://www.ncbi.nlm.nih.gov/pubmed/16530042 [Accessed October 21, 2013].
Kumagai, A. et al., 2010. Treslin Collaborates with TopBP1 in Triggering the Initiation of DNA Replication. *Cell*, 140(3), pp.349–359. Available at: http://dx.doi.org/10.1016/j.cell.2009.12.049.
Kumagai, A. & Dunphy, W.G., 2000. Claspin, a Novel Protein Required for the Activation of Chk1 during a DNA Replication Checkpoint Response in Xenopus Egg Extracts. *Molecular Cell*, 6(4), pp.839–849. Available at: http://linkinghub.elsevier.com/retrieve/pii/S1097276505000924.

Kumagai, A. & Dunphy, W.G., 2003. Repeated phosphopeptide motifs in Claspin mediate the regulated binding of Chk1. *Nature Cell Biology*, 5(2), pp.161–165. Available at: http://www.nature.com/doifinder/10.1038/ncb921.

Kumagai, A., Kim, S.M. & Dunphy, W.G., 2004. Claspin and the activated form of ATR-ATRIP collaborate in the activation of Chk1. *Journal of Biological Chemistry*, 279(48), pp.49599–49608.

Kuo, L.J. & Yang, L.-X., 2008. Gamma-H2AX - a novel biomarker for DNA double-strand breaks. *In vivo (Athens, Greece)*, 22(3), pp.305–9.

Lahkim Bennani-Belhaj, K. et al., 2010. BLM Deficiency Is Not Associated with Sensitivity to Hydroxyurea-Induced Replication Stress. *Journal of nucleic acids*, 2010. Available at: http://www.pubmedcentral.nih.gov/articlerender.fcgi?artid=2945640&tool=pmcentrez&rendertype=abstract.

Larrea, A. & Lujan, S., 2010. Genome-wide model for the normal eukaryotic DNA replication fork. *Proceedings of the …*. Available at: http://www.pnas.org/content/107/41/17674.short.

Lee, A.Y.L., Liu, E. & Wu, X., 2007. The Mre11/Rad50/Nbs1 complex plays an important role in the prevention of DNA rereplication in mammalian cells. *Journal of Biological Chemistry*, 282(44), pp.32243–32255.

Lee, J. & Dunphy, W., 2010. Rad17 plays a central role in establishment of the interaction between TopBP1 and the Rad9-Hus1-Rad1 complex at stalled replication forks. *Molecular biology of the cell*, 21, pp.926–935. Available at: http://www.molbiolcell.org/content/21/6/926.short [Accessed October 27, 2014].

Lee, J., Kumagai, A. & Dunphy, W.G., 2003. Claspin, a Chk1-regulatory protein, monitors DNA replication on chromatin independently of RPA, ATR, and Rad17. *Molecular Cell*, 11(2), pp.329–340.

Lee, J., Kumagai, A. & Dunphy, W.G., 2007. The Rad9-Hus1-Rad1 Checkpoint Clamp Regulates Interaction of TopBP1 with ATR. *Journal of Biological Chemistry*, 282(38), pp.28036–28044. Available at: http://www.ncbi.nlm.nih.gov/pubmed/17636252 [Accessed October 21, 2013].

Lee, Y.-C. et al., 2016. RPA-Binding Protein ETAA1 Is an ATR Activator Involved in DNA Replication Stress Response. *Current Biology*, pp.1–12. Available at: http://linkinghub.elsevier.com/retrieve/pii/S0960982216312568.

Leung-Pineda, V., Ryan, C.E. & Piwnica-Worms, H., 2006. Phosphorylation of Chk1 by ATR is antagonized by a Chk1-regulated protein phosphatase 2A circuit. *Molecular and cellular biology*, 26(20), pp.7529–7538.

Li, L. et al., 1998. Carrier frequency of the Bloom syndrome blm(Ash) mutation in the Ashkenazi Jewish population. *Molecular Genetics and Metabolism*, 64(4), pp.286–290.

Lin, S.-J. et al., 2012. The Rad4(TopBP1) ATR-activation domain functions in G1/S phase in a chromatin-dependent manner. *PLoS genetics*, 8(6), p.e1002801. Available at: http://www.pubmedcentral.nih.gov/articlerender.fcgi?artid=3386226&tool=pmcentrez&rendertype=abstract [Accessed October 18, 2013].

Lindqvist, A. et al., 2005. Cdc25B cooperates with Cdc25A to induce mitosis but has a unique role in activating cyclin B1-Cdk1 at the centrosome. *Journal of Cell Biology*, 171(1), pp.35–45.

Liu, Q. et al., 2000. Chk1 is an essential kinase that is regulated by Atr and required for the G(2)/M DNA damage checkpoint. *Genes & development*, 14(12), pp.1448–59. Available at: http://www.pubmedcentral.nih.gov/articlerender.fcgi?artid=316686&tool=pmcentrez&rendertype=abstract.

Liu, Q. et al., 2000. Chk1 is an essential kinase that is regulated by Atr and required for the G2/M DNA damage checkpoint. *Genes and Development*, 14(12), pp.1448–1459.

Lomonosov, M. et al., 2003. Stabilization of stalled DNA replication forks by the BRCA2 breast cancer susceptibility protein service Stabilization of stalled DNA replication forks by the BRCA2 breast cancer susceptibility protein. , pp.3017–3022.

Lopez-Girona, A. et al., 2001. Serine-345 is required for Rad3-dependent phosphorylation and function of checkpoint kinase Chk1 in fission yeast. *Proceedings of the National Academy of Sciences*, 98(20), pp.11289–11294. Available at: http://www.pnas.org/cgi/doi/10.1073/pnas.191557598.

Lopez-Martinez, D., Liang, C.-C. & Cohn, M.A., 2016. Cellular response to DNA interstrand crosslinks: the Fanconi anemia pathway. *Cellular and Molecular Life Sciences*, 73(16), pp.3097–3114. Available at: http://link.springer.com/10.1007/s00018-016-2218-x.

Lord, C.J. & Ashworth, A., 2017. PARP inhibitors: Synthetic lethality in the clinic. *Science*, 355(6330), pp.1152–1158. Available at: http://www.sciencemag.org/lookup/doi/10.1126/science.aam7344.

MacDougall, C.A. et al., 2007. The structural determinants of checkpoint activation. *Genes & development*, 21(8), pp.898–903. Available at: http://www.ncbi.nlm.nih.gov/pubmed/17437996.

Mailand, N. et al., 2000. Rapid destruction of human Cdc25A in response to DNA damage. *Science*, 288(5470), pp.1425–1429.

Majka, J., Binz, S.K., et al., 2006. Replication protein A directs loading of the DNA damage checkpoint clamp to 5'-DNA junctions. *The Journal of biological chemistry*, 281(38), pp.27855–61. Available at: http://www.ncbi.nlm.nih.gov/pubmed/16864589.

Majka, J., Niedziela-Majka, A. & Burgers, P.M.J., 2006. The Checkpoint Clamp Activates Mec1 Kinase during Initiation of the DNA Damage Checkpoint. *Molecular Cell*, 24(6), pp.891–901.

Mäkiniemi, M. et al., 2001. BRCT Domain-containing Protein TopBP1 Functions in DNA Replication and Damage Response. *Journal of Biological Chemistry*, 276(32), pp.30399–30406. Available at: http://www.jbc.org/lookup/doi/10.1074/jbc.M102245200.

Manke, I.A. et al., 2003. BRCT repeats as phosphopeptide-binding modules involved in protein targeting. *Science (New York, N.Y.)*, 302(5645), pp.636–9. Available at: http://www.sciencemag.org/cgi/doi/10.1126/science.1088877.

Mankouri, H.W.H., Ashton, T.M. & Hickson, I.D., 2011. Holliday junction-containing DNA structures persist in cells lacking Sgs1 or Top3 following exposure to DNA damage. *Proceedings of the …*, 108(12), pp.4944–4949. Available at: http://buonmathuot.vn/ws/r/www.pnas.org/content/108/12/4944.full.

Maréchal, A. & Zou, L., 2013. DNA Damage Sensing by the ATM and ATR kinases. *Cold Spring Harbor perspectives in biology*, pp.1–18.

Marheineke, K. & Hyrien, O., 2004. Control of replication origin density and firing time in Xenopus egg extracts. Role of a caffeine-sensitive, ATR-dependent checkpoint. *Journal of Biological Chemistry*, 279(27), pp.28071–28081.

Maric, M. et al., 2014. Cdc48 and a ubiquitin ligase drive disassembly of the CMG helicase at the end of DNA replication. *Science*, 346(6208), pp.1253596–1253596. Available at: http://www.sciencemag.org/cgi/doi/10.1126/science.1253596.

Marteijn, J.A. et al., 2014. Understanding nucleotide excision repair and its roles in cancer and ageing. *Nature Reviews Molecular Cell Biology*, 15(7), pp.465–481. Available at: http://www.nature.com/doifinder/10.1038/nrm3822.

Matos, J. & West, S.C., 2014. Holliday junction resolution: Regulation in space and time. *DNA Repair*, 19, pp.176–181. Available at: http://dx.doi.org/10.1016/j.dnarep.2014.03.013.

Matsuoka, S., Huang, M. & Elledge, S.J., 1998. Linkage of ATM to cell cycle regulation by the Chk2 protein kinase. *Science (New York, N.Y.)*, 282(5395), pp.1893–1897.

Maya-Mendoza, A. et al., 2007. Chk1 regulates the density of active replication origins during the vertebrate S phase. *The EMBO Journal*, 26(11), pp.2719–2731. Available at: http://emboj.embopress.org/cgi/doi/10.1038/sj.emboj.7601714.

Mazouzi, A., Velimezi, G. & Loizou, J.I., 2014. DNA replication stress: Causes, resolution and disease. *Experimental Cell Research*, 329(1), pp.85–93. Available at: http://linkinghub.elsevier.com/retrieve/pii/S0014482714004352.

Meijer, L. et al., 1997. Biochemical and cellular effects of roscovitine, a potent and selective inhibitor of the cyclin-dependent kinases cdc2, cdk2 and cdk5. *European Journal of Biochemistry*, 243(1–2), pp.527–536. Available at: http://www.ncbi.nlm.nih.gov/pubmed/9030781%5Cnpapers3://publication/uuid/6CBCC5C0-EFB2-4F14-9555-059944D0760C.

Melo, J.A., Cohen, J. & Toczyski, D.P., 2001. Two checkpoint complexes are independently recruited to sites of DNA damage in vivo. *Genes and Development*, 15(21), pp.2809–2821.

Michael, W.M. et al., 2000. Activation of the DNA Replication Checkpoint Through RNA Synthesis by Primase. *Science*, 289(5487), pp.2133–2137. Available at: http://www.sciencemag.org/cgi/doi/10.1126/science.289.5487.2133.

Mijic, S. et al., 2017. Replication fork reversal triggers fork degradation in BRCA2-defective cells. *Nature Communications*, 8(1), pp.1–11.

Mimitou, E.P. & Symington, L.S., 2008. Sae2, Exo1 and Sgs1 collaborate in DNA double-strand break processing. *Nature*, 455(7214), pp.770–774. Available at: http://www.nature.com/doifinder/10.1038/nature07312.

Mohaghegh, P. & Hickson, I.D., 2001. DNA helicase deficiencies associated with cancer predisposition and premature ageing disorders. *Human molecular genetics*, 10(7), pp.741–6. Available at: http://www.ncbi.nlm.nih.gov/pubmed/11257107.

Moldovan, G.-L. & D'Andrea, A.D., 2009. How the Fanconi Anemia Pathway Guards the Genome. *Annual Review of Genetics*, 43(1), pp.223–249. Available at: http://www.annualreviews.org/doi/10.1146/annurev-genet-102108-134222.

Molinari, M. et al., 2000. Human Cdc25 A inactivation in response to S phase inhibition and its role in preventing premature mitosis. *EMBO Reports*, 1(1), pp.71–79.

Mordes, D.A. et al., 2008. TopBP1 activates ATR through ATRIP and a PIKK regulatory domain. *Genes and Development*, 22(11), pp.1478–1489.

Moyer, S.E., Lewis, P.W. & Botchan, M.R., 2006. Isolation of the Cdc45/Mcm2-7/GINS

(CMG) complex, a candidate for the eukaryotic DNA replication fork helicase. *Proceedings of the National Academy of Sciences*, 103(27), pp.10236–10241. Available at: http://www.pnas.org/cgi/doi/10.1073/pnas.0602400103.

Murga, M. et al., 2009. A mouse model of ATR-Seckel shows embryonic replicative stress and accelerated aging. *Nature Genetics*, 41(8), pp.891–898. Available at: http://www.pubmedcentral.nih.gov/articlerender.fcgi?artid=2902278&tool=pmcentrez&rendertype=abstract [Accessed October 18, 2013].

Muzi-Falconi, M. et al., 2003. The DNA Polymerase _-Primase Complex: Multiple Functions and Interactions. *The Scientific World JOURNAL*, 3, pp.21–33. Available at: http://www.hindawi.com/journals/tswj/2003/575271/abs/.

Nam, E.A. et al., 2011. Thr-1989 phosphorylation is a marker of active ataxia telangiectasia- mutated and Rad3-related (ATR) kinase. *Journal of Biological Chemistry*, 286(33), pp.28707–28714.

Neff, N.F. et al., 1999. The DNA helicase activity of BLM is necessary for the correction of the genomic instability of bloom syndrome cells. *Molecular biology of the cell*, 10(3), pp.665–76. Available at: http://www.pubmedcentral.nih.gov/articlerender.fcgi?artid=25194&tool=pmcentrez&rendertype=abstract.

Nick McElhinny, S.A. et al., 2008. Division of labor at the eukaryotic replication fork. *Molecular cell*, 30(2), pp.137–44. Available at: http://www.ncbi.nlm.nih.gov/pubmed/18439893.

Nicolette, M.L. et al., 2010. Mre11–Rad50–Xrs2 and Sae2 promote 5' strand resection of DNA double-strand breaks. *Nature Structural & Molecular Biology*, 17(12), pp.1478–1485. Available at: http://www.nature.com/doifinder/10.1038/nsmb.1957.

Nieduszynski, C. a, Knox, Y. & Donaldson, A.D., 2006. Genome-wide identification of replication origins in yeast by comparative genomics service Genome-wide identification of replication origins in yeast by comparative genomics. *Genes & Development*, 20, pp.1874–1879.

Nieminuszczy, J., Schwab, R.A. & Niedzwiedz, W., 2016. The DNA fibre technique - tracking helicases at work. *Methods*. Available at: http://dx.doi.org/10.1016/j.ymeth.2016.04.019.

Niida, H. & Nakanishi, M., 2006. DNA damage checkpoints in mammals. *Mutagenesis*, 21(1), pp.3–9. Available at: http://www.ncbi.nlm.nih.gov/pubmed/16314342 [Accessed July 11, 2014].

Nimonkar, A. V. et al., 2011. BLM-DNA2-RPA-MRN and EXO1-BLM-RPA-MRN constitute two DNA end resection machineries for human DNA break repair. *Genes and Development*, 25(4), pp.350–362.

Nimonkar, A. V. et al., 2008. Human exonuclease 1 and BLM helicase interact to resect DNA and initiate DNA repair. *Proceedings of the National Academy of Sciences*, 105(44), pp.16906–16911. Available at: http://www.pnas.org/cgi/doi/10.1073/pnas.0809380105.

O'Connor, M.J., 2015. Targeting the DNA Damage Response in Cancer. *Molecular Cell*, 60(4), pp.547–560. Available at: http://dx.doi.org/10.1016/j.molcel.2015.10.040.

O'Driscoll, M. et al., 2003. A splicing mutation affecting expression of ataxia–telangiectasia and Rad3–related protein (ATR) results in Seckel syndrome. *Nature Genetics*, 33(4), pp.497–501. Available at:

http://www.nature.com/doifinder/10.1038/ng1129.
O'Driscoll, M. et al., 2004. An overview of three new disorders associated with genetic instability: LIG4 syndrome, RS-SCID and ATR-Seckel syndrome. *DNA Repair*, 3(8–9), pp.1227–1235.
O'Neill, T. et al., 2000. Utilization of oriented peptide libraries to identify substrate motifs selected by ATM. *Journal of Biological Chemistry*, 275(30), pp.22719–22727.
Ochi, T. et al., 2015. PAXX, a paralog of XRCC4 and XLF, interacts with Ku to promote DNA double-strand break repair. *Science*, 347(6218), pp.185–188. Available at: http://www.sciencemag.org/cgi/doi/10.1126/science.1261971.
Olson, E. et al., 2006. RPA2 is a direct downstream target for ATR to regulate the S-phase checkpoint. *Journal of Biological Chemistry*, 281(51), pp.39517–39533.
St. Onge, R.P. et al., 2003. A role for the phosphorylation of hRad9 in checkpoint signaling. *Journal of Biological Chemistry*, 278(29), pp.26620–26628.
Ouyang, K.J., Woo, L.L. & Ellis, N.A., 2008. Homologous recombination and maintenance of genome integrity: Cancer and aging through the prism of human RecQ helicases. *Mechanisms of Ageing and Development*, 129(7–8), pp.425–440.
Parker, L.L. & Piwnica-Worms, H., 1992. Inactivation of the p34cdc2-Cyclin B Complex by the Human WEE1 Tyrosine Kinase. *Science*, 257(1989), pp.1955–1957.
Paull, T.T. & Gellert, M., 1998. The 3' to 5' Exonuclease Activity of Mre11 Facilitates Repair of DNA Double-Strand Breaks. *Molecular Cell*, 1(7), pp.969–979. Available at: http://linkinghub.elsevier.com/retrieve/pii/S1097276500800970.
Peng, C. et al., 1997. Mitotic and G2 Checkpoint Control: Regulation of 14-3-3 Protein Binding by Phosphorylation of Cdc25C on Serine-216. *Science*, 277(5331), pp.1501–1505. Available at: http://www.sciencemag.org/cgi/doi/10.1126/science.277.5331.1501.
Perry, J. & Kleckner, N., 2003. The ATRs, ATMs, and TORs are giant HEAT repeat proteins. *Cell*, 112(2), pp.151–155.
Petermann, E. et al., 2006. Chk1 requirement for high global rates of replication fork progression during normal vertebrate S phase. *Molecular and cellular biology*, 26(8), pp.3319–26. Available at: http://mcb.asm.org/content/26/8/3319.full.
Petermann, E., Orta, M.L., et al., 2010. Hydroxyurea-Stalled Replication Forks Become Progressively Inactivated and Require Two Different RAD51-Mediated Pathways for Restart and Repair. *Molecular Cell*, 37(4), pp.492–502.
Petermann, E., Woodcock, M. & Helleday, T., 2010. Chk1 promotes replication fork progression by controlling replication initiation. *Proceedings of the National Academy of Sciences of the United States of America*, 107(37), pp.16090–16095.
Piwnica-Worms, Z.H. and, 2001. ATR-Mediated Checkpoint Pathways Regulate Phosphorylation and Activation of ATR-Mediated Checkpoint Pathways Regulate Phosphorylation and Activation of Human Chk1. *Mol. Cell. Biol.*, 21(13), pp.4129–4139.
Podhorecka, M., Skladanowski, A. & Bozko, P., 2010. H2AX Phosphorylation: Its Role in DNA Damage Response and Cancer Therapy. *Journal of Nucleic Acids*, 2010, pp.1–9. Available at: http://www.hindawi.com/journals/jna/2010/920161/.
Priego Moreno, S. et al., 2014. Polyubiquitylation drives replisome disassembly at the termination of DNA replication. *Science*, 346(6208), pp.477–481. Available at: http://www.sciencemag.org/cgi/doi/10.1126/science.1253585.

Prioleau, M. & MacAlpine, D.M., 2016. DNA replication origins-where do we begin? *Genes & development*, 30(15), pp.1683–97. Available at: http://www.ncbi.nlm.nih.gov/pubmed/27542827.

Pursell, Z.F. et al., 2007. Yeast DNA polymerase epsilon participates in leading-strand DNA replication. *Science (New York, N.Y.)*, 317(5834), pp.127–30. Available at: http://science.sciencemag.org/content/sci/317/5834/127.full.pdf.

Ran, F.A. et al., 2013. Genome engineering using the CRISPR-Cas9 system. *Nature Protocols*, 8(11), pp.2281–2308. Available at: http://www.nature.com/doifinder/10.1038/nprot.2013.143.

Rao, V.A. et al., 2007. Endogenous gamma-H2AX-ATM-Chk2 checkpoint activation in Bloom's syndrome helicase deficient cells is related to DNA replication arrested forks. *Molecular cancer research : MCR*, 5(July), pp.713–724.

Rauen, M. et al., 2000. The human checkpoint protein hRad17 interacts with the PCNA-like proteins hRad1, hHus1, and hRad9. *Journal of Biological Chemistry*, 275(38), pp.29767–29771.

Ray Chaudhuri, A. et al., 2012. Topoisomerase i poisoning results in PARP-mediated replication fork reversal. *Nature Structural and Molecular Biology*, 19(4), pp.417–423. Available at: http://dx.doi.org/10.1038/nsmb.2258.

Raynard, S. et al., 2008. Functional role of BLAP75 in BLM-topoisomerase IIIalpha-dependent holliday junction processing. *The Journal of biological chemistry*, 283(23), pp.15701–8. Available at: http://www.ncbi.nlm.nih.gov/pubmed/18390547.

Raynard, S., Bussen, W. & Sung, P., 2006. A double Holliday junction dissolvasome comprising BLM, topoisomerase IIIalpha, and BLAP75. *The Journal of biological chemistry*, 281(20), pp.13861–4. Available at: http://www.ncbi.nlm.nih.gov/pubmed/16595695.

Recolin, B. et al., 2014. Molecular mechanisms of DNA replication checkpoint activation. *Genes*, 5(1), pp.147–175.

Remus, D. & Diffley, J.F., 2009. Eukaryotic DNA replication control: Lock and load, then fire. *Current Opinion in Cell Biology*, 21(6), pp.771–777.

Riballo, E. et al., 2004. A pathway of double-strand break rejoining dependent upon ATM, Artemis, and proteins locating to ??-H2AX foci. *Molecular Cell*, 16(5), pp.715–724.

Roberts, S.A. et al., 2012. Clustered Mutations in Yeast and in Human Cancers Can Arise from Damaged Long Single-Strand DNA Regions. *Molecular Cell*, 46(4), pp.424–435. Available at: http://dx.doi.org/10.1016/j.molcel.2012.03.030.

Robertson, A.B. et al., 2009. Base excision repair: The long and short of it. *Cellular and Molecular Life Sciences*, 66(6), pp.981–993.

Roos-Mattjus, P. et al., 2003. Phosphorylation of Human Rad9 Is Required for Genotoxin-activated Checkpoint Signaling. *Journal of Biological Chemistry*, 278(27), pp.24428–24437.

Rubnitz, J. & Subramani, S., 1984. The minimum amount of homology required for homologous recombination in mammalian cells. *Mol Cell Biol*, 4(11), pp.2253–2258. Available at: http://www.ncbi.nlm.nih.gov/entrez/query.fcgi?cmd=Retrieve&db=PubMed&dopt=Citation&list_uids=6096689.

Sacco, E. et al., 2012. Comparative analysis of the molecular mechanisms controlling

the initiation of chromosomal DNA replication in yeast and in mammalian cells. *Biotechnology Advances*, 30(1), pp.73–98. Available at: http://dx.doi.org/10.1016/j.biotechadv.2011.09.009.

Saldivar, J.C., Cortez, D. & Cimprich, K.A., 2017. The essential kinase ATR: ensuring faithful duplication of a challenging genome. *Nature Reviews Molecular Cell Biology*. Available at: http://www.nature.com/doifinder/10.1038/nrm.2017.67.

San Filippo, J., Sung, P. & Klein, H., 2008. Mechanism of Eukaryotic Homologous Recombination. *Annual Review of Biochemistry*, 77(1), pp.229–257. Available at: http://www.annualreviews.org/doi/10.1146/annurev.biochem.77.061306.125255.

Sanchez-Pulido, L., Diffley, J.F.X. & Ponting, C.P., 2010. Homology explains the functional similarities of Treslin/Ticrr and Sld3. *Current Biology*, 20(12), pp.509–510.

Sanchez, Y. et al., 1997. Conservation of the Chk1 Checkpoint Pathway in Mammals: Linkage of DNA Damage to Cdk Regulation Through Cdc25. *Science*, 277(5331), pp.1497–1501. Available at: http://www.sciencemag.org/cgi/doi/10.1126/science.277.5331.1497.

Sanjiv, K. et al., 2016. Cancer-Specific Synthetic Lethality between ATR and CHK1 Kinase Activities. *Cell Reports*, 14(2), pp.298–309.

Sansam, C.L. et al., 2010. A vertebrate gene, ticrr, is an essential checkpoint and replication regulator. *Genes and Development*, 24(2), pp.183–194.

Santocanale, C. & Diffley, J.F., 1998. A Mec1- and Rad53-dependent checkpoint controls late-firing origins of DNA replication. *Nature*, 395(6702), pp.615–618.

Sartori, A. a et al., 2007. Human CtIP promotes DNA end resection. *Nature*, 450(7169), pp.509–14. Available at: http://www.pubmedcentral.nih.gov/articlerender.fcgi?artid=2409435&tool=pmcentrez&rendertype=abstract [Accessed November 10, 2014].

Sawicka, M. et al., 2016. The Dimeric Architecture of Checkpoint Kinases Mec1ATR and Tel1ATM Reveal a Common Structural Organization. *The Journal of biological chemistry*, 291(26), pp.13436–47. Available at: http://www.ncbi.nlm.nih.gov/pubmed/27129217.

Schlacher, K. et al., 2011. Double-strand break repair-independent role for BRCA2 in blocking stalled replication fork degradation by MRE11. *Cell*, 145(4), pp.529–542. Available at: http://dx.doi.org/10.1016/j.cell.2011.03.041.

Schwab, R. a, Blackford, A.N. & Niedzwiedz, W., 2010. ATR activation and replication fork restart are defective in FANCM-deficient cells. *The EMBO journal*, 29(4), pp.806–18. Available at: http://www.pubmedcentral.nih.gov/articlerender.fcgi?artid=2829160&tool=pmcentrez&rendertype=abstract [Accessed October 21, 2013].

Seiler, J.A. et al., 2007. The Intra-S-Phase Checkpoint Affects both DNA Replication Initiation and Elongation: Single-Cell and -DNA Fiber Analyses. *Molecular and Cellular Biology*, 27(16), pp.5806–5818. Available at: http://mcb.asm.org/cgi/doi/10.1128/MCB.02278-06.

Semlow, D.R. et al., 2016. Replication-Dependent Unhooking of DNA Interstrand Cross-Links by the NEIL3 Glycosylase. *Cell*, 167(2), p.498–511.e14. Available at: http://dx.doi.org/10.1016/j.cell.2016.09.008.

Shastri, V.M. & Schmidt, K.H., 2016. Cellular defects caused by hypomorphic variants

of the Bloom syndrome helicase gene BLM. *Molecular genetics & genomic medicine*, 4(1), pp.106–19. Available at: http://www.ncbi.nlm.nih.gov/pubmed/26788541%5Cnhttp://www.pubmedcentral.nih.gov/articlerender.fcgi?artid=PMC4707026.

Shechter, D., Costanzo, V. & Gautier, J., 2004. ATR and ATM regulate the timing of DNA replication origin firing. *Nature Cell Biology*, 6(7), pp.648–655. Available at: http://www.nature.com/doifinder/10.1038/ncb1145.

Shiotani, B., Nguyen, H. & Håkansson, P., 2013. Two distinct modes of ATR activation orchestrated by Rad17 and Nbs1. *Cell reports*, pp.1651–1662. Available at: http://www.sciencedirect.com/science/article/pii/S2211124713002003 [Accessed October 27, 2014].

Silva, J. et al., 2018. EXD2 governs germ stem cell homeostasis and lifespan by promoting mitoribosome integrity and translation. *Nature Cell Biology*, 20(February). Available at: http://www.nature.com/articles/s41556-017-0016-9.

Sirbu, B.M. et al., 2013. Identification of proteins at active, stalled, and collapsed replication forks using isolation of proteins on nascent DNA (iPOND) coupled with mass spectrometry. *The Journal of biological chemistry*, 288(44), pp.31458–67. Available at: http://www.pubmedcentral.nih.gov/articlerender.fcgi?artid=3814742&tool=pmcentrez&rendertype=abstract [Accessed November 10, 2014].

Slater, M.L., 1973. Effect of reversible inhibition of deoxyribonucleic acid synthesis on the yeast cell cycle. *Journal of Bacteriology*, 113(1), pp.263–270.

Sleigh, M.J., 1976. The mechanism of DNA breakage by phleomycin in vitro. *Nucleic Acids Research*, 3(4), pp.891–902. Available at: https://academic.oup.com/nar/article-lookup/doi/10.1093/nar/3.4.891.

Smits, V.A.J., Reaper, P.M. & Jackson, S.P., 2006. Rapid PIKK-dependent release of Chk1 from chromatin promotes the DNA-damage checkpoint response. *Current Biology*, 16(2), pp.150–159.

Smogorzewska, A. et al., 2010. A Genetic Screen Identifies FAN1, a Fanconi Anemia-Associated Nuclease Necessary for DNA Interstrand Crosslink Repair. *Molecular Cell*, 39(1), pp.36–47.

Sogo, J.M., Lopes, M. & Foiani, M., 2002. Fork reversal and ssDNA accumulation at stalled replication forks owing to checkpoint defects. *Science*, 297(5581), pp.599–602.

Sonoda, E. et al., 1999. Sister chromatid exchanges are mediated by homologous recombination in vertebrate cells. *Molecular and cellular biology*, 19(7), pp.5166–9. Available at: http://www.pubmedcentral.nih.gov/articlerender.fcgi?artid=84359&tool=pmcentrez&rendertype=abstract.

Spagnolo, L. et al., 2006. Three-Dimensional Structure of the Human DNA-PKcs/Ku70/Ku80 Complex Assembled on DNA and Its Implications for DNA DSB Repair. *Molecular Cell*, 22(4), pp.511–519.

Stinchcomb, D.T., Struhl, K. & Davis, R.W., 1979. Isolation and characterisation of a yeast chromosomal replicator. *Nature*, 282(5734), pp.39–43. Available at: http://www.nature.com/doifinder/10.1038/282039a0.

Straughen, J.E. et al., 1998. A rapid method for detecting the predominant Ashkenazi Jewish mutation in the Bloom's syndrome gene. *Human mutation*, 11(2), pp.175–

8. Available at: http://www.ncbi.nlm.nih.gov/pubmed/9482582.
Sturzenegger, A. et al., 2014. DNA2 cooperates with the WRN and BLM RecQ helicases to mediate long-range DNA end resection in human cells. *Journal of Biological Chemistry*, 289(39), pp.27314–27326.
Sun, L. et al., 2017. Structural Insight into BLM Recognition by TopBP1. *Structure*, pp.1–7. Available at: http://linkinghub.elsevier.com/retrieve/pii/S0969212617302587.
Sun, Y. et al., 2007. DNA Damage-Induced Acetylation of Lysine 3016 of ATM Activates ATM Kinase Activity. *Molecular and Cellular Biology*, 27(24), pp.8502–8509. Available at: http://mcb.asm.org/cgi/doi/10.1128/MCB.01382-07.
Sung, P., 1994. Catalysis of ATP-dependent homologous DNA pairing and strand exchange by yeast RAD51 protein. *Science*, 265(5176), pp.1241–1243. Available at: http://www.sciencemag.org/cgi/doi/10.1126/science.8066464.
Técher, H. et al., 2016. Signaling from Mus81-Eme2-Dependent DNA Damage Elicited by Chk1 Deficiency Modulates Replication Fork Speed and Origin Usage. *Cell Reports*, 14(5), pp.1114–1127.
Técher, H. et al., 2017. The impact of replication stress on replication dynamics and DNA damage in vertebrate cells. *Nature reviews. Genetics*, 18(9), pp.535–550. Available at: http://www.nature.com/doifinder/10.1038/nrg.2017.46.
Thangavel, S. et al., 2015. DNA2 drives processing and restart of reversed replication forks in human cells. *The Journal of Cell Biology*, 208(5), pp.545–562. Available at: http://www.jcb.org/cgi/doi/10.1083/jcb.201406100.
Toledo, L.I. et al., 2011. A cell-based screen identifies ATR inhibitors with synthetic lethal properties for cancer-associated mutations. *Nat Struct Mol Biol*, 18(6), pp.721–727.
Toledo, L.I. et al., 2008. ATR signaling can drive cells into senescence in the absence of DNA breaks. *Genes and Development*, 22(3), pp.297–302.
Tsao, C.-C., Geisen, C. & Abraham, R.T., 2004. Interaction between human MCM7 and Rad17 proteins is required for replication checkpoint signaling. *The EMBO Journal*, 23(23), pp.4660–4669. Available at: http://emboj.embopress.org/cgi/doi/10.1038/sj.emboj.7600463.
Van, C. et al., 2010. Continued primer synthesis at stalled replication forks contributes to checkpoint activation. *Journal of Cell Biology*, 189(2), pp.233–246.
De Voer, R.M. et al., 2015. Deleterious Germline BLM mutations and the risk for early-onset colorectal cancer. *Scientific Reports*, 5, pp.1–7. Available at: http://dx.doi.org/10.1038/srep14060.
Walworth, N.C. & Bernards, R., 1996. rad-Dependent Response of the chk1-Encoded Protein Kinase at the DNA Damage Checkpoint. *Science*, 271(5247), pp.353–356. Available at: http://www.sciencemag.org/cgi/doi/10.1126/science.271.5247.353.
Wang, J., Chen, J. & Gong, Z., 2013. TopBP1 Controls BLM Protein Level to Maintain Genome Stability. *Molecular Cell*, 52(5), pp.667–678. Available at: http://www.ncbi.nlm.nih.gov/pubmed/24239288 [Accessed July 23, 2014].
Wang, J., Gong, Z. & Chen, J., 2011. MDC1 collaborates with TopBP1 in DNA replication checkpoint control. *Journal of Cell Biology*, 193(2), pp.267–273.
Wang, W., Seki, M. & Narita, Y., 2000. Possible association of BLM in decreasing DNA double strand breaks during DNA replication. *The EMBO Journal*, 19(13), pp.3428–3435. Available at:

http://onlinelibrary.wiley.com/doi/10.1093/emboj/19.13.3428/full.
Wang, Y. & Qin, J., 2003. MSH2 and ATR form a signaling module and regulate two branches of the damage response to DNA methylation. *Proceedings of the National Academy of Sciences of the United States of America*, 100(26), pp.15387–15392.
Ward, I.M. & Chen, J., 2001. Histone H2AX Is Phosphorylated in an ATR-dependent Manner in Response to Replicational Stress. *Journal of Biological Chemistry*, 276(51), pp.47759–47762.
Wardlaw, C.P., Carr, A.M. & Oliver, A.W., 2014. TopBP1: A BRCT-scaffold protein functioning in multiple cellular pathways. *DNA repair*, 22, pp.165–74. Available at: http://www.ncbi.nlm.nih.gov/pubmed/25087188 [Accessed December 15, 2014].
Warren, M. et al., 2010. Irradiated Blm-deficient mice are a highly tumor prone model for analysis of a broad spectrum of hematologic malignancies. *Leukemia research*, 34(2), pp.210–20. Available at: http://www.pubmedcentral.nih.gov/articlerender.fcgi?artid=2815150&tool=pmcentrez&rendertype=abstract [Accessed October 22, 2013].
Watanabe, N., Broome, M. & Hunter, T., 1995. Regulation of the human WEE1Hu CDK tyrosine 15-kinase during the cell cycle. *The EMBO journal*, 14(9), pp.1878–91. Available at: http://www.pubmedcentral.nih.gov/articlerender.fcgi?artid=398287&tool=pmcentrez&rendertype=abstract.
Watt, P.M. & Hickson, I.D., 1996. Genome stability: Failure to unwind causes cancer. *Current Biology*, 6(3), pp.265–267.
Wechsler, T., Newman, S. & West, S.C., 2011. Aberrant chromosome morphology in human cells defective for Holliday junction resolution. *Nature*, 471(7340), pp.642–646. Available at: http://dx.doi.org/10.1038/nature09790.
Wilsker, D. et al., 2008. Essential function of Chk1 can be uncoupled from DNA damage checkpoint and replication control. *Proceedings of the National Academy of Sciences of the United States of America*, 105(52), pp.20752–7. Available at: http://www.pubmedcentral.nih.gov/articlerender.fcgi?artid=2634938&tool=pmcentrez&rendertype=abstract.
Winding, P. & Berchtold, M.W., 2001. The chicken B cell line DT40: A novel tool for gene disruption experiments. *Journal of Immunological Methods*, 249(1–2), pp.1–16.
Wold, M.S. & Kelly, T., 1988. Purification and characterization of replication protein A, a cellular protein required for in vitro replication of simian virus 40 DNA. *Proceedings of the National Academy of Sciences of the United States of America*, 85(8), pp.2523–7. Available at: http://www.pubmedcentral.nih.gov/articlerender.fcgi?artid=280029&tool=pmcentrez&rendertype=abstract.
Woodward, A.M. et al., 2006. Excess Mcm2-7 license dormant origins of replication that can be used under conditions of replicative stress. *Journal of Cell Biology*, 173(5), pp.673–683.
Wu, L., 2007. Role of the BLM helicase in replication fork management. *DNA repair*, 6(7), pp.936–44. Available at: http://www.ncbi.nlm.nih.gov/pubmed/17363339 [Accessed August 13, 2014].
Wu, L. & Hickson, I.D., 2006. DNA helicases required for homologous recombination

and repair of damaged replication forks. *Annual review of genetics*, 40, pp.279–306.

Wu, P.-Y. et al., 2009. Structural and functional interaction between the human DNA repair proteins DNA ligase IV and XRCC4. *Molecular and cellular biology*, 29(11), pp.3163–72. Available at: http://www.pubmedcentral.nih.gov/articlerender.fcgi?artid=2682001&tool=pmcentrez&rendertype=abstract%5Cnhttp://www.ncbi.nlm.nih.gov/pubmed/19332554%5Cnhttp://www.pubmedcentral.nih.gov/articlerender.fcgi?artid=PMC2682001.

Wyatt, H.D.M. & West, S.C., 2014. Holliday junction resolvases. *Cold Spring Harbor Perspectives in Biology*, 6(9), pp.1–30.

Wyman, C. & Kanaar, R., 2006. DNA Double-Strand Break Repair: All's Well that Ends Well. *Annual Review of Genetics*, 40(1), pp.363–383. Available at: http://www.annualreviews.org/doi/10.1146/annurev.genet.40.110405.090451.

Xiao, Z. et al., 2003. Chk1 mediates S and G2 arrests through Cdc25A degradation in response to DNA-damaging agents. *Journal of Biological Chemistry*, 278(24), pp.21767–21773.

Yamane, K., Wu, X. & Chen, J., 2002. A DNA Damage-Regulated BRCT-Containing Protein, TopBP1, Is Required for Cell Survival. *Molecular and Cellular Biology*, 22(2), pp.555–566. Available at: http://mcb.asm.org/cgi/doi/10.1128/MCB.22.2.555-566.2002.

Yamazaki, S., Hayano, M. & Masai, H., 2013. Replication timing regulation of eukaryotic replicons: Rif1 as a global regulator of replication timing. *Trends in Genetics*, 29(8), pp.449–460. Available at: http://dx.doi.org/10.1016/j.tig.2013.05.001.

Yan, S. & Michael, W., 2009. TopBP1 and DNA polymerase α-mediated recruitment of the 9-1-1 complex to stalled replication forks. *Cell Cycle*, pp.2877–2884. Available at: http://www.landesbioscience.com/journals/cc/YanCC8-18.pdf [Accessed January 15, 2015].

Yarbro, J.W., 1992. Mechanism of action of hydroxyurea. *Seminars in oncology*, 19(3 Suppl 9), pp.1–10. Available at: http://www.ncbi.nlm.nih.gov/pubmed/1641648.

Yazinski, S.A. & Zou, L., 2016. Functions, Regulation, and Therapeutic Implications of the ATR Checkpoint Pathway. *Annual Review of Genetics*, 50(1), pp.155–173. Available at: http://www.annualreviews.org/doi/10.1146/annurev-genet-121415-121658.

Yoo, H.Y. et al., 2009. The Mre11-Rad50-Nbs1 Complex Mediates Activation of TopBP1 by ATM. *Molecular Biology of the Cell*, 20(9), pp.2351–2360. Available at: http://www.ncbi.nlm.nih.gov/pubmed/20496754.

Yu, X. et al., 2003. The BRCT domain is a phospho-protein binding domain. *Science (New York, N.Y.)*, 302(5645), pp.639–42. Available at: http://www.sciencemag.org/cgi/doi/10.1126/science.1088753.

Zellweger, R. et al., 2015. Rad51-mediated replication fork reversal is a global response to genotoxic treatments in human cells. *Journal of Cell Biology*, 208(5), pp.563–579.

Zeman, M.K. & Cimprich, K.A., 2014. Causes and consequences of replication stress. *Nature cell biology*, 16(1), pp.2–9. Available at: http://www.ncbi.nlm.nih.gov/pubmed/24366029%5Cnhttp://www.pubmedcentr

al.nih.gov/articlerender.fcgi?artid=PMC4354890.
Zhang, Y.W. et al., 2005. Genotoxic stress targets human Chk1 for degradation by the ubiquitin-proteasome pathway. *Molecular Cell*, 19(5), pp.607–618.
Zhou, B.S. & Elledge, S.J., 2000. The DNA damage response: putting checkpoints in perspective. *Nature*, 408(6811), pp.433–439. Available at: http://www.nature.com/doifinder/10.1038/35044005.
Zhou, Z.-W. et al., 2013. An essential function for the ATR-activation-domain (AAD) of TopBP1 in mouse development and cellular senescence. *PLoS genetics*, 9(8), p.e1003702. Available at: http://www.pubmedcentral.nih.gov/articlerender.fcgi?artid=3738440&tool=pmcentrez&rendertype=abstract [Accessed October 18, 2013].
Zhu, Z. et al., 2008. Sgs1 Helicase and Two Nucleases Dna2 and Exo1 Resect DNA Double-Strand Break Ends. *Cell*, 134(6), pp.981–994.
Zid, B.M. & Kapahi, P., 2018. Exonuclease EXD2 in mitochondrial translation. *Nature Cell Biology*, 20(2), p.120. Available at: http://www.nature.com/articles/s41556-017-0031-x.
Zou, L., Cortez, D. & Elledge, S.J., 2002. Regulation of ATR substrate selection by Rad17-dependent loading of Rad9 complexes onto chromatin. *Genes and Development*, 16(2), pp.198–208.
Zou, L. & Elledge, S.J., 2003. Sensing DNA damage through ATRIP recognition of RPA-ssDNA complexes. *Science (New York, N.Y.)*, 300(5625), pp.1542–8. Available at: http://www.ncbi.nlm.nih.gov/pubmed/12791985.